STABILITY ANALYSIS OF COMPOSITE LAMINATES USING SIMPLE HIGHER ORDER SHEAR DEFORMATION THEORY

By

Arindam Chakraborty

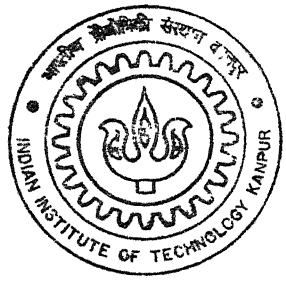

DEPARTMENT OF AEROSPACE ENGINEERING

Indian Institute of Technology Kanpur

FEBRUARY, 2003

STABILITY ANALYSIS OF COMPOSITE LAMINATES USING SIMPLE HIGHER ORDER SHEAR DEFORMATION THEORY

A thesis Submitted

in Partial fulfilment of the Requirements

for the Degree of

Master of Technology

by

ARINDAM CHAKRABORTY

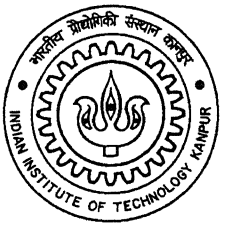

to the

DEPARTMENT OF AEROSPACE ENGINEERING

INDIAN INSTITUTE OF TECHNOLOGY, KANPUR

February 2003

CERTIFICATE

It is certified that work contained in this thesis titled **STABILITY ANALYSIS OF COMPOSITE LAMINATES USING SIMPLE HIGHER ORDER SHEAR DEFORMATION THEORY**, by **Arindam Chakraborty**, has been carried out under my supervision and that this work has not been submitted elsewhere for a degree.

February, 2003

Dr. N. G. R. Iyengar
Professor
Department of Aerospace Engineering
Indian Institute of Technology
Kanpur
India

DEDICATED

TO

THE LOVING MEMORY

OF MY

GRANDFATHER

ACKNOWLEDGEMENTS

I take this opportunity to express my deep sense of gratitude to my thesis supervisor Dr. N. G. R. Iyengar for his constant support and guidance throughout this work. Working with him has been a rich experience and shall always be a pleasant memory.His valuable suggestions and innovative ideas helped me a lot in completing this work. I am extremely thankful to him for giving me the appropriate milieu for research.He has also introduced me to the rapidly expanding world of composite materials.

I would also like to express my deep regard to Dr. C. S. Upadhyay for introducing me to the exciting world of Finite Elements and for extending his help whenever I required them.My deep regards are also due to Dr. C. Venkatesan, Dr. Kunal Ghosh and Dr. V. K. Gupta for the courses they have taught me which greatly enhanced my knowledge in Aerospace Engineering.

Words are not enough to express my appreciation and gratitude for the unbounded love and affection from my parents and brother.I will never be able to make up for the hardship my parents had to undertake to bring me here. I am also indebted to dola for her love and encouragement.

I will also cherish the memory of my friends mjyoti,mrinal,sudip, debasish,saumyadip ,liton,anirban,suman,tirtha,arpan,rameshwar,shankar,ishaq and palash for making my stay at IIT Kanpur the most pleasant one.My seniors amit and mohite helped me in many ways.A note of thanks is also due to Mr. Alok Gupta for his help regarding software problems which I faced during my thesis work.And last but not the least, atul, your cheering attitude will always be a pleasant memory for me.

IIT Kanpur — Arindam Chakraborty

February, 2003

ABSTRACT

Response of composite laminates under in-plane compressive loading is of interest to the analysts and designers.Since they are generally thin, they are prone to instability under inplane loads.One aspect which distinguishes composite materials from isotropic materials is the shear strength of the materials used.In the case of isotropic materials elastic modulus(E) is generally about 2.5-2.8 times shear modulus(G), for composite materials since E is independent of G it can have any value.Hence the transverse shear effect becomes important for predicting the response of even moderately thick composite laminates.For very thick laminates neglecting transverse shear will lead to completely erroneous results.A number of different theories have been suggested by different investigators which take into account of this transverse shear effect.

In the present study an attempt has been made to take into account the effect of transverse shear for the stability analysis of moderately thick/very thick composite laminated plates under in-plane compressive and shear loading using a "**Simple Higher Order Shear Deformation Theory**"based on **four unknown displacement functions** instead of five which is commonly used for most of the other higher order theories.The finite element method is employed to study the initial buckling load of square/rectangular laminates.A $\mathbf{C^1}$ **continuous shear flexible** finite element based on the proposed HSDT is developed using the **Hermite cubic rectangular element**.The plate geometry has been modeled using **linear Lagrange rectangular element** and hence a **Subparametric** formulation has been adopted.

The analytically obtained results using the present formulation have been compared with the results obtained employing different shear diformation theories.The change in initial buckling response of thick rectangular laminated plates with respect to the orientation angle has been studied.The interaction curves (between $\mathbf{N_x}$ and $\mathbf{N_y}$ and between $\mathbf{N_x}$ and $\mathbf{N_{xy}}$ for different aspect ratios) are studied in details.Several new results have been presented for different parameters like, aspect ratio, fibre orientation angle, a/h ratio, etc.

Contents

List of Figures

List of Tables

LIST OF SYMBOLS

X, Y, Z	Caretsian coordinates
a, b, h	Length,width and thickness of the laminated plate
a/b	Aspect ratio of laminate
a/h	Length/thickness ratio of laminate
θ	Lamina orientation angle
NL	Number of layers
z_k	Thickness of k^{th} lamina
u, v, w	Displacements along X, Y and Z directions respectively
w_b, w_s	Components of transverse displacement w
$\{\delta\}$	Generalized displacement vector
$\{\bar{\delta}\}$	Element nodal displacement vector
$[Q_k]$	2 D - stiffness matrix for k^{th} lamina
$[\bar{Q}_k]$	Transformed stiffness matrix for k^{th} lamina
N_x, N_y, N_{xy}	In-plane stress resultants
M_x, M_y, M_{xy}	Stress couples
P_x, P_y, P_{xy}	Higher order stress couples
Q_x, Q_y	Transverse shear forces in the laminate
$[A_{ij}]$	Extensional stiffness matrix
$[B_{ij}]$	Bending-extensional coupling matrix
$[D_{ij}]$	Bending stiffness matrix
$[E_{ij}]$	Higher order stiffness matrix
$[F_{ij}]$	Higher order stiffness matrix
$[G_{lm}]$	Transverse shear rigidity matrix
$[H_{ij}]$	Higher order stiffness matrix
$[D_r]$	Overall stiffness matrix
$\{\epsilon_0\}$	Mid-surface strains
$\{\kappa_0\}$	Mid-surface bending and twisting curvatures
$\{\kappa_l\}$	Higher order terms
$\{\gamma\}$	Transverse shear slope
N_i	Element shape functions in global co-ordinates

N_i'	Element shape functions in local co-ordinates
$\hat{N}_i'$	Element shape functions in natural co-ordinates
$\bar{a}, \bar{b}$	Length and width of rectangular element in local co-ordinate
Π	Total potential
U	Internal strain energy
T	Work done due to inplane loads
$[\bar{K}]$	Overall stiffness matrix
$[K]$	Elastic stiffness matrix
$[K_g]$	Geometric stiffness matrix
λ_{min}	Scaled initial buckling load
$\bar{N}_x, \bar{N}_y, \bar{N}_{xy}$	Nondimensionalized initial buckling loads

Chapter 1

INTRODUCTION

1.1 COMPOSITE MATERIALS

Composites can be broadly defined at a macroscopic scale as a combination of two or more materials in which the materials remain in seperate phases and they donot interact chemically.Common materials which can be included in this broad definition include reinforced concrete, fibre reinforced plastic, plywood, etc.Among the two phases one is a binder or matrix and the other is a reinforcement.The composite material discussed in the present work belongs to this category.

A combination of dissimilar materials can have unique and very advantageous properties if the materials have appropriate characteristics.It may result in better properties than either of the materials alone.For instance, the FRP pipe will be stronger aginst other traditional pipe materials such as all plastic PVC pipe.By forming a composite material one can improve a number of structural and behavioural properties such as specific strength, specific stiffness, fatigue life, hygro-thermal behaviour, corrossion resistance, wear resistance, etc.

Broadly, composites can be classifed into two types:

a) Particle-reinforced composites

b) Fibre-reinforced composites.

In the present investigation **laminated continuous fibre reinforced compos-**

ite is considered.Some of the commonly used fibre materials are E-glass, S-glass, kevlar, graphite, boron, silica, tungsten, etc.Fibres are used to provide the necessary strength and stiffness to the structure.Matrix materials (Polymers) can be classified into two types depending on their structure and thermal behaviour.These are namely:

1) Thermoplastic Polymers - Soften and melt on heating.Polyethylene, polystyrene, nylon, polyacetals belong to this group.

2) Thermosetting Polymers - Do not soften but decompose on heating. Once solidified by a crosslinking (curing) process, they cannot be reshaped.Common examples of this kind include epoxides, polyesters, phenolics, silicone, etc.

The main advantages of polymeric matrix are low cost, easy processibility, good chemical resistance and low specific gravity.

Composite offers unique opportunities in design.Apart from being lighter it is a good substitute for conventional metallic materials.The structural performance offered by it is far versatile than can be realised with conventional materials.An in-depth understanding of the principles governing their structural behaviour can help us explore this versatility to maximum possible extent.

1.2 MOTIVATION

As mentioned above the key factor in utilising the underlying strength and uniqueness of composite materials is the proper understanding of its structural response under different working load conditions.One structural component which is being extensively used in aerospace, automobile and other applications is laminated composite plates.Earlier, classical lamination theory which is an extension of the classical plate theory was used to analyse laminated composite plate.Unfortunately this theory though simple, completely ignores the transverse shear effect which has significant effect on the structural behaviour of laminated plate.The reason behind this is the very high ratio of effective elastic moduli along the fibre direction to effective shear moduli which can be achieved in case of composite materials as the shear

moduli can be varied independent of elastic moduli though the same is not the case for isotropic materials.This when coupled with thickness effect makes classical laminate theory unusable for the analysis of even moderately thick composite laminated plates.

One behavioural aspect of composite laminated plates which is vital for its safe design is the initiation of buckling under the action of in-plane compressive and shear loads.The load at which an initially flat configuration of the plate under the action of in-plane forces suddenly changes to a bent configuration is known as initial buckling load.As the structure undergoes form failure at this point it is imperative that a considerable amount of attention must be paid to find its initial buckling load.The exact determination of this load governs the safe designing of plate structures.

So, for a better estimation of the initial buckling of composite laminated plates, many theories have been proposed over the years which includes the effect of transverse shear deformation.The first order shear deformaion theory (FSDT) includes shear correction factor in their formulation, the exact evaluation of which is very difficult as the shear correction factor depends on the geometry and Poisson ratio.The higher order theories (HSDT) which take into account the parabolic variation of transverse shear stresses, normally involves five unknown displacement functions and requires C^0 continuous element for a finite element analysis.This requires numerical strategies such as reduced/selective integration to avoid shear locking effect (see [1]).A higher order theory proposed by Lim et al. [2] involves only four unknown displacement functions which allows C^1 continuous plate bending element and therefore doesnot necessitate numerical strategies to avoid shear locking effect.Also as this theory involves lesser number of unknowns it is expected to be computationally more effective than the other theories which involve more (five) unknowns.

1.3 LITERATURE SURVEY

Over three decades analysis of laminated composite plates is under intensive investigation.Some of the studies ([3] and [4]) have shown that the transverse shear effect

is quite significant in the layered composite plates due to high ratio of inplane elastic modulus to transverse shear modulus which made classical laminate theory unusable for analysis.To overcome this difficulty a modified bending theory was formulated which accounts for the transverse shear deformation in isotropic plates. This plate bending theory is known as Reissner/Mindlin plate bending theory ([5] and [6]).This theory was applied for anisotropic plates by Whitney and Pagano (see [3] and [4]).In this theory the transverse shear strains are constant throughout the thickness of the plate.A shear correction factor has to be introduced to account for the discrepency between the theory and the actual behaviour.Though this theory gives better results than classical laminate theory, however, gives erroneous results when the plate thickness to side ratio increases.Thus to account for a better representation of shear distribution across the thickness, Reddy [7] proposed a higher order theory.Reddy and his co-researchers studied the initial buckling of laminated composite plates using this higher order shear deformation theory ([8] and [9]).A simplified higher order theory proposed by Lim et al. [2] involves only four unknowns instead of five for Reddy [7].The simplified theory allows to use C^1 continuous plate bending element which is free from any shear locking effect.Gajbir Singh [10] used this model for the response of laminated composite beams and plates.His work was related to nonlinear bending, vibration and thermal postbuckling of composite plates.To the best of the author's knowledge no results are available for the initial buckling analysis under uniaxial and biaxial compressive and shear inplane loading in the published literature using this simple higher order shear deformation theory.

1.4 PRESENT INVESTIGATION

In the present investigation the following studies have been made:

1. Initial buckling behaviour of laminated composite plate under in-plane compressive loading using the simple higher order shear deformation theory as mentioned in section 1.3 and compare the results of other investigators using other higher order theories.

2. The effect of various parameters like, plate aspect ratio, length to thickness

ratio and lamination angle on the initial buckling load of laminates.

3. Development of interaction curves for biaxial loading (N_x and N_y, N_x and $+N_{xy}$, N_x and $-N_{xy}$) of symmetric laminate for different aspect ratio, length to thickness ratio and lamination angles. This will help in the design of laminates subjected to combined loads.

1.5 LAYOUT OF THESIS

The organisation of the thesis is given as:

1. The **first chapter** is devoted to the motivation for present study, the literature review and the goals pertinent to the present study and the layout of the thesis.

2. The **second chapter** is devoted to the discussion of the plate model and laminate constitutive equations.

3. The **third chapter** deals with the finite element formulation of the problem using energy principle.

4. In the **fourth chapter**, first the validation of the present model is presented and afterwards various numerical results are furnished to detail the present investigation and inferences on them are drawn.

5. Concluding remarks and observations from this study along with some suggestions for further extensions of the work are given in **Chapter five**.

Chapter 2

HIGHER ORDER PLATE THEORY

2.1 INTRODUCTION

In this chapter, details of a plate theory proposed by Lim et al. [2] for isotropic plate is discussed and extended to laminated composite plate.The displacement field includes classical plate theory and first order shear deformation theory as its subset and accounts for the parabolic variation of the transverse shear strains which also accounts for the surface boundary condition of zero transverse shear stresses (and hence shear strains) at the top end bottom surfaces of the plate.

The displacement field presented by Reddy [7] is modified by reducing the number of variables to four (five, in case of Reddy's theory).This simplification is based on the assumption that in-plane rotation tensor is constant through the thickness and the transverse displacement can be seperated into two components in such a way that the transverse shear strains are functions of only one of these components.

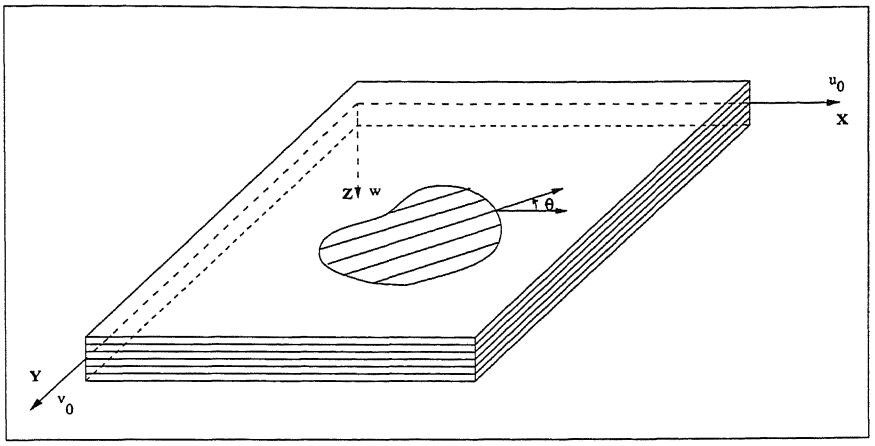

Figure 2.1: **Laminated plate with orientation of global co-ordinates**

2.2 FORMULATION OF DISPLACEMENT FIELD

The displacement field is expressed as:

$$\{V(x,y,z)\} = [\, u(x,y,z),\ v(x,y,z),\ w(x,y,z)\,]^T\ .$$

where $u(x,y,z)$, $v(x,y,z)$ and $w(x,y,z)$ are:

$$\begin{aligned} u(x,y,z) &= u_0(x,y) - z w_{b,x}(x,y) + z^2\phi_x(x,y) + z^3\psi_x(x,y); \\ v(x,y,z) &= v_0(x,y) - z w_{b,y}(x,y) + z^2\phi_y(x,y) + z^3\psi_y(x,y); \\ w(x,y,z) &= w_b(x,y) + w_s(x,y) \end{aligned} \tag{2.1}$$

The transverse displacement component w_b is such that its derivatives are numerically equal to the rotation of the cross-section (i.e. $\phi = -\bigtriangledown w_b$) and w_s is the displacement due to the effect of transverse shear deformation of the cross-section.The assumption that w_b and w_s are functions of x and y only is justified, since the transverse normal stress is of the order of $(h/a)^2$ times the in-plane normal stress.

The von-Karman type non-linear strain-displacement relationships for the higher order theory under consideration can be written as follows:

$$\begin{aligned}
\epsilon_{xx} &= u_{0,x} + \tfrac{1}{2}\,(w_{b,x} + w_{s,x})^2 - z\,w_{b,xx} + z^2\,\phi_{x,x} + z^3\,\psi_{x,x};\\
\epsilon_{yy} &= v_{0,y} + \tfrac{1}{2}\,(w_{b,y} + w_{s,y})^2 - z\,w_{b,yy} + z^2\,\phi_{y,y} + z^3\,\psi_{y,y};\\
\epsilon_{zz} &= 0;\\
\gamma_{xy} &= u_{0,y} + v_{0,x} + (w_{b,x} + w_{s,x})(w_{b,y} + w_{s,y}) - 2\,z\,w_{b,xy}\\
&\quad + z^2\,(\phi_{y,x} + \phi_{x,y}) + z^3\,(\psi_{y,x} + \psi_{x,y});\\
\gamma_{xz} &= w_{s,x} + 2\,z\,\phi_x + 3\,z^2\,\psi_x;\\
\gamma_{yz} &= w_{s,y} + 2\,z\,\phi_y + 3\,z^2\,\psi_y
\end{aligned} \tag{2.2}$$

where comma (,) denotes the partial derivatives.

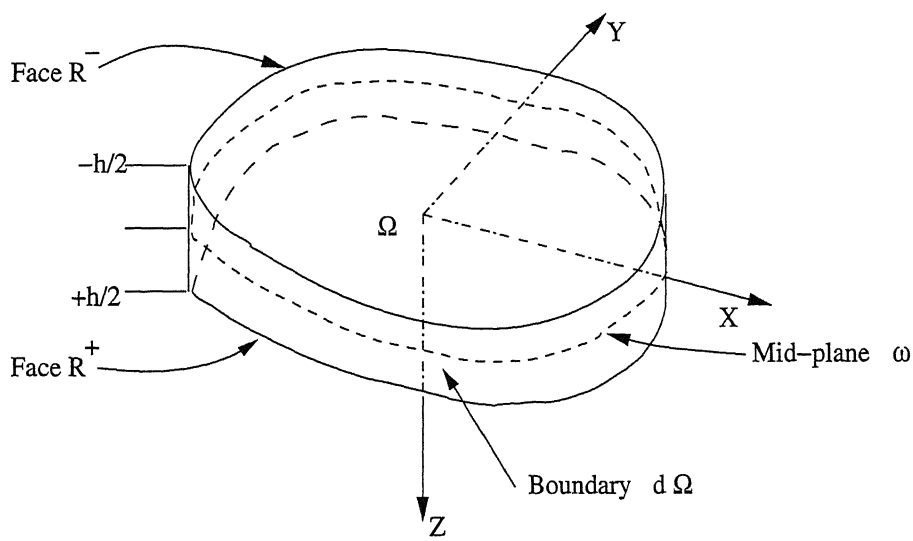

Figure 2.2: **Representation of arbitrary three dimensional domain**

The surface boundary condition that the transverse shear stresses vanish on the plate's top and bottom faces (see Fig. 2.2) is equivalent to the requirement that the corresponding strains be zero on these surfaces, i.e.

$$\gamma_{xz}(x, y, \pm\tfrac{h}{2}) = \gamma_{yz}(x, y, \pm\tfrac{h}{2}) = 0$$

On introduction of the conditions as given above in the expressions for transverse shear strains (from Eq. 2.2), the following relations are obtained.

$$\begin{aligned}
&\phi_x = \phi_y = 0 \qquad \text{and}\\
&\psi_x = -\tfrac{4}{3h^2}\,w_{s,x}\;; \quad \psi_y = -\tfrac{4}{3h^2}\,w_{s,y}
\end{aligned} \tag{2.3}$$

The displacement field of Eq. (2.1) is modified by setting ϕ_x and ϕ_y to be zero according to conditions of Eq. (2.3). The resulting displacement field is written below:

$$\begin{aligned} u(x,y,z) &= u_0(x,y) - z\, w_{b,x}(x,y) - \tfrac{4z^3}{3h^2}\, w_{s,x}(x,y); \\ v(x,y,z) &= v_0(x,y) - z\, w_{b,y}(x,y) - \tfrac{4z^3}{3h^2}\, w_{s,y}(x,y); \\ w(x,y,z) &= w_b(x,y) + w_s(x,y) \end{aligned} \tag{2.4}$$

In Eq. (2.4) u, v and w are the displacements along x, y and z directions respectively. u_0, v_0 and w (w_b and w_s) are the mid-plane displacements.Thus, the generalised displacement vector $\{\delta\}$ of the mid-surface contains four degrees of freedom (DOF) and is given by:

$$\{\delta\} = \{u_0, v_0, w_b, w_s\}^T.$$

The corresponding strain-displacement relationships are:

$$\begin{aligned} \epsilon_{xx} &= u_{0,x} + \tfrac{1}{2}\,(w_{b,x} + w_{s,x})^2 - z\, w_{b,xx} - \tfrac{4z^3}{3h^2}\, w_{s,xx}; \\ \epsilon_{yy} &= v_{0,y} + \tfrac{1}{2}\,(w_{b,y} + w_{s,y})^2 - z\, w_{b,yy} - \tfrac{4z^3}{3h^2}\, w_{s,yy}; \\ \epsilon_{zz} &= 0; \\ \gamma_{xy} &= u_{0,y} + v_{0,x} + (w_{b,x} + w_{s,x})(w_{b,y} + w_{s,y}) - 2\, z\, w_{b,xy} \\ &\quad - \tfrac{8z^3}{3h^2}\, w_{s,xy}; \\ \gamma_{xz} &= (1 - \tfrac{4z^2}{h^2})\, w_{s,x}; \\ \gamma_{yz} &= (1 - \tfrac{4z^2}{h^2})\, w_{s,y} \end{aligned} \tag{2.5}$$

It can be noted that these kinematics can be obtained by substituting $\psi_x = -w_{b,x}$, $\psi_y = -w_{b,y}$ and $w = w_b + w_s$ in Reddy's [7] higher order theory involving five unknowns $(u_0, v_0, w_0, \psi_x, \psi_y)$.

It can also be shown that the present formulation degenerates to first order shear deformation theory by suitably dropping higher order terms and incorporating appropriate shear correction factors (for isotropic plate whose value is 5/6).The classical laminate theory (CLT) can be derived from the present theory by equating w_s to zero.

The strain-displacement relationships given in Eq. (2.5) can be rewritten as:

$$\begin{aligned}
\epsilon_{xx} &= \epsilon_{0x} + z\,\kappa_{0x} + z^3\,\kappa_{lx};\\
\epsilon_{yy} &= \epsilon_{0y} + z\,\kappa_{0y} + z^3\,\kappa_{ly};\\
\epsilon_{zz} &= 0;\\
\gamma_{xy} &= \gamma_{0xy} + z\,\kappa_{0xy} + z^3\,\kappa_{lxy};\\
\gamma_{xz} &= (1 - \tfrac{4z^2}{h^2})\,w_{s,x};\\
\gamma_{yz} &= (1 - \tfrac{4z^2}{h^2})\,w_{s,y}
\end{aligned} \tag{2.6}$$

where:

$$\begin{aligned}
\epsilon_{0x} &= u_{0,x} + \tfrac{1}{2}\,(w_{b,x} + w_{s,x})^2;\\
\epsilon_{0y} &= v_{0,y} + \tfrac{1}{2}\,(w_{b,y} + w_{s,y})^2;\\
\gamma_{0xy} &= u_{0,y} + v_{0,x} + (w_{b,x} + w_{s,x})(w_{b,y} + w_{s,y});\\
\kappa_{0x} &= -w_{b,xx}; \quad \kappa_{0y} = -w_{b,yy}; \quad \kappa_{0xy} = -2w_{b,xy};\\
\kappa_{lx} &= -\tfrac{4}{3h^2}\,w_{s,xx}; \quad \kappa_{ly} = -\tfrac{4}{3h^2}\,w_{s,yy}; \quad \kappa_{lxy} = -\tfrac{8}{3h^2}\,w_{s,xy}
\end{aligned}$$

2.3 LAMINATE CONSTITUTIVE EQUATIONS

A lamina (considered a unidirectional composite) is characterised by having all fibres (either a single ply or multiple plies) oriented in the same direction.This model allows one to treat the lamina as an orthotropic material whose material symmetry planes are parallel and transverse to the fibre direction.The model used to represent a lamina consists of unidirectional fibres per layer which is further assumed as perfectly straight and uniformly oriented within the lamina.

In the following Fig. (2.3) the material co-ordinate axes L and T are defined parallel and perpendicular to the fibre direction respectively, while global co-ordinates are X, Y and Z. The material co-ordinate axis T' is further assumed to be along Z axis.The angle between global co-ordinate axis X and fibre direction, material co-ordinate axis L, is θ and is known as the orientation angle. As a sign convention anticlockwise angle from $+ve$ X direction is taken as positive.

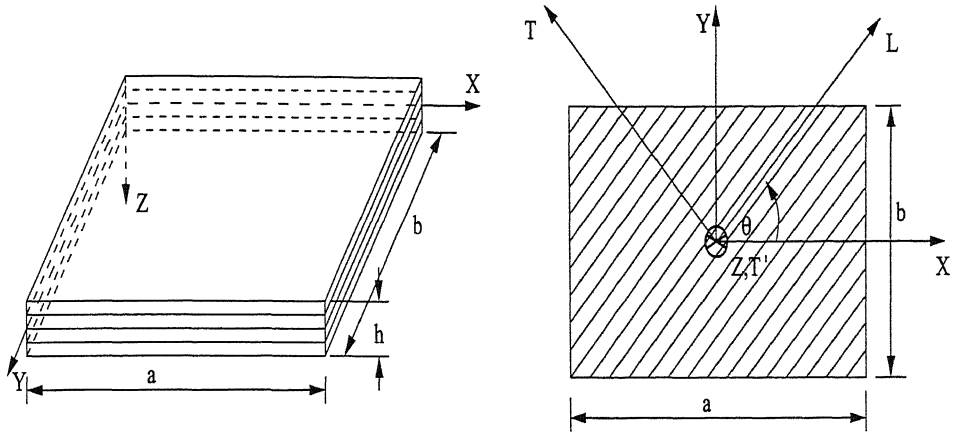

Figure 2.3: **Co-rdinate axes for the lamina**

Generalized Hooke's law

In the derivation of lamina constitutive equations, following two assumptions are made.

1. The lamina is a continuum.
2. It behaves as a linearly elastic material.

Further, at the micro-level the following assumptions are made about the material.

1. Perfect bonding between fibres and matrix exists.
2. Fibres are parallel and uniformly distributed throughout.
3. The matrix is free of voids or micro cracks and initially in a stress free state.
4. Both fibres and matrix are isotropic and obey Hooke's law.

Stress-strain relations for the k^{th} lamina in the material coordinate axes, whose fibres are oriented at an angle θ with reference to the X axis is given as (see [11], [12]):

$$\left\{ \sigma_i \right\}_k = [\, Q_{ij}]_k \left\{ \epsilon_j \right\}_k \tag{2.7}$$

where $\{\sigma_i\}$ is the vector of stress components, $[Q_{ij}]$ is the 2 D - stiffness matrix with respect to material co-ordinate axes, and $\{\epsilon_j\}$ are the engineering strain components, for the k^{th} lamina.

In expanded form, the above relation can be written as:

$$\begin{Bmatrix} \sigma_L \\ \sigma_T \\ \tau_{LT} \\ \tau_{LT'} \\ \tau_{TT'} \end{Bmatrix}_k = \begin{bmatrix} Q_{11} & Q_{12} & 0 & 0 & 0 \\ Q_{21} & Q_{22} & 0 & 0 & 0 \\ 0 & 0 & Q_{66} & 0 & 0 \\ 0 & 0 & 0 & Q_{44} & 0 \\ 0 & 0 & 0 & 0 & Q_{55} \end{bmatrix}_k \begin{Bmatrix} \epsilon_L \\ \epsilon_T \\ \gamma_{LT} \\ \gamma_{LT'} \\ \gamma_{TT'} \end{Bmatrix}_k$$

where:

$$Q_{11} = \frac{E_L}{(1-\nu_{LT}\nu_{TL})}; \qquad Q_{12} = Q_{21} = \frac{E_T\nu_{LT}}{(1-\nu_{LT}\nu_{TL})};$$
$$Q_{22} = \frac{E_T}{(1-\nu_{LT}\nu_{TL})}; \qquad Q_{66} = G_{LT};$$
$$Q_{44} = G_{LT'}; \qquad Q_{55} = G_{TT'}$$

The stresses and strains in the X, Y and Z directions are obtained by transformation of the relations given in equation (2.7). The transformed stress strain relations for the k^{th} lamina are given as:

$$\begin{Bmatrix} \sigma_x \\ \sigma_y \\ \tau_{xy} \\ \tau_{xz} \\ \tau_{yz} \end{Bmatrix}_k = \begin{bmatrix} \bar{Q}_{11} & \bar{Q}_{12} & \bar{Q}_{16} & 0 & 0 \\ \bar{Q}_{12} & \bar{Q}_{22} & \bar{Q}_{26} & 0 & 0 \\ \bar{Q}_{16} & \bar{Q}_{26} & \bar{Q}_{66} & 0 & 0 \\ 0 & 0 & 0 & \bar{Q}_{44} & \bar{Q}_{45} \\ 0 & 0 & 0 & \bar{Q}_{45} & \bar{Q}_{55} \end{bmatrix}_k \begin{Bmatrix} \epsilon_x \\ \epsilon_y \\ \gamma_{xy} \\ \gamma_{xz} \\ \gamma_{yz} \end{Bmatrix}_k \tag{2.8}$$

where:

$$\bar{Q}_{11} = Q_{11}c^4 + (2Q_{12} + 4Q_{66})s^2c^2 + Q_{22}s^4;$$
$$\bar{Q}_{12} = Q_{12}(s^4 + c^4) + (Q_{11} + Q_{22} - 4Q_{66})s^2c^2;$$
$$\bar{Q}_{16} = (Q_{11} - Q_{12} - 2Q66)sc^3 + (Q_{12} - Q_{22} + 2Q66)s^3c;$$
$$\bar{Q}_{22} = Q_{11}s^4 + (2Q_{12} + 4Q_{66})s^2c^2 + Q_{22}c^4;$$
$$\bar{Q}_{26} = (Q_{11} - Q_{12} - 2Q66)s^3c + (Q_{12} - Q_{22} + 2Q66)sc^3;$$
$$\bar{Q}_{66} = (Q_{11} - 2Q_{12} + Q_{22} - 2Q66)s^2c^2 + Q_{66}(c^4 + s^4);$$
$$\bar{Q}_{44} = Q_{44}c^2 + Q_{55}s^2;$$
$$\bar{Q}_{45} = (Q_{44} - Q_{55})cs;$$
$$\bar{Q}_{55} = Q_{55}c^2 + Q_{44}s^2$$

where, $[\bar{Q}_{ij}]$ is the transformed stiffness matrix , $c = Cos(\theta)$ and $s = Sin(\theta)$ with θ denoting the angle of orientation of k^{th} lamina.

Using the above lamina constitutive equations and integrating the stresses over the laminate thickness, the stress resultants in terms of inplane forces, moments, shear forces and higher order stress couples per unit length, for a laminate with NL laminae are,

$$\begin{Bmatrix} \{\mathbf{N_i}\} \\ \{\mathbf{M_i}\} \\ \{\mathbf{P_i}\} \\ \{\mathbf{Q_l}\} \end{Bmatrix} = \begin{bmatrix} [A_{ij}] & [B_{ij}] & [E_{ij}] & [0] \\ [B_{ij}] & [D_{ij}] & [F_{ij}] & [0] \\ [E_{ij}] & [F_{ij}] & [H_{ij}] & [0] \\ [0] & [0] & [0] & [G_{lm}] \end{bmatrix} \begin{Bmatrix} \{\epsilon_{0j}\} \\ \{\kappa_{0j}\} \\ \{\kappa_{lj}\} \\ \{\gamma_m\} \end{Bmatrix} \tag{2.9}$$

$$(\text{i , j} = 1 \text{ , } 2 \text{ and } 6)$$

$$(\text{l , m} = 4 \text{ , } 5)$$

(Detailed expansion of Eq. (2.9) is given in Appendix A.)

Where $\{\epsilon_0\}$ are the mid-surface strains, $\{\kappa_0\}$ are the mid-surface bending and twisting curvatures, $\{\kappa_l\}$ are the higher order terms and $\{\gamma\}$ are the transverse shear slope and

$$\{\mathbf{N_i}\}^{\mathbf{T}} = (N_x, N_y, N_{xy}) = \sum_{k=1}^{NL} \int_{z_k}^{z_{k-1}} (\sigma_x, \sigma_y, \tau_{xy})^k \quad dz; \tag{2.10}$$

$$\{\mathbf{M_i}\}^{\mathbf{T}} = (M_x, M_y, M_{xy}) = \sum_{k=1}^{NL} \int_{z_k}^{z_{k-1}} (\sigma_x, \sigma_y, \tau_{xy})^k \; z \; dz; \tag{2.11}$$

$$\{\mathbf{P_i}\}^{\mathbf{T}} = (P_x, P_y, P_{xy}) = \sum_{k=1}^{NL} \int_{z_k}^{z_{k-1}} (\sigma_x, \sigma_y, \tau_{xy})^k \; z^3 \; dz; \tag{2.12}$$

$$\{\mathbf{Q_l}\}^{\mathbf{T}} = (Q_x, Q_y) = \sum_{k=1}^{NL} \int_{z_k}^{z_{k-1}} (\tau_{xz}, \tau_{yz})^k \quad (1 - \frac{4z^2}{h^2}) \; dz. \tag{2.13}$$

Here, z_i are the z coordinates corresponding to the laminae interfaces as shown in Fig 2.4.

Thus, with the assumed displacement model, the various stiffness matrices derived are:

$[A_{ij}]$ = Extensional; $[B_{ij}]$ = Bending-extensional coupling;

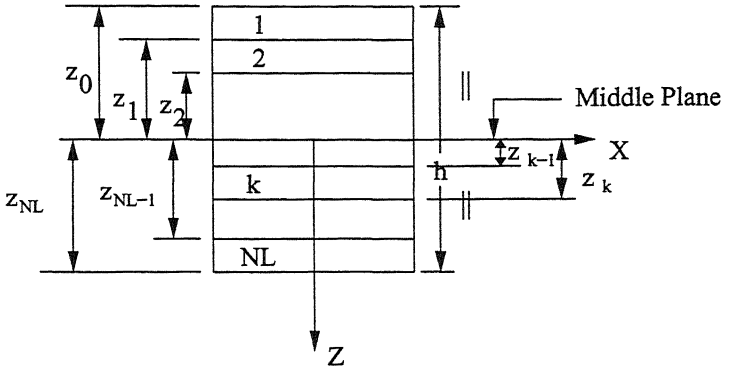

Figure 2.4: **Geometry of multilayered laminate**

$[D_{ij}]$ = Bending; $[G_{lm}]$ = Transverse shear stiffness and

$[E_{ij}]$, $[F_{ij}]$, $[H_{ij}]$ = Higher order stiffnesses.

The set of stiffness matrices $[A_{ij}], [B_{ij}], [D_{ij}]$, $[E_{ij}]$, $[F_{ij}]$, $[H_{ij}]$ and $[G_{lm}]$ are used in forming overall stiffness matrix $[D_r]$ for the laminate.

Chapter 3

FINITE ELEMENT FORMULATION

For the finite element approximation of the problem under investigation rectangular four noded elements are used, along with linear Lagrange interpolation function to model the geometry of the plate.A C^1 continuous shear flexible element based on the presented higher order theory is developed using the Hermite interpolation formulae as indicated by Bogner et al [13]. A typical mesh, generated over the rectangular plate domain is shown in Fig. 3.1. The node (both local and global) and element numbering scheme is also shown in the figure. In what follows the finite element formulation is presented.

3.1 DEFINITIONS

Let $\{V\}$ be the displacement vector defined as:

$$\{V\} = \begin{Bmatrix} u \\ v \\ w \end{Bmatrix} \tag{3.1}$$

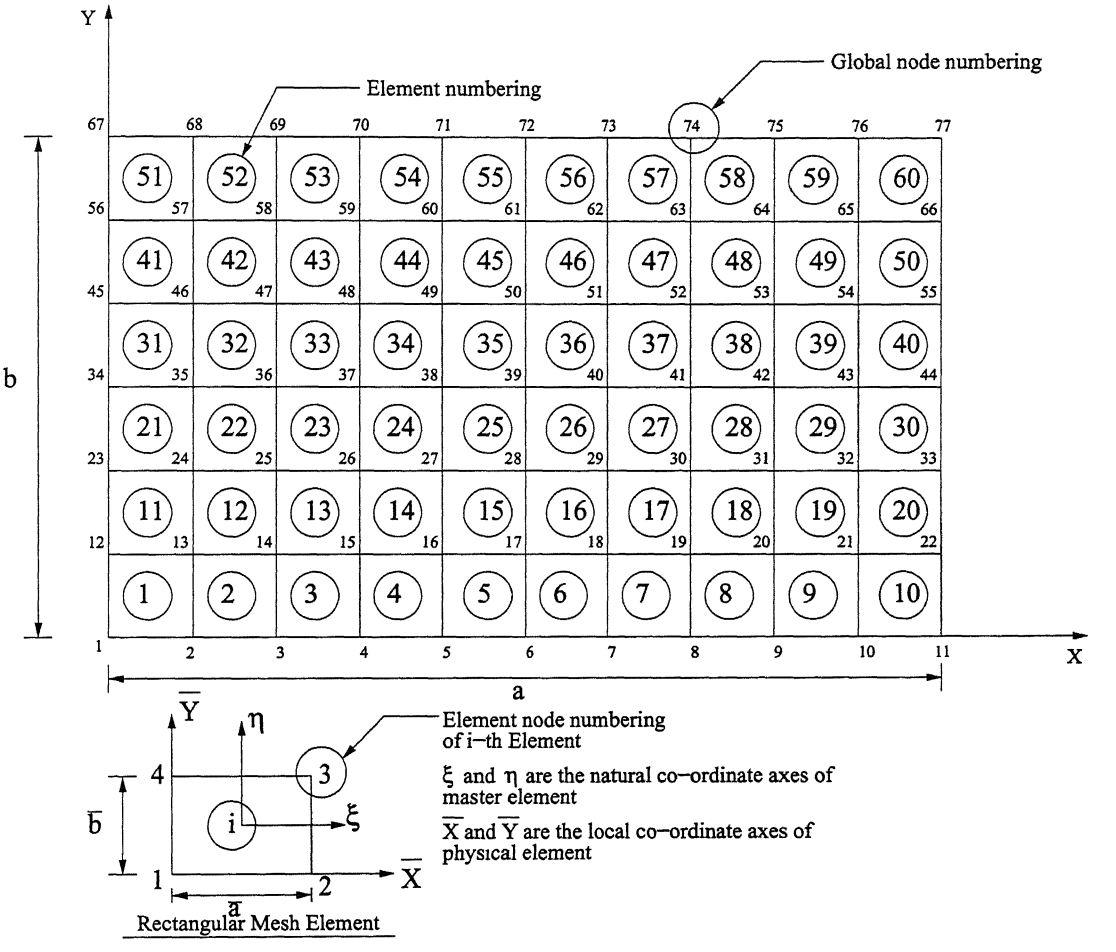

Figure 3.1: **Typical meshing of Rectangular plate domain**

The stress and strain vectors corresponding to $\{V\}$ be $\{\sigma\}$ and $\{\epsilon\}$ can be defined as:

$$\{\sigma\} = \begin{Bmatrix} \sigma_x \\ \sigma_y \\ \tau_{xy} \\ \tau_{xz} \\ \tau_{yz} \end{Bmatrix} \qquad \{\epsilon\} = \begin{Bmatrix} \epsilon_x \\ \epsilon_y \\ \gamma_{xy} \\ \gamma_{xz} \\ \gamma_{yz} \end{Bmatrix} \tag{3.2}$$

From the generalized Hooke's law which relates stress components to the respective strain components in global coordinate system:

$$\{\sigma\} = [\bar{Q}]\ \{\epsilon\} \tag{3.3}$$

The material stiffness matrix $[\bar{Q}]$ for orthotropic material is given in Eq. (2.8) for each lamina.

We are concerned with initial buckling of the laminate.Hence, the non-linear terms in the strain-displacement relationships as described in Eq. (2.5) are neglected for our study because the transverse deflection (both w_b and w_s) is assumed to be very small.

The linear strain-displacement relationships can be written as:

$$\begin{aligned}
\epsilon_{xx} &= u_{0,x} - z\, w_{b,xx} - \tfrac{4z^3}{3h^2}\, w_{s,xx}; \\
\epsilon_{yy} &= v_{0,y} - z\, w_{b,yy} - \tfrac{4z^3}{3h^2}\, w_{s,yy}; \\
\epsilon_{zz} &= 0; \\
\gamma_{xy} &= u_{0,y} + v_{0,x} - 2\, z\, w_{b,xy} \\
&\quad - \tfrac{8z^3}{3h^2}\, w_{s,xy}; \\
\gamma_{xz} &= (1 - \tfrac{4z^2}{h^2})\, w_{s,x}; \\
\gamma_{yz} &= (1 - \tfrac{4z^2}{h^2})\, w_{s,y}
\end{aligned} \tag{3.4}$$

The above relations is expressed in matrix form as:

$$\{\epsilon\} = [\bar{D}]\ \{V\} \tag{3.5}$$

where $[\bar{D}]$ is a differential operator in terms of global coordinates, defined as

$$[\bar{D}] = \begin{bmatrix} \frac{\partial}{\partial x} & 0 & 0 \\ 0 & \frac{\partial}{\partial y} & 0 \\ \frac{\partial}{\partial y} & \frac{\partial}{\partial x} & 0 \\ \frac{\partial}{\partial z} & 0 & \frac{\partial}{\partial x} \\ 0 & \frac{\partial}{\partial z} & \frac{\partial}{\partial y} \end{bmatrix} \tag{3.6}$$

The components of displacement can be expressed in terms of the four unknowns, which can be written as:

$$\{\delta\}^T = \{u_0, v_0, w_b, w_s\}$$

For any element the field variables in terms of shape functions and nodal variables can be written as:

$$\begin{aligned}
u_0(x,y) &= \sum_{i=1}^{4} N_i' \, u_{0i} + \sum_{i=1}^{4} N_{i+4}' \, u_{0,x_i} + \sum_{i=1}^{4} N_{i+8}' \, u_{0,y_i}; \\
v_0(x,y) &= \sum_{i=1}^{4} N_i' \, v_{0i} + \sum_{i=1}^{4} N_{i+4}' \, v_{0,xi} + \sum_{i=1}^{4} N_{i+8}' \, v_{0,y_i}; \\
w_b(x,y) &= \sum_{i=1}^{4} N_i' \, w_{bi} + \sum_{i=1}^{4} N_{i+4}' \, w_{b,xi} + \sum_{i=1}^{4} N_{i+8}' \, w_{b,y_i} + \\
&\quad \sum_{i=1}^{4} N_{i+12}' \, w_{b,xy_i}; \\
w_s(x,y) &= \sum_{i=1}^{4} N_i' \, w_{si} + \sum_{i=1}^{4}{}' \, N_{i+4} \, w_{s,x_i} + \sum_{i=1}^{4} N_{i+8}' \, w_{s,y_i} + \\
&\quad \sum_{i=1}^{4} N_{i+12}' \, w_{s,xy_i}
\end{aligned} \tag{3.7}$$

In the above expression u_{0i}, $u_{0,xi}$, u_{0,y_i}, v_{0i}, v_{0,x_i}, v_{0,y_i}, w_{bi}, $w_{b,xi}$, w_{b,y_i}, w_{b,xy_i}, w_{si}, w_{s,x_i}, w_{s,y_i}, w_{s,xy_i} $(i = 1,4)$ are the fourteen degrees of freedom per node, N_i's are the element shape functions in local co-ordinates (in terms of $\bar{X}$ and $\bar{Y}$ as shown in Fig. 3.2).In natural co-ordinates (in terms of ξ and η as shown in Fig. 3.2) N_i's can be expressed as $\hat{N}_i'$s (see [1]).The details of the element shape functions (both N_i' and $\hat{N}_i'$) are given in Appendix B.

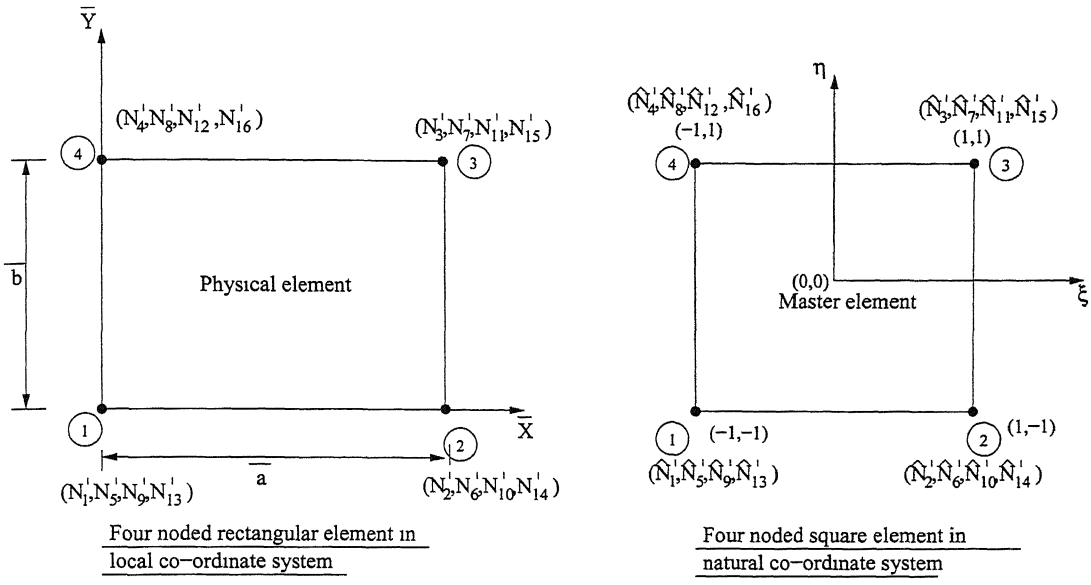

Figure 3.2: **Four noded rectangular element**

Substituting Eq. (3.7) in the strain-displacement relations given in Eqn. (3.4) the following relations can be established:

$$\left\{\begin{array}{c} \epsilon_{0x} \\ \epsilon_{0y} \\ \gamma_{0xy} \\ \kappa_{0x} \\ \kappa_{0y} \\ \kappa_{0xy} \\ \kappa_{lx} \\ \kappa_{ly} \\ \kappa_{lxy} \\ w_{s,x} \\ w_{s,y} \end{array}\right\}_{11\times1} = [B_0]_{11\times56}\,\{\bar{\delta}\}_{56\times1} \tag{3.8}$$

where:

$$\{\bar{\delta}\}^T = \{\ u_{0i},\ u_{0,x_i},\ u_{0,y_i},\ v_{0i},\ v_{0,x_i},\ v_{0,y_i},\ w_{bi},\ w_{b,x_i},\ w_{b,y_i},\ w_{b,xy_i},\ w_{si},\ w_{s,x_i},\ w_{s,y_i},$$
$$w_{s,xy_i}\},\ (i = 1,...,4)$$

and:

$$\epsilon_{0x} = u_{0,x}; \quad \epsilon_{0y} = v_{0,y}; \quad \gamma_{0xy} = u_{0,y} + v_{0,x};$$
$$\kappa_{0x} = -w_{b,xx}; \quad \kappa_{0y} = -w_{b,yy}; \quad \kappa_{0xy} = -2w_{b,xy};$$
$$\kappa_{lx} = -\tfrac{4}{3h^2}\, w_{s,xx}; \quad \kappa_{ly} = -\tfrac{4}{3h^2}\, w_{s,yy}; \quad \kappa_{lxy} = -\tfrac{8}{3h^2}\, w_{s,xy}$$

The details of $[B_0]$ are given in Appendix C.

3.2 FINITE ELEMENT FORMULATION USING ENERGY PRINCIPLE

The total potential for the plate is given by

$$\Pi\left(\delta\right) = \sum_{e=1}^{N} \pi^e\left(\delta\right), \tag{3.9}$$

where π^e is the total potential of the non-intersecting (but adjacent) sub-domains e which are part of the domain (N sub-domains are considered here). The total potential can be expressed in terms of internal strain energy $U^{(e)}$, external work done due to transverse loads $W^{(e)}$ and work done due to inplane forces $T^{(e)}$, as follows:

$$\pi^e\left(\delta\right) = U^{(e)} - W^{(e)} - T^{(e)} \tag{3.10}$$

Strain energy of the laminate can expressed as follows:

$$U^{(e)} = \frac{1}{2}\int_{V^{(e)}} \{\epsilon\}^T\, [\sigma]\, dV^{(e)} \tag{3.11}$$

Work done by the applied external transverse load is,

$$\begin{aligned} W^{(e)} &= \textstyle\int_{A^{(e)}} \{V\}_{z=\pm\frac{h}{2}}^T\, f\, dA^{(e)} \\ &= \textstyle\int_{R^{+(e)}} w\, f^+\, dA^{(e)} + \int_{R^{-(e)}} w\, f^-\, dA^{(e)} \end{aligned} \tag{3.12}$$

where f^+ is the transverse load on the top face R^+ and f^- is the transverse load on the top face R^- and $w = w_b + w_s$.

For initial buckling problem we can assume that the plate, which is stressed by forces acting in the middle plane of the plate (i.e. N_x, N_y and N_{xy}), undergoes some small lateral bending consistent with the given boundary conditions and in-plane forces remain constant during bending.Such limited bending can be produced

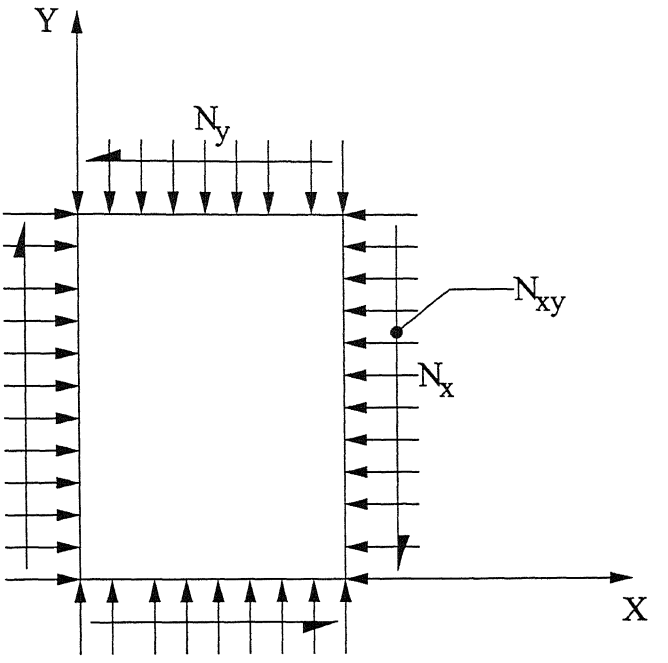

Figure 3.3: **The orientation of negative in-plane forces**

without stretching of the middle plane.Hence the work done by the applied in-plane loads (considered negative in sense) can be expressed as follows:

$$T^{(e)} = \frac{1}{2}\int_{A^{(e)}} [N_x\, w_{,x}^2 + N_x\, w_{,y}^2 + 2\, N_{xy}\, w_{,x} w_{,y}]\, dA \tag{3.13}$$

Where the directions of the inplane forces are as shown in Fig 3.3 . It can also be noted here that in case of initial buckling problem the applied external transverse load is kept zero (i.e. $W^{(e)} = 0$).

The exact solution $\{V_{ex}\}$ to this problem is the minimizer of the total potential Π. This can be obtained as:

$$\delta^{(1)}\, \Pi = 0 \tag{3.14}$$

which is also the *Virtual Work Formulation* of the problem in terms of the components of δ(and hence $\bar{\delta}$). This leads to the generalised finite element formulation which can be expressed as:

$$[\bar{K}]\, \{\bar{\delta}\} = \{F\} \tag{3.15}$$

Where $[\bar{K}]$ is the global stiffness matrix which is composed of two components (i.e. global elastic stiffness matrix $[K]$ and global geometric stiffness matrix $[K_g]$) and $\{F\}$ is the global load vector which is zero in our case as $W^{(e)} = 0$.

Hence Eqn. (3.15) can be rewritten as:

$$\Big[\,[K] - [K_g]\,\Big]\,\{\bar{\delta}\} = 0 \tag{3.16}$$

In the following sections, we are going to employ the virtual work formulation to derive the finite element equations governing the initial buckling problem.

3.3 COMPUTATION OF ELEMENT ELASTIC STIFFNESS MATRIX

The elastic stiffness matrix corresponding to assumed deformation state of an element can be defined by expressing the internal strain energy in terms of unknown nodal displacements. In the formulation of unsymmetric laminates the membrane, the flexure, membrane-flexure coupling and shear strains contribute to strain energy.

From Eqn. (2.9 - 2.13) and Eqn. 3.11 the internal starin energy of an element (given by area A^e) can be expressed as:

$$U^e = \frac{1}{2}\int_{A^{(e)}} (\, N_x\,\epsilon_{0x} + N_y\,\epsilon_{0y} + N_{xy}\,\epsilon_{0xy} + M_x\,\kappa_{0x} + M_y\,\kappa_{0y} + M_{xy}\,\kappa_{0xy} + P_x\,\kappa_{lx} + P_y\,\kappa_{ly} + P_{xy}\,\kappa_{lxy} + Q_x\,w_{s,x} + Q_y\,w_{s,y}\,)dA \tag{3.17}$$

The Eq. (3.8) along with Eq. (2.9) can be used to express the internal strain energy as:

$$U^e = \frac{1}{2}\int_{A^{(e)}} (\,\{\bar{\delta}^e\}^T\,[{B_0}^T]\,[D_r]\,[B_0]\,\{\bar{\delta}^e\}\,)\,dA \tag{3.18}$$

The strain energy expression can be written in a concise form as:

$$U^{(e)} = \frac{1}{2}\,\{\bar{\delta}^e\}^T\,[K^e]\,\{\bar{\delta}^e\} \tag{3.19}$$

where $[K^e]$ is the elastic stiffness matrix and $\{\bar{\delta}^e\}$ are the unknown displacements corresponding to the finite element solution in an element e.

$[K^e]$ is given by:

$$[K^e] = \int_{A^{(e)}} [B_0]^T [D_r] [B_0] \, dA \tag{3.20}$$

Numerical integration is carried out to get the element elastic stiffness matrix.

3.4 COMPUTATION OF ELEMENT GEOMETRIC STIFFNESS MATRIX

The total work done by in-plane applied loads in an element can be expressed as:

$$T^e = \frac{1}{2} \int_{A^{(e)}} (\{\bar{\delta}^e\}^T [{B_g}^T] [N] [B_g] \{\bar{\delta}^e\}) \, dA \tag{3.21}$$

This can be written in a concise form as:

$$T^{(e)} = \frac{1}{2} \{\bar{\delta}^e\}^T [K_g^e] \{\bar{\delta}^e\} \tag{3.22}$$

The details of $[B_g]$ are given in Appendix C.

whereas:

$$[N] = \begin{bmatrix} N_x & N_{xy} \\ N_{xy} & N_y \end{bmatrix}$$

Assuming that forces N_x, N_y and N_{xy} are represented by certain expression with a common factor λ, so that

$$N_x = \lambda \hat{N}_x, \quad N_y = \lambda \hat{N}_y, \text{ and } N_{xy} = \lambda \hat{N}_{xy}$$

then:

$$[N] = \lambda \begin{bmatrix} \hat{N}_x & \hat{N}_{xy} \\ \hat{N}_{xy} & \hat{N}_y \end{bmatrix}$$

or:

$$[N] = \lambda [\bar{N}]$$

where:

$$[\bar{N}] = \begin{bmatrix} \hat{N}_x & \hat{N}_{xy} \\ \hat{N}_{xy} & \hat{N}_y \end{bmatrix}$$

$[K_g^e]$ is the geometric stiffness matrix and $\{\bar{\delta}^e\}$ are the unknown displacements corresponding to the finite element solution in an element e.

$[K_g^e]$ is given by:

$$\begin{aligned} [K_g^e] &= \lambda \int_{A^{(e)}} [B_g]^T \, [\bar{N}] \, [B_g] \, dA; \\ \text{Or } [K_g^e] &= \lambda \, [\bar{K}_g^e] \end{aligned} \tag{3.23}$$

Numerical integration is carried out to get the element geometric stiffness matrix.

3.5 METHODOLOGY FOR FINDING INITIAL BUCKLING LOAD

In the present analysis the goal is to find the initial buckling load for laminated composite plate under different conditions of loading (uniaxial or biaxial) with different boundary conditions, plate aspect ratios, plate thickness ratios, fibre orientation angles, etc.

This is an eigenvalue type of problem which is described below.

From Eqns. (3.16), (3.20) and (3.23) we get the final FEM equation as follows:

$$\left[[K] - \lambda[\bar{K}_g] \right] \{\bar{\delta}\} = 0 \tag{3.24}$$

The characteristic equation of the above eigenvalue problem can be expressed as:

$$\left| [K] - \lambda[\bar{K}_g] \right| = 0 \tag{3.25}$$

Eqn. (3.25) is solved using NAG ROUTINES to obtain the eigenvalues λ_i (i = 1,M) where M is the dimension of the matrices $[K]$ and $[\bar{K}_g]$ (and is equal to the total degrees of freedom in the analysis set of the problem).The minimum value of

λ corresponds to the scaled initial buckling load from which we can get the initial buckling load as follows:

$$N_x \text{ (or } N_y \text{ or } N_{xy} \text{)} = \lambda_{min} \hat{N}_x \text{ (or } \hat{N}_y \text{ or } \hat{N}_{xy} \text{)}$$

The corresponding eigenvector (which is also found using NAG ROUTINES) gives the mode shape (not the exact displacements) corresponding to the initial buckling load.

3.6 GEOMETRIC APPROXIMATION

3.6.1 LINEAR MAPPING OF STRAIGHT EDGE RECTANGULAR ELEMENTS

As mentioned earlier, the plate domain is divided into a number of straight edge rectangular elements. For the aforementioned geometry the geometric transformation from physical element to the master element can be done by linear mapping which is discussed below.

LINEAR MAPPING:

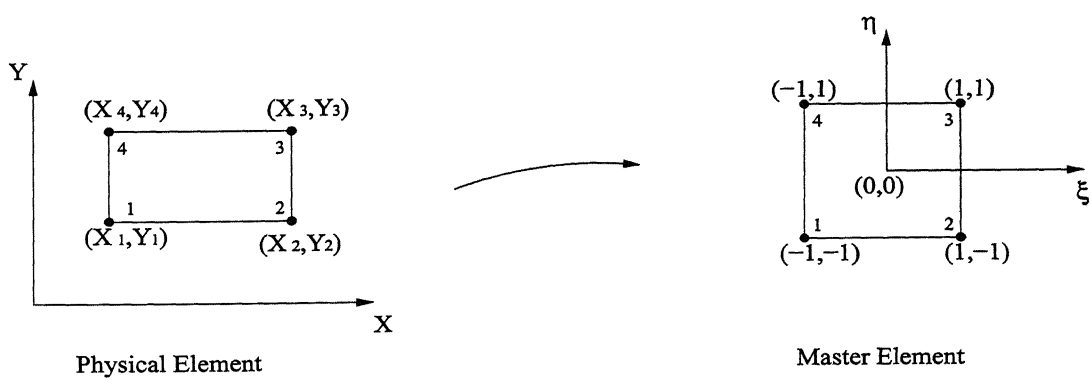

Figure 3.4: **Linear mapping in two dimensional domain**

The transformation between (X, Y) co-ordinates and (ξ, η) co-ordinates is accomplished by the following co-ordinate transformation:

$$\begin{aligned} x(\xi,\eta) &= \sum_{j=1}^{4} X_j^e \, \hat{\psi}_j^e; \\ y(\xi,\eta) &= \sum_{j=1}^{4} Y_j^e \, \hat{\psi}_j^e \end{aligned} \tag{3.26}$$

Where X_j^e and Y_j^e are the global co-ordinates of the physical element nodes and $\hat{\psi}_j^e$ denote the finite element interpolation functions of the master element.In the present study bilinear Lagrange interpolation functions are employed.

$\hat{\psi}_j^e$ are defined in the following way:

$$\begin{aligned} \hat{\psi}_1^e &= \frac{1}{4}(1-\xi)\,(1-\eta)\,; \\ \hat{\psi}_2^e &= \frac{1}{4}(1+\xi)\,(1-\eta)\,; \\ \hat{\psi}_3^e &= \frac{1}{4}(1+\xi)\,(1+\eta)\,; \\ \hat{\psi}_4^e &= \frac{1}{4}(1-\xi)\,(1+\eta) \end{aligned} \tag{3.27}$$

It is obvious from the above relations that:

$$\begin{aligned} \frac{\partial x}{\partial \xi} &= \frac{1}{4}\left[-X_1\,(1-\eta) + X_2\,(1-\eta) + X_3\,(1+\eta) - X_4\,(1+\eta)\right]; \\ \frac{\partial x}{\partial \eta} &= \frac{1}{4}\left[-X_1\,(1-\xi) - X_2\,(1+\xi) + X_3\,(1+\xi) + X_4\,(1-\xi)\right]; \\ \frac{\partial y}{\partial \xi} &= \frac{1}{4}\left[-Y_1\,(1-\eta) + Y_2\,(1-\eta) + Y_3\,(1+\eta) - Y_4\,(1+\eta)\right]; \\ \frac{\partial y}{\partial \eta} &= \frac{1}{4}\left[-Y_1\,(1-\xi) - Y_2\,(1+\xi) + Y_3\,(1+\xi) + Y_4\,(1-\xi)\right] \end{aligned} \tag{3.28}$$

Transforming $dxdy$ into $d\xi d\eta$:

Let the differential area $dxdy$ is formed through vectors $\hat{dx}$ and $\hat{dy}$ with magnitude dA and direction normal to the elemental area is $\hat{k}$

$$dA = dx\,dy = [\hat{dx} \times \hat{dy}] \cdot \hat{k} \tag{3.29}$$

$$\begin{aligned} dx\,dy &= \left[\left(\tfrac{\partial x}{\partial \xi}\,d\xi\,\hat{i} + \tfrac{\partial x}{\partial \eta}\,d\eta\,\hat{j}\right) \times \left(\tfrac{\partial y}{\partial \xi}\,d\xi\,\hat{i} + \tfrac{\partial y}{\partial \eta}\,d\eta\,\hat{j}\right)\right] \cdot \hat{k} \\ &= \left[\tfrac{\partial x}{\partial \xi} \cdot \tfrac{\partial y}{\partial \eta} - \tfrac{\partial x}{\partial \eta} \cdot \tfrac{\partial y}{\partial \xi}\right] d\xi\,d\eta \\ &= |J|\,d\xi\,d\eta \end{aligned} \tag{3.30}$$

or the Jacobian matrix is given by

$$[J] = \begin{bmatrix} \frac{\partial x}{\partial \xi} & \frac{\partial y}{\partial \xi} \\ \frac{\partial x}{\partial \eta} & \frac{\partial y}{\partial \eta} \end{bmatrix} \tag{3.31}$$

or:

$$|J| = \frac{\partial x}{\partial \xi}\frac{\partial y}{\partial \eta} - \frac{\partial y}{\partial \xi}\frac{\partial x}{\partial \eta} \tag{3.32}$$

Hence $\int_e f\,(x, y)\,dx\,dy$ can be written as

$$\int_e f\,(x, y)\,dx\,dy = \int_{e_m} \hat{f}\,(\xi, \eta)\,d\xi\,d\eta \tag{3.33}$$

such that $\hat{f}\,(\xi, \eta) = |J|\,f\,(x(\xi, \eta), y(\xi, \eta))$.

The condition which must to be satisfied for physically meaningful mapping of the physical element to the master element is that, $|J| > 0$.

Numerical Integration:

To compute $\int_{A_m} \hat{f}\,(\xi, \eta)\,d\xi\,d\eta$ *Gaussian quadrature* for two-dimentional integrals is used through which

$$\int_{A_m} \hat{f}\,(\xi, \eta)\,d\xi\,d\eta \approx \sum_{i=1}^{M}\sum_{j=1}^{N} \hat{f}\,(\xi_i, \eta_j)\,W_i\,W_j \tag{3.34}$$

where, M and N denote the number of quadrature points in ξ and η directions respectively, (ξ_i, η_j) denote the Gauss points, W_i and W_j are the Gauss weights at quadrature point (ξ_i, η_j) and geometrically the Jacobian $|J|$ is the ratio of an area element in the physical element to the corresponding area element in the master element e.

Order of numerical integration is greater than or equal to $(p+1)/2$ where, p is the order of the integrand.

In our problem we have chosen $5X5$ Gauss quadrature points.

3.6.2 SHAPE FUNCTION DERIVATIVES

Shape functions are defined in the master element i.e. $\hat{N}_i' = \hat{N}_i'(\xi, \eta)$. Its derivatives with respect to global co-ordinates (X and Y) are related to their derivatives with

respect to the natural co-ordinates (ξ and η) by:

$$\left\{ \begin{array}{c} N_{i,x} \\ N_{i,y} \end{array} \right\}_e = \left[J \right]_e^{-1} \left\{ \begin{array}{c} \hat{N}'_{i,\xi} \\ \hat{N}'_{i,\eta} \end{array} \right\}_{e_m} \tag{3.35}$$

and

$$\begin{aligned} \left\{ \begin{array}{c} N_{i,xx} \\ N_{i,yy} \\ N_{i,xy} \end{array} \right\}_e &= \left[\begin{array}{ccc} x_{,\xi}^2 & y_{,\xi}^2 & 2\, x_{,\xi}\, y_{,\xi} \\ x_{,\eta}^2 & y_{,\eta}^2 & 2\, x_{,\eta}\, y_{,\eta} \\ x_{,\xi}\, x_{,\eta} & y_{,\xi}\, y_{,\eta} & x_{,\eta}\, y_{,\xi} + x_{,\xi}\, y_{,\eta} \end{array} \right]_e^{-1} \\ \times \left(\left\{ \begin{array}{c} \hat{N}'_{i,\xi\xi} \\ \hat{N}'_{i,\eta\eta} \\ \hat{N}'_{i,\xi\eta} \end{array} \right\}_{e_m} - \left[\begin{array}{cc} x_{,\xi\xi} & y_{,\xi\xi} \\ x_{,\eta\eta} & y_{,\eta\eta} \\ x_{,\xi\eta} & y_{,\xi\eta} \end{array} \right]_e \left\{ \begin{array}{c} N_{i,x} \\ N_{i,y} \end{array} \right\}_e \right) \end{aligned} \tag{3.36}$$

Chapter 4

RESULTS AND DISCUSSION

4.1 INTRODUCTION

The finite element formulation presented in Chapter 3, is used to study the initial buckling of laminated composite plates using a simple higher order shear deformation theory.For the present study it is assumed that there is no coupling between the in-plane and out-of-plane quantities.If this is not true, then even for an infinitesimally small inplane compressive force the laminated composite plate will undergo flexure.For symmetric laminate this condition is automatically satisfied but for antisymmetric laminate there is always coupling between in-plane and out-of-plane quantities.In the case of antisymmetric laminate we have assumed that this coupling effect is negligibly small and was ignored to find the initial buckling load.This assumtion although seems strong it can be shown that if the number of plies is increased the coupling effect dies out rapidly and the solution approaches the orthotropic solution (see [12]).

In the present study the following assumptions are made.

1. The thickness of each layer is constant.
2. There is no delamination/slip between the layers.
3. No micro-buckling takes place before the initial buckling.
4. There is no fibre breakage or matrix cracking before the onset of initial buck-

ling.

In the current investigation the following nomenclatures are assumed to denote the thickness of laminate.

- $a/h \geq 100$: Thin laminate .
- $20 \leq a/h \leq 50$: Moderately thick laminate .
- $a/h \leq 10$: Very thick laminate .

This classification is tentative and actual definition depends on a variety of factors such as loadings, boundary conditions etc.

4.2 BOUNDARY CONDITIONS

The following types of geometric boundary conditions are considered in the analysis.

- Simply-Supported (S) : $w_b = w_s = 0$.
- Clamped (C) : $w_b = w_s = w_{b,n} = w_{s,n} = 0$;
  where, $n = x$ or y depending on the side of the plate.

To define the complete set of boundary conditions on all four sides of the plate the following scheme has been adopted which is explained through an example.

A set of boundary conditions say, SCCS denotes the following:

$$w_b = w_s = 0 \qquad \text{at } x = 0 \,\forall\, y$$

$$w_b = w_s = w_{b,y} = w_{s,y} = 0 \qquad \text{at } y = 0 \,\forall\, x$$

$$w_b = w_s = w_{b,x} = w_{s,x} = 0 \qquad \text{at } x = a \,\forall\, y$$

$$w_b = w_s = 0 \qquad \text{at } y = b \,\forall\, x$$

4.3 MATERIAL PROPERTIES USED

For the present investigation the following material properties are used.

Table 4.1: **Material properties**

Material code	$E_L(GPa)$	$\frac{E_L}{E_T}$	$\frac{G_{LT}}{E_T}$	$\frac{G_{LT'}}{E_T}$	$\frac{G_{TT'}}{E_T}$	ν_{LT}
M1 [14]	130	13	0.5	0.5	0.2	0.35
M2 [9]	200	40	0 6	0.6	0.5	0.25
M3	100	isotropic				0.25
M4 [15]	153	15.904	0.616	0.616	0.336	0.32

4.4 CONVERGENCE STUDY

In this section the following set of problems are considered for the convergence study.

Table 4.2: **Problem definitions for convergence study**

Problem number	Material code	Aspect (a/b)	Length/thickness ratio(a/h)	Boundary conditions	laminae lay-up sequence
P1	M1	1.0	10	SSSS	$[90/0]_s$
P2	M1	1.0	50	SSSS	$[90/0]_s$
P3	M1	1.0	100	SSSS	$[90/0]_s$
P4	M1	1.0	10	CCCC	$[90/0]_s$
P5	M1	1.0	50	CCCC	$[90/0]_s$
P6	M1	1.0	100	CCCC	$[90/0]_s$
P7	M1	1.0	10	SSSS	$[90/0/90/0]_2$
P8	M1	1.0	50	SSSS	$[90/0/90/0]_2$
P9	M1	1.0	100	SSSS	$[90/0/90/0]_2$
P10	M1	1.0	10	CCCC	$[90/0/90/0]_2$
P11	M1	1.0	50	CCCC	$[90/0/90/0]_2$
P12	M1	1.0	100	CCCC	$[90/0/90/0]_2$

Convergence of the initial buckling load with mesh refinement (by decreasing the mesh size or in other words by increasing the number of meshes in the plate domain) for the problems defined in Table 4.2 is as shown in Table 4.3 .

From Table 4.3 it can be concluded that for a square plate, 10×10 mesh gives sufficient accurate results (for both simply supported and clamped boundary conditions) from engineering point of view.Hence for further studies of square plates, the plate domain is divided into 10×10 mesh.

For rectangular plates, convergence study was done for each problem (with different aspect ratios) seperately, trying to keep the element aspect ratio almost equal to one.It has been observed that for $a/b = 2$ sufficiently converged result can be obtained for 10×5 mesh whereas for $a/b = 3$ it is 15×5, for both simply supported and clamped boundary conditions.

Table 4.3: **Convergence study**

Problem number	Mesh size	Nondimensionalized buckling load, $\bar{N}_x$ ($\bar{N}_x = N_x b^2/E_t h^3$)
P1	2×2	7.4943
	4×4	9.3565
	8×8	9.4372
	10×10	9.4441
P2	2×2	9.9005
	4×4	12.4832
	8×8	12.5253
	10×10	12.5259
P3	2×2	10.0013
	4×4	12.6150
	8×8	12.6554
	10×10	12.6554
P4	2×2	12.6457
	4×4	15.3898
	8×8	15.9465
	10×10	16.0501

Problem number	Mesh size	Nondimensionalized buckling load, $\bar{N}_x$ ($\bar{N}_x = N_x b^2/E_t h^3$)
P5	2×2	20.3343
	4×4	26.1606
	8×8	27.4415
	10×10	27.7342
P6	2×2	20.6987
	4×4	26.7411
	8×8	28.0754
	10×10	28.3809
P7	2×2	10.3057
	4×4	10.9218
	8×8	11.0400
	10×10	11.0477
P8	2×2	13.1137
	4×4	13.4850
	8×8	13.4996
	10×10	13.4997
P9	2×2	13.2234
	4×4	13.5846
	8×8	13.5957
	10×10	13.5962
P10	2×2	18.9513
	4×4	21.2392
	8×8	21.7043
	10×10	21.7440
P11	2×2	39.8804
	4×4	42.6732
	8×8	44.5310
	10×10	44.7049

Problem number	Mesh size	Nondimensionalized buckling load, $\bar{N}_x$ ($\bar{N}_x = N_x b^2/E_t h^3$)
P12	2×2	40.7152
	4×4	43.8164
	8×8	45.8574
	10×10	46.0485

4.5 VALIDATION STUDY

The validation of the plate model for finite element formulation is done by comparing the results of the following set of problems with standard results published in the literature.

Table 4.4: **Problem definitions for validation study**

Problem number	Material code	Aspect (a/b)	Thickness ratio(a/h)	Boundary conditions	laminae lay-up sequence
P13	M3	1.0	100	SSSS	isotropic
P14	M3	1.0	100	CCCC	isotropic
P15	M2	1.0	10	SSSS	$[0/90]_5$
P16	M2	1.0	10	SSCS	$[0/90]_5$
P17	M2	1.0	10	CSCS	$[0/90]_5$
P18	M2	1.0	5	SSSS	$[0/90]_5$
P19	M2	1.0	5	SSCS	$[0/90]_5$
P20	M2	1.0	5	CSCS	$[0/90]_5$

The comparative study of the analytical results from the present investigation with the results available in the published literature is presented in Table 4.5 .

From Table 4.5 it can be observed that the difference in the results obtained from the present study and that from the published literature is less than 2.5% in all the cases.Hence we can conclude that the present formulation gives results which are in

good agreement and validates the present formulation.

Table 4.5: **Comparison of results**

Problem number	Laminate theory [ref. no.]	Reference		Present	
		$\bar{N}_x$	$\bar{N}_y$	$\bar{N}_x$	$\bar{N}_y$
P13	CLT [16]	4.0	-	3.997	-
	HSDT	-	-	-	-
P14	CLT [16]	10.15	-	10.032	-
	HSDT	-	-	-	-
P15	CLT [9]	35.232[a]	35.232[a]	36.198[c]	36.198[c]
	HSDT [9]	24.424[b]	25.828[b]	25.943	25.943
P16	CLT [9]	-	59.288[a]	-	60.563[c]
	HSDT [9]	-	33.662[b]	-	33.969
P17	CLT [9]	-	89.770[a]	-	91.015[c]
	HSDT [9]	-	36.657[b]	-	35.958
P18	CLT [9]	-	35.232[a]	-	36.198[c]
	HSDT [9]	-	12.224[b]	-	12.603
P19	CLT [9]	-	59.288[a]	-	60.563[c]
	HSDT [9]	-	12.800[b]	-	12.969
P20	CLT [9]	-	89.770[a]	-	91.015[c]
	HSDT [9]	-	13.659[b]	-	13.426

[a] Results obtained with the exact solution developed in the corresponding reference.

[b] Results using the finite element solution in the corresponding reference.

[c] Results obtained by subpressing w_s over the entire domain of the plate.

$\bar{N}_x/\bar{N}_y$ are the dimensionless initial buckling values where the nondimensionalizing factor is as given in the corresponding references.

4.6 PARAMETRIC STUDY OF COMPOSITE LAMINATES SUBJECTED TO UNIAXIAL IN-PLANE LOADINGS

In the following section the effects of transverse shear deformation, plate aspect ratio (a/b), length/thickness ratio (a/h) and fibre orientation angle (θ) on the initial buckling loads of laminated (8 layer antisymmetric, $[\pm\theta]_4$) composite plates is studied (using HSDT) keeping the same material properties (Material- M2).

The loads considered are uniaxial in-plane compressive and negative shear buckling load whereas the geometric boundary condition is taken as simply supported on all four sides.

Results are also obtained using CLT for thin laminate ($a/h = 100$).

The results presented in Figs. 4.1 - 4.3 show that for thin laminate ($a/h = 100$) the fibre orientation angle for the maximum value of the fundamental initial buckling load (henceforth the fibre orientation angle for the maximum value of the fundamental initial buckling load is denoted as $\theta_{cric.}$ and the corresponding initial buckling load as the critical initial buckling load) is around 45° for aspect ratios $a/b = 1, 2, 3$.The critical initial buckling load decreases very slightly with the increase in aspect ratio.Further comparing the graphs for $a/h = 100$ in Figs. 4.1 - 4.3 (obtained using HSDT) with that of the graphs in Fig. 4.4 (obtained using CLT) it can be concluded that the effect of neglecting transverse shear in the analysis is negligible for thin laminates.The initial buckling values for thin laminate using HSDT are slightly less than the corresponding values obtained using CLT.

With increase in the thickness of the laminate (decreasing the length/thickness ratio) transverse shear effect plays a dominant role in the buckling behaviour of the laminate.For $a/h = 50$ the fibre orientation angles for critical initial buckling load are about 45°, 42° and 40° respectively, for aspect ratios $a/b = 1, 2, 3$.Hence the critical fibre orientaion angle for $a/h = 50$ is lesser than that for $a/h = 100$ and changes slightly with the change in aspect ratio.

changes slightly with the change in aspect ratio.

As the laminate becomes thicker there is a shift in the critical fibre orientation angle towards lesser values.Also this shift is more as the aspect ratio increases.For thick laminate ($a/h = 20, 10, 5$) the effect of fibre orientation angle on the value of critical buckling load decreses with the increase in aspect ratio.Further, it can be observed that as the length/thickness ratio decreases (the laminate becomes thicker) the initial buckling load changes very little with the change in fibre orientation angle (for all aspect ratios).

The decrease in the values of initial buckling loads (for any orientation of the fibre) is more pronounced for thick laminates.This brings out the fact that for thick laminates one should consider transverse shear effects.

From Fig. 4.5 it can be observed that for shear buckling load (considered negative here) the critical fibre orientation angle changes slightly with the change in aspect ratio.This critical fibre orientation angle is around 45° for thick laminates ($a/h = 10$).

The critical fibre orientation angles and associated critical initial buckling loads (uniaxial in-plane compressive, N_x) for different aspect ratios and length/thickness ratio are presented in Table 4.6 .

In Figs. 4.6 - 4.27 the mode shapes of the buckled plates are shown for various aspect ratios and length/thickness ratios at different fibre orientation angles.The mode shapes are non-dimensionalized as $\bar{w} = \frac{w}{h}$ where $w = w_b + w_s$.The mode shapes are found to be either symmetric or antisymmetric in nature.It can be observed from the figures that there is a change in the mode shapes as the fibre orientation angle changes.

Table 4.6: **Effect of aspect ratio and length/thickness ratio upon the critical initial buckling load of antisymmetrically laminated angle ply plates,** $[\pm\theta]_4$

Aspect (a/b)	Thickness ratio(a/h)	Critical fibre orientation angle($\theta_{cric.}$)		Critical initial buckling load($\bar{N}_x = N_x b^2/E_T h^3$)	
		HSDT	CLT	HSDT	CLT
1	100	45	45	67.04	67.54
1	50	45	45	65.59	67.54
1	10	42	45	40.12	67.54
1	5	15	45	14.66	67.54
2	100	45	45	65.56	67.52
2	50	42	45	61.02	67.52
2	20	35	45	36.65	67.52
2	10	16	45	14.63	67.52
2	5	15	45	4.88	67.52
3	100	45	45	63.195	67.48
3	50	40	45	52.02	67.48
3	20	27	45	22.13	67.48
3	10	10	45	7.64	67.48
3	5	0	45	2.65	67.48

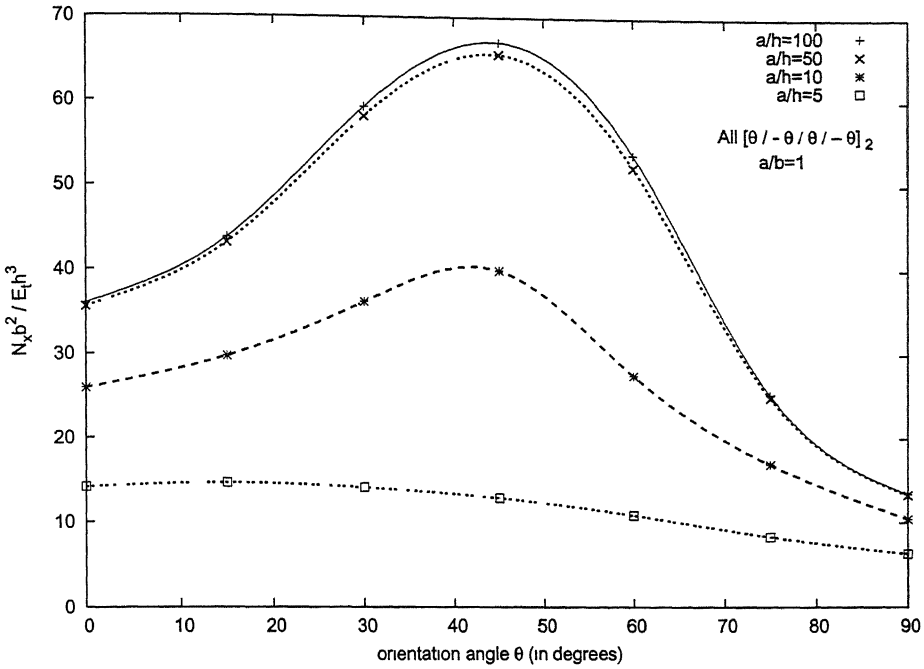

Figure 4.1: **Non-dimensionalized initial buckling load versus fibre orientation (θ), (Material- M2).**

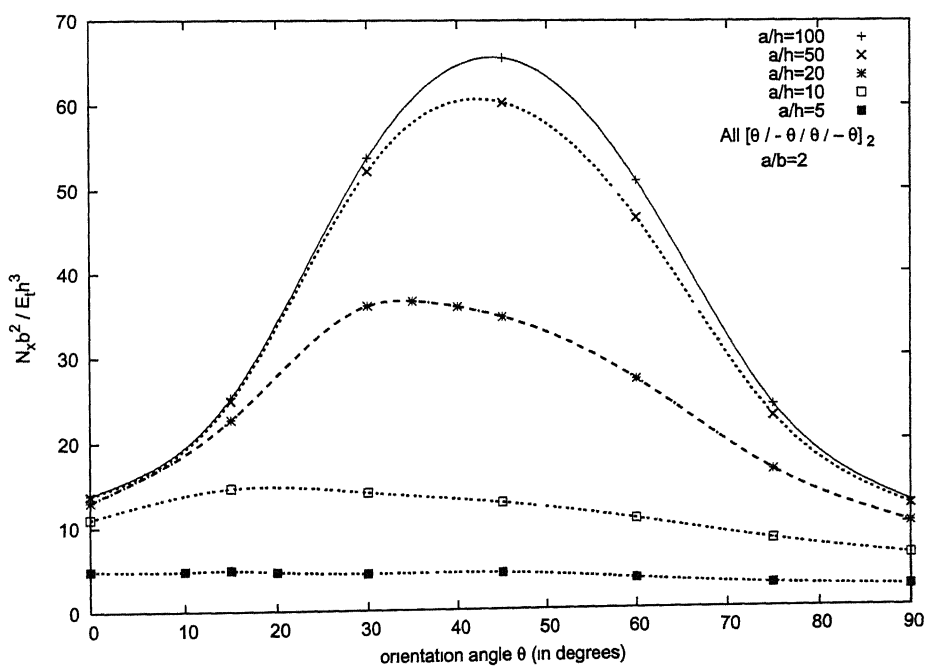

Figure 4.2: **Non-dimensionalized initial buckling load versus fibre orientation (θ), (Material- M2).**

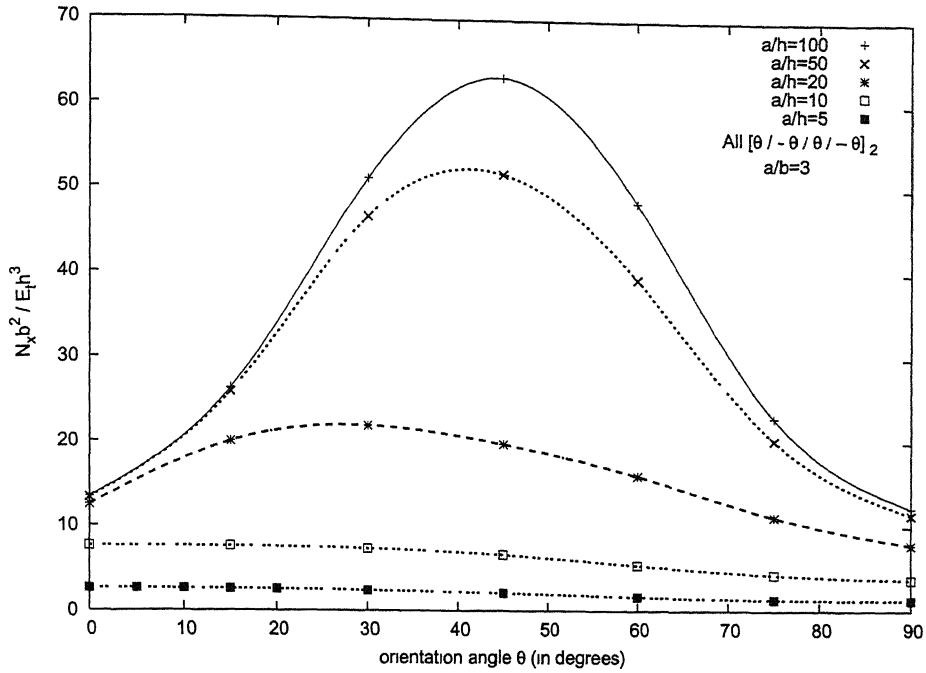

Figure 4.3: **Non-dimensionalized initial buckling load versus fibre orientation (θ), (Material- M2).**

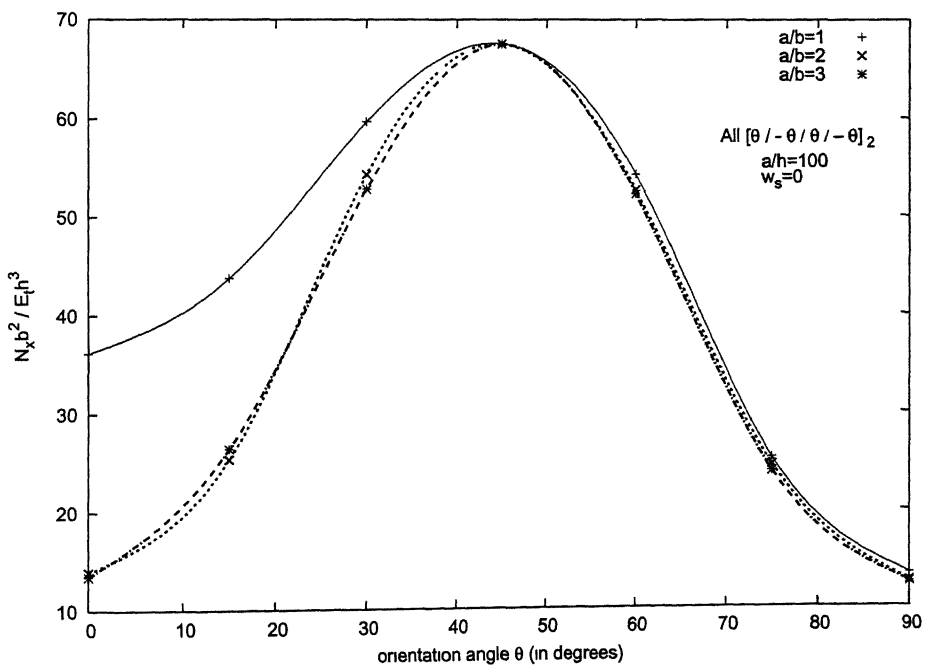

Figure 4.4: **Non-dimensionalized initial buckling load versus fibre orientation (θ) using CLT (Material- M2).**

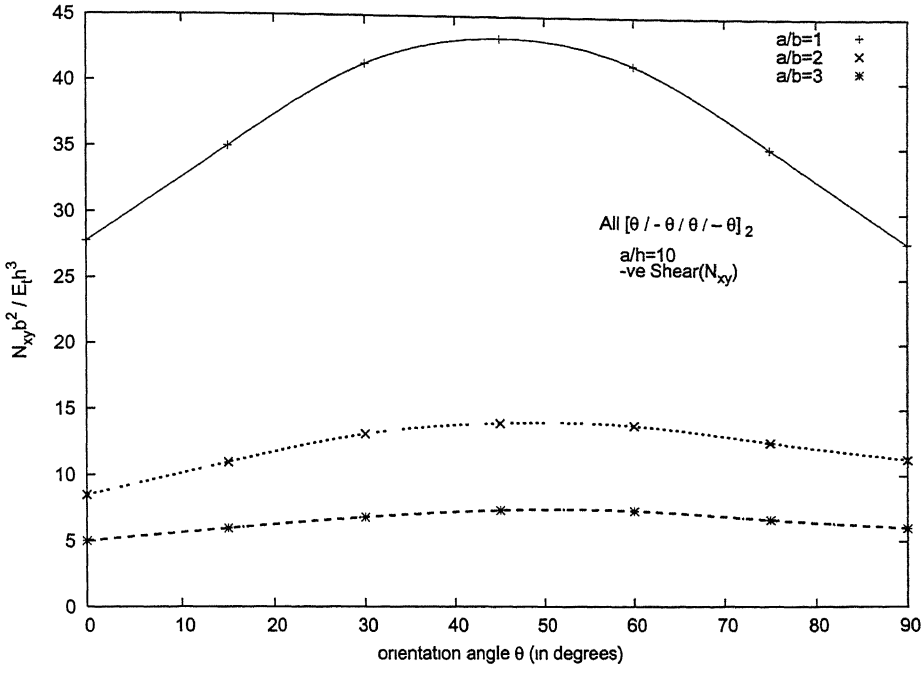

Figure 4.5: **Non-dimensionalized initial shear(-ve) buckling load versus fibre orientation (θ), (Material- M2).**

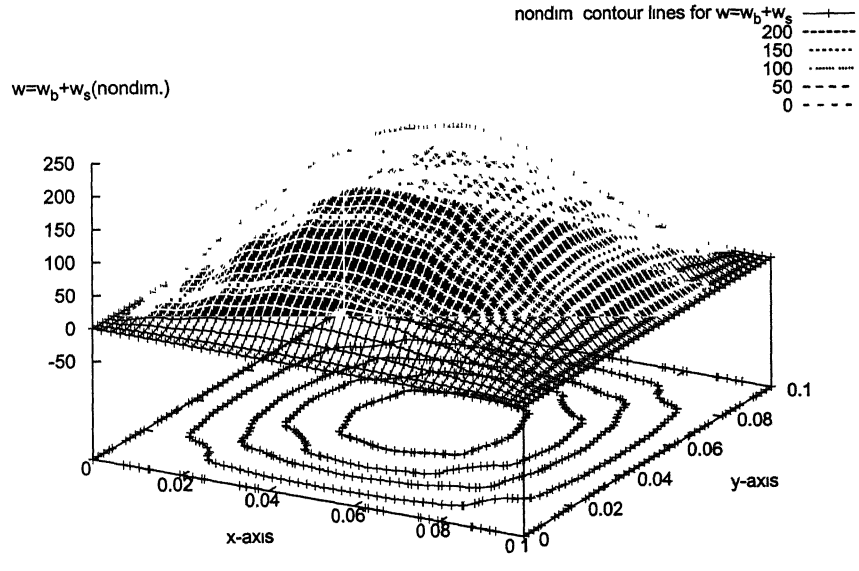

Figure 4.6: **Mode shape of antisymmetric angle ply laminate $[\pm\theta]_4$ for $a/b = 1, a/h = 100, \theta = 30$ under application of N_x.**

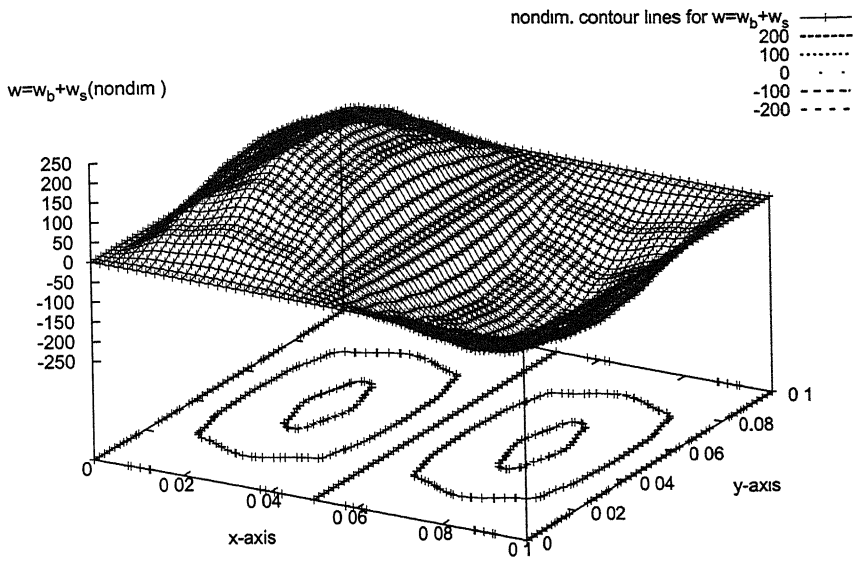

Figure 4.7: **Mode shape of antisymmetric angle ply laminate $[\pm\theta]_4$ for $a/b = 1, a/h = 100, \theta = 70$ under application of N_x.**

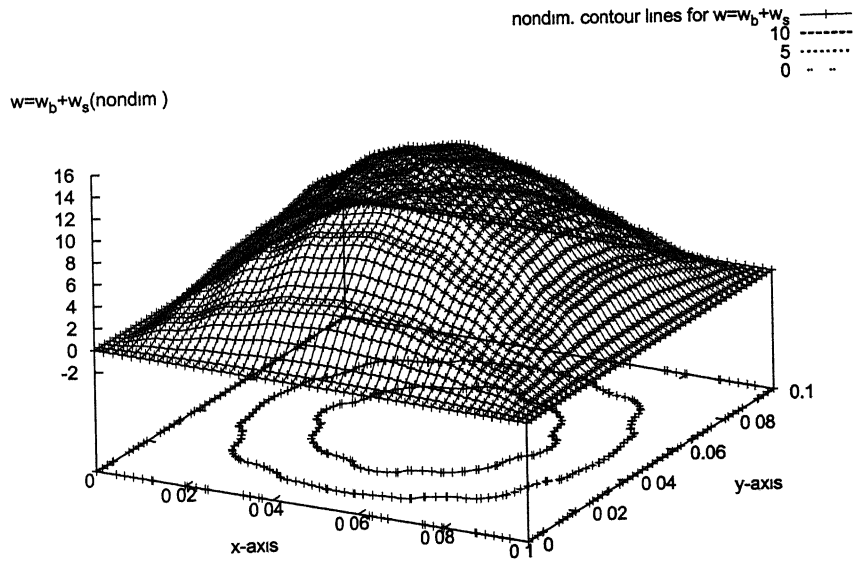

Figure 4.8: **Mode shape of antisymmetric angle ply laminate $[\pm\theta]_4$ for $a/b = 1, a/h = 5, \theta = 10$ under application of N_x.**

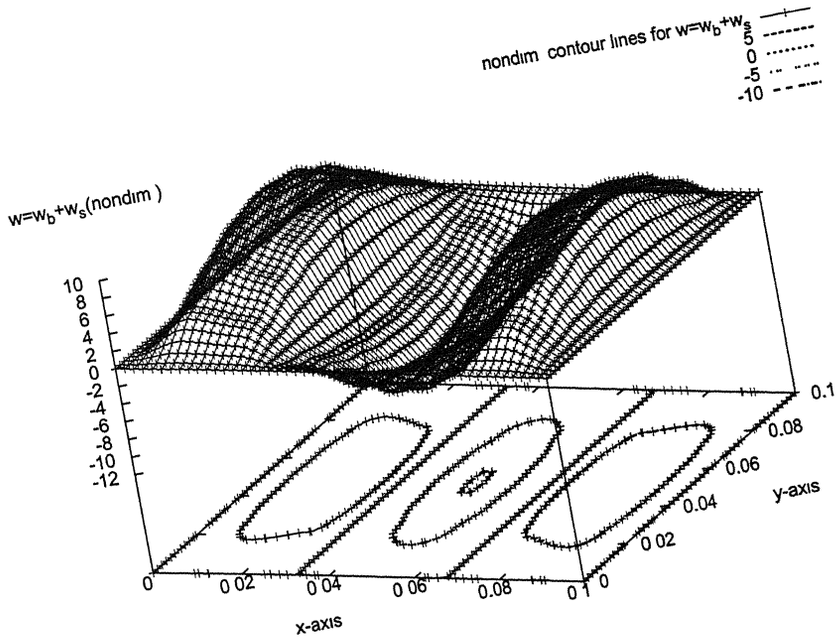

Figure 4.9: **Mode shape of antisymmetric angle ply laminate $[\pm\theta]_4$ for $a/b = 1, a/h = 5, \theta = 70$ under application of N_x.**

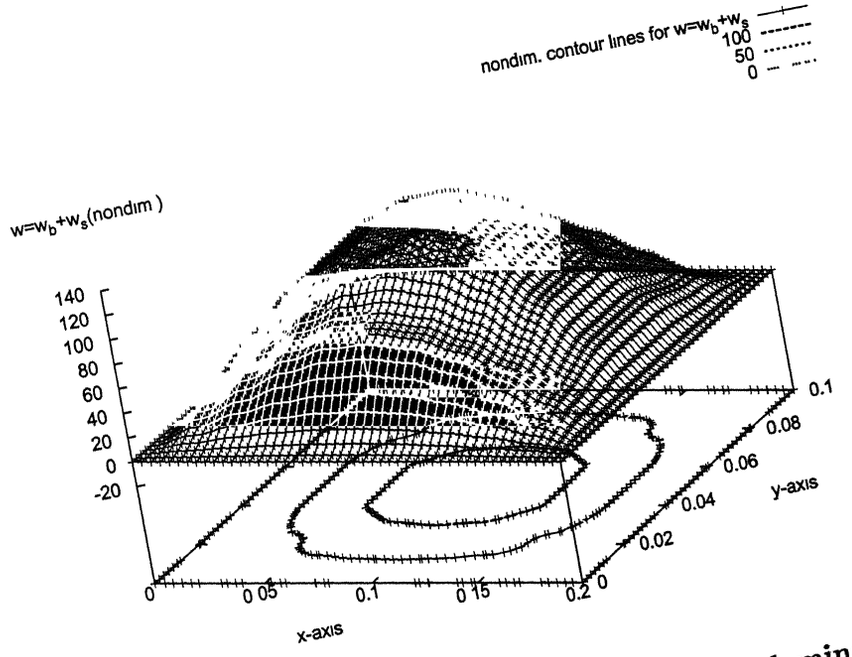

Figure 4.10: **Mode shape of antisymmetric angle ply laminate $[\pm\theta]_4$ for $a/b = 2, a/h = 100, \theta = 20$ under application of N_x.**

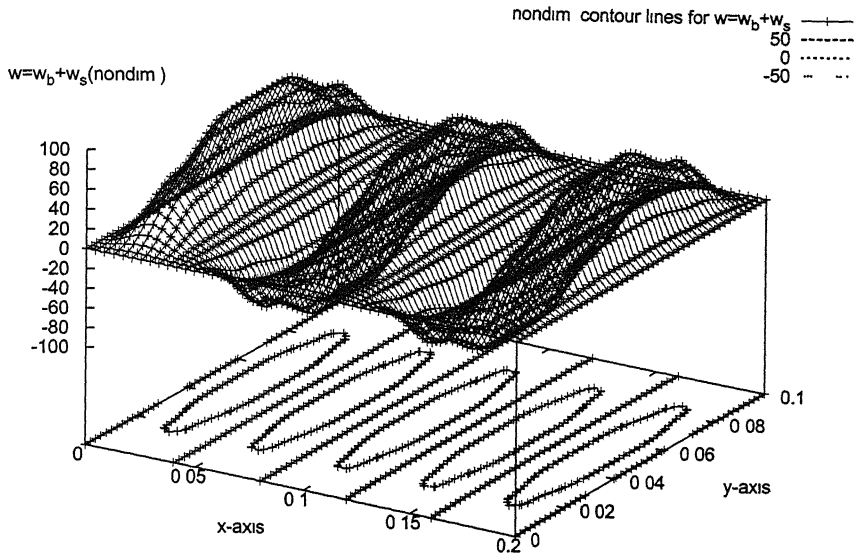

Figure 4.11: **Mode shape of antisymmetric angle ply laminate $[\pm\theta]_4$ for $a/b = 2, a/h = 100, \theta = 75$ under application of N_x.**

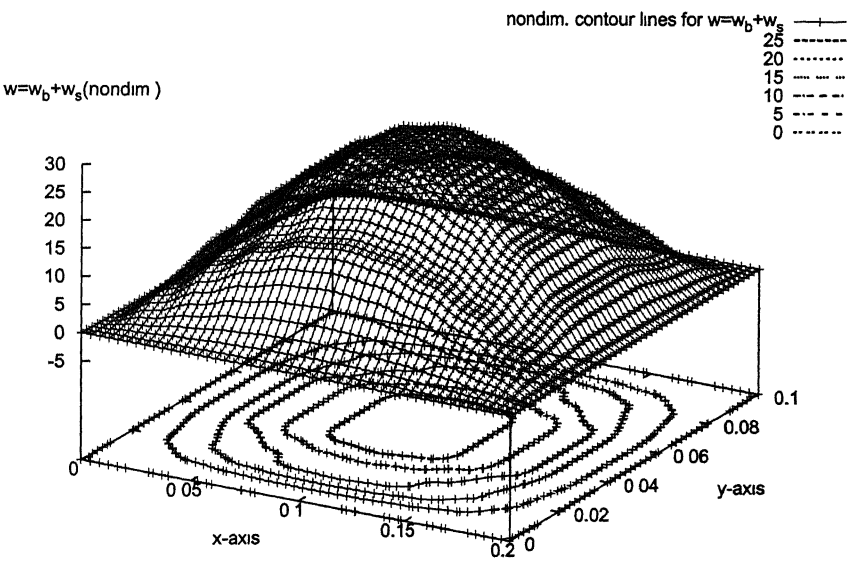

Figure 4.12: **Mode shape of antisymmetric angle ply laminate $[\pm\theta]_4$ for $a/b = 2, a/h = 20, \theta = 20$ under application of N_x.**

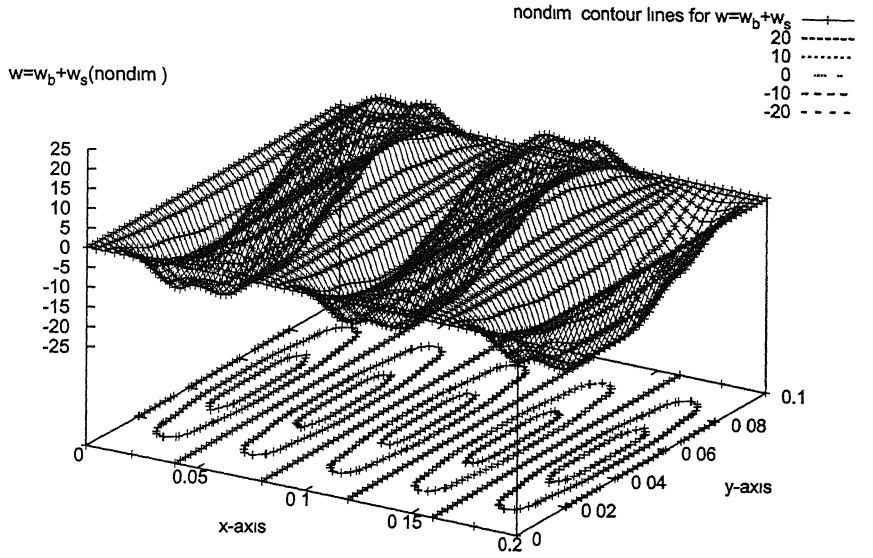

Figure 4.13: **Mode shape of antisymmetric angle ply laminate $[\pm\theta]_4$ for $a/b = 2, a/h = 20, \theta = 75$ under application of N_x.**

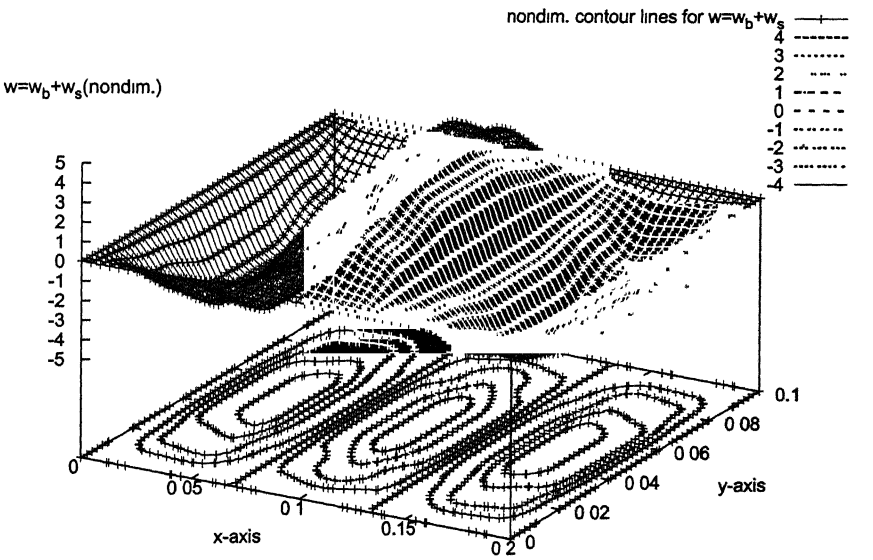

Figure 4.14: **Mode shape of antisymmetric angle ply laminate $[\pm\theta]_4$ for $a/b = 2, a/h = 5, \theta = 10$ under application of N_x.**

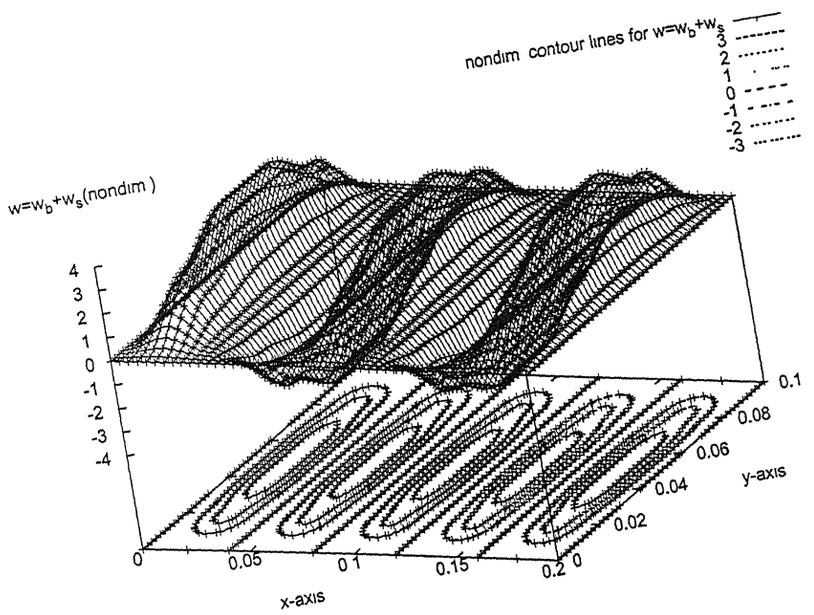

Figure 4.15: **Mode shape of antisymmetric angle ply laminate $[\pm\theta]_4$ for $a/b = 2, a/h = 5, \theta = 50$ under application of N_x.**

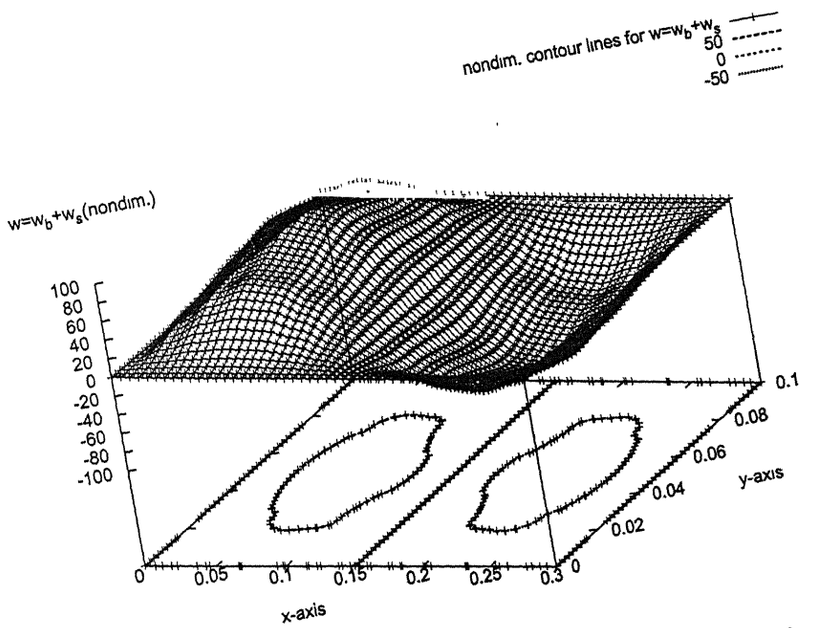

Figure 4.16: **Mode shape of antisymmetric angle ply laminate $[\pm\theta]_4$ for $a/b = 3, a/h = 100, \theta = 20$ under application of N_x.**

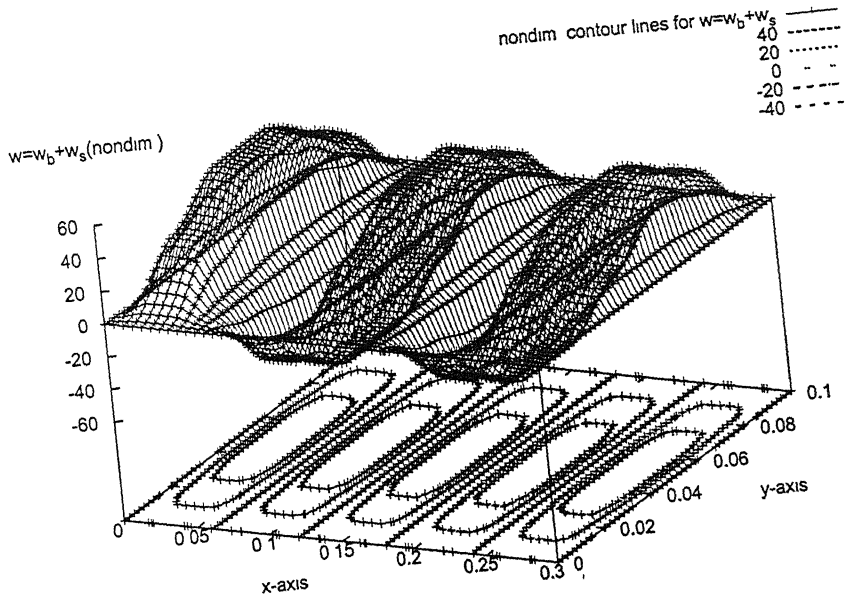

Figure 4.17: Mode shape of antisymmetric angle ply laminate $[\pm\theta]_4$ for $a/b = 3, a/h = 100, \theta = 60$ under application of N_x.

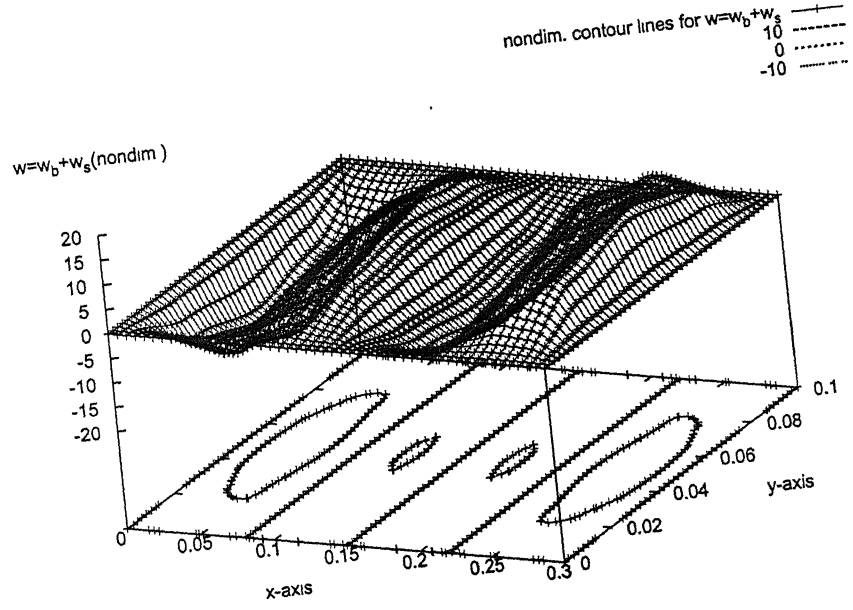

Figure 4.18: Mode shape of antisymmetric angle ply laminate $[\pm\theta]_4$ for $a/b = 3, a/h = 20, \theta = 15$ under application of N_x.

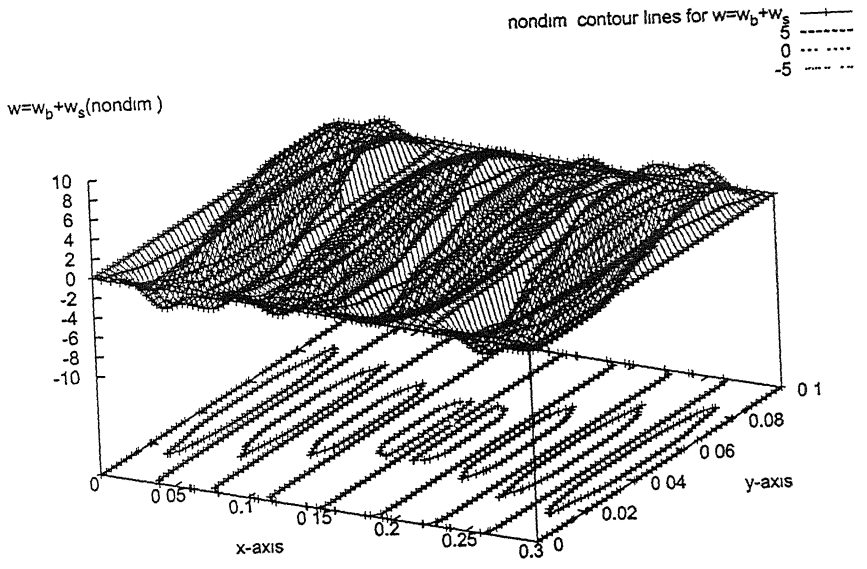

Figure 4.19: Mode shape of antisymmetric angle ply laminate $[\pm\theta]_4$ for $a/b = 3, a/h = 20, \theta = 50$ under application of N_x.

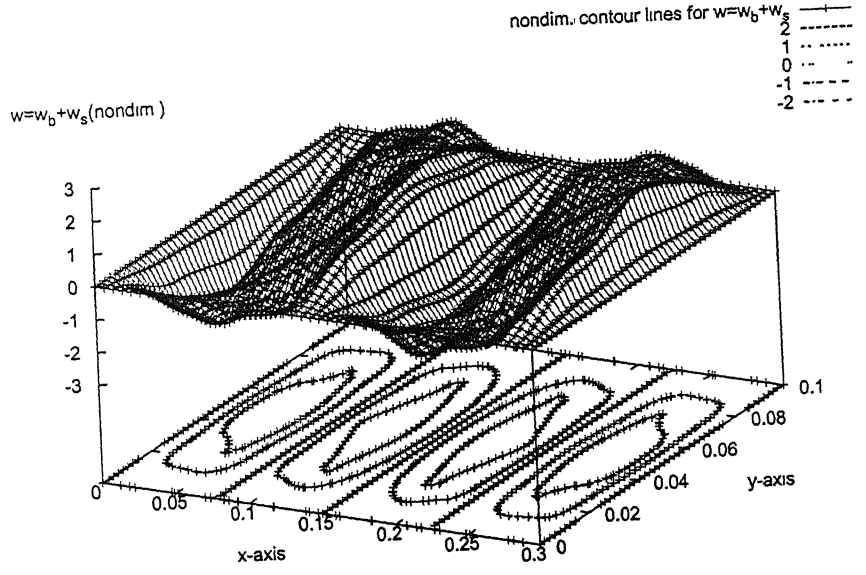

Figure 4.20: Mode shape of antisymmetric angle ply laminate $[\pm\theta]_4$ for $a/b = 3, a/h = 5, \theta = 0$ under application of N_x.

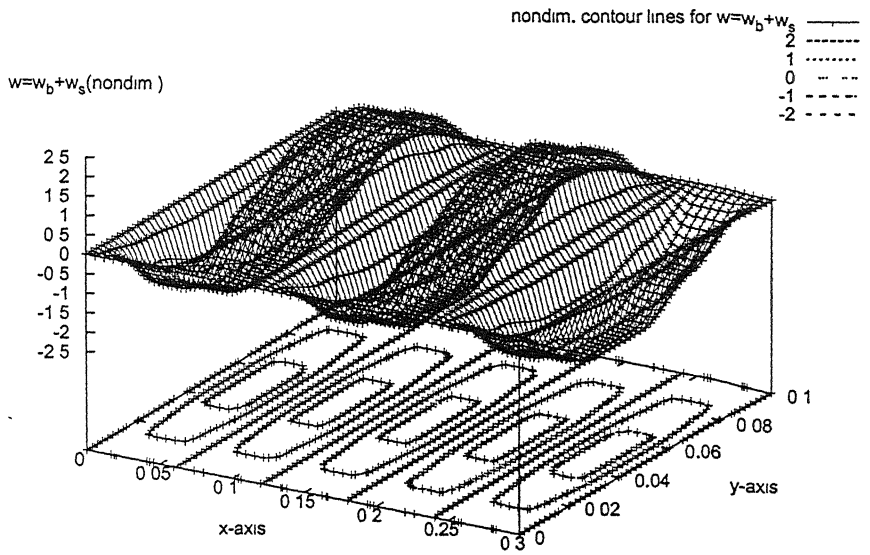

Figure 4.21: **Mode shape of antisymmetric angle ply laminate $[\pm\theta]_4$ for $a/b = 3, a/h = 5, \theta = 40$ under application of N_x.**

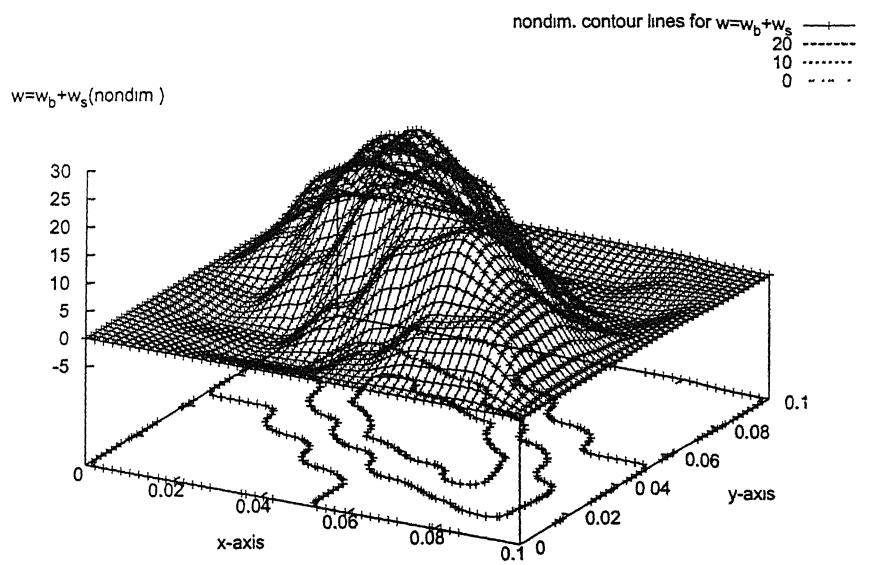

Figure 4.22: **Mode shape of antisymmetric angle ply laminate $[\pm\theta]_4$ for $a/b = 1, a/h = 10, \theta = 30$ under application of N_{xy}.**

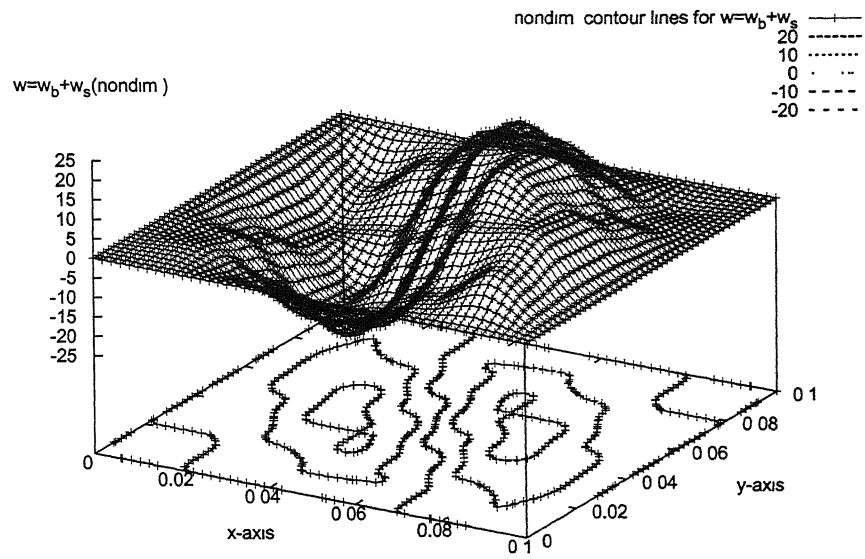

Figure 4.23: **Mode shape of antisymmetric angle ply laminate $[\pm\theta]_4$ for $a/b = 1, a/h = 10, \theta = 75$ under application of N_{xy}.**

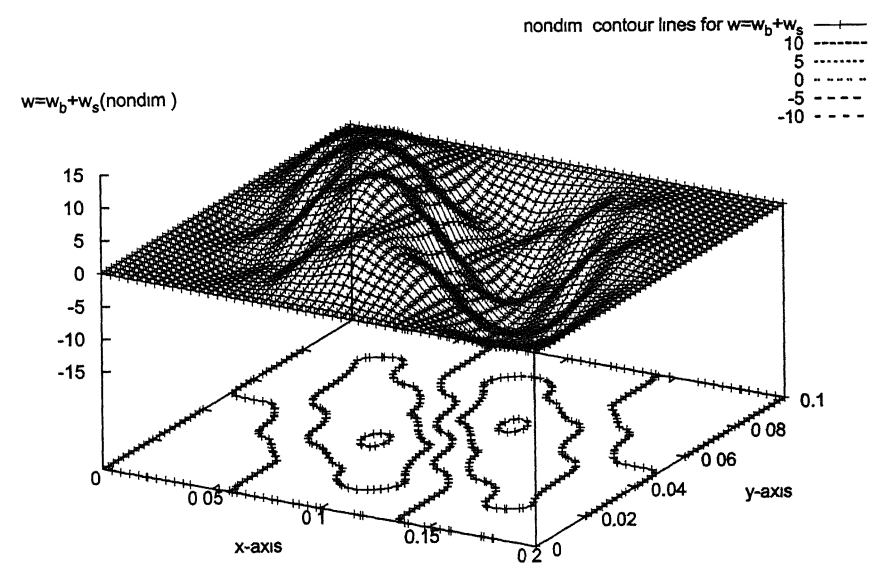

Figure 4.24: **Mode shape of antisymmetric angle ply laminate $[\pm\theta]_4$ for $a/b = 2, a/h = 10, \theta = 30$ under application of N_{xy}.**

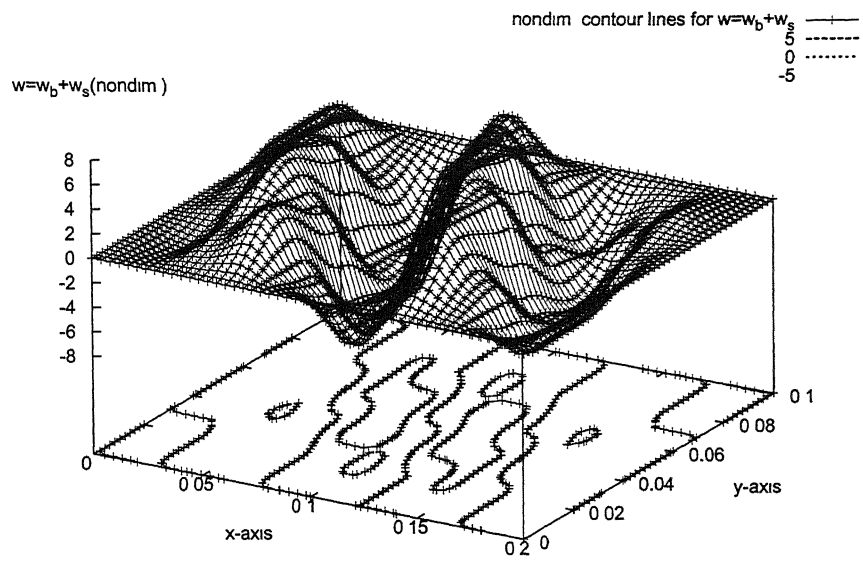

Figure 4.25: **Mode shape of antisymmetric angle ply laminate $[\pm\theta]_4$ for $a/b = 2, a/h = 10, \theta = 75$ under application of-N_{xy}.**

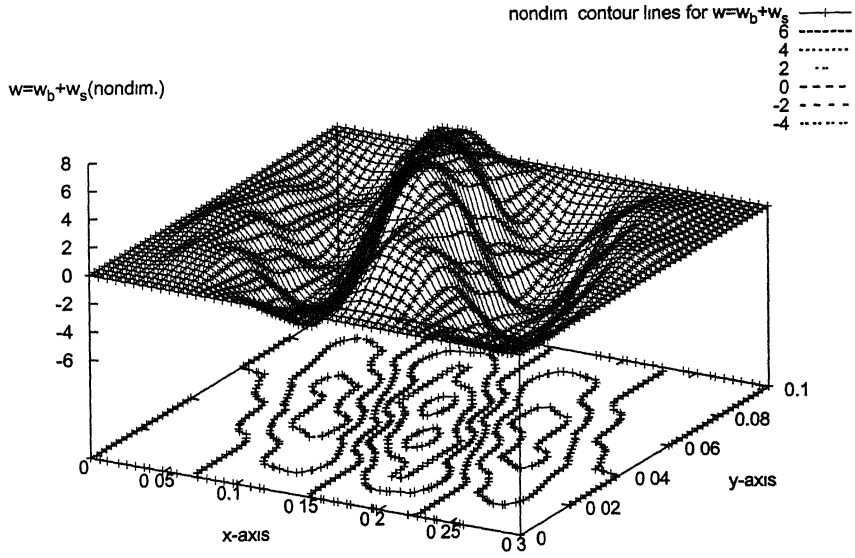

Figure 4.26: **Mode shape of antisymmetric angle ply laminate $[\pm\theta]_4$ for $a/b = 3, a/h = 10, \theta = 30$ under application of-N_{xy}.**

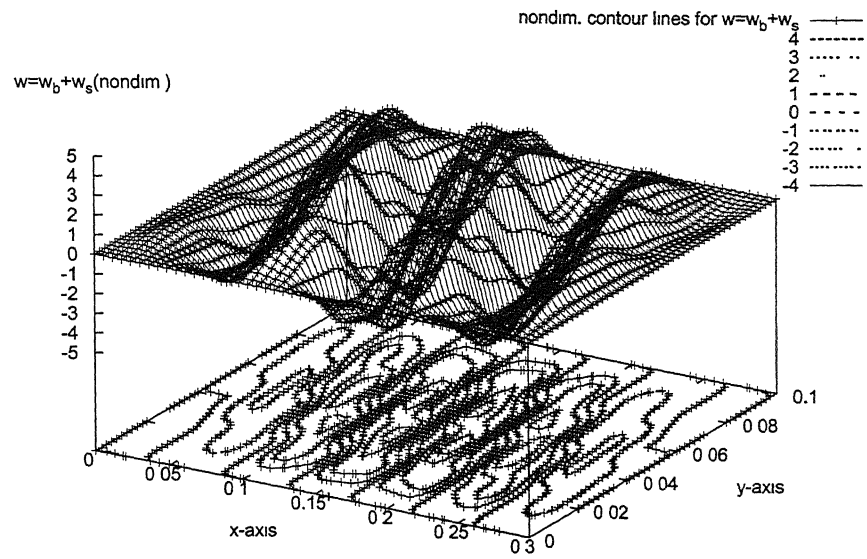

Figure 4.27: **Mode shape of antisymmetric angle ply laminate $[\pm\theta]_4$ for $a/b = 3, a/h = 10, \theta = 75$ under application of N_{xy}.**

4.7 INTERACTION CURVES FOR BIAXIAL IN-PLANE LOADINGS

In the present investigation stability boundaries are obtained for two cases of biaxial loading.

- In-plane compressive loads in both X and Y directions (i.e. N_x and N_y).
- In-plane compressive loads in X direction and in-plane (both negative and positive) shear (i.e.N_x and $\pm N_{xy}$).

Computations are carried out for laminates simply supported on all the four edges (SSSS).

It can be noted here that in this section N_x, N_y *and* N_{xy} all denotes nondimensionalized in-plane initial buckling loads, nondimensionalized by a factor $(b^2/E_T h^3)$.

4.7.1 BIAXIAL IN-PLANE LOADINGS N_x AND N_y

First the results from the present study are compared with standard results available in the literature [15].It is found that the results from the present study are in good agreement with the results cited in the reference.These are shown in Fig 4.28 (for $a/b = 1$) and Fig 4.29 (for $a/b = 2$).It can be observed, that, for rectangular laminates (in Fig. 4.29) there is a unique point (at about $\frac{N_y}{N_x} = 0.2667$) at which for both the laminates ($[45/90/-45/90]_{2s}$ and $[\pm 45]_{4s}$) the buckling load is same.For the combinations of loads where N_x is less than this critical value $[\pm 45]_{4s}$ laminate buckles at a lower value of N_y for a given N_x and for the combinations of loads where N_y is less than this critical value $[\pm 45]_{4s}$ laminate buckles at a greater value of N_x for the same amount of N_y.For square laminate no such unique point is observed.

Next the effect of neglecting transverse shear is studied for square laminated plates.It is found, that, for thin laminates the effect is negligible.It is observed, that, for $a/b = 1$ (Figs. 4.30 and 4.31) the values of initial buckling load obtained using CLT are somewhat more than that obtained using HSDT, but this difference is very small and can be neglected for all practical purposes.However, for thick laminates the effect is not the same. Here the initial buckling loads obtained using CLT are far greater than that obtained using HSDT (Figs. 4.32 and 4.33).Hence if one uses CLT to estimate the initial buckling load for thick laminates, it will be grossly erroneous.So in this case one has to use HSDT to obtain accurate values of initial buckling load.

In the following section the stability envelops are shown for both cross ply and angle ply symmetric laminates $[\pm\theta]_{2s}$ for plate aspect ratios 1 and 2 and length/thickness ratios 100 and 10 for both square and rectangular laminates.The analysis is done using simple HSDT for all the cases.

For $a/b = 1$ and $a/h = 100$ (Fig. 4.34) the following observations can be made.

- The stability envelops in general are either linear or piecewise linear.
- $\theta = 45°$ laminate gives the highest value of $(N_x + N_y)$ for any combination of the loads and for cross ply laminate $(N_x + N_y)$ is the minimum.

- There is a sudden change in slope of the stability envelops for laminates with $\theta = 30°$ and $\theta = 60°$.For $\theta = 30°$ laminate, this slope change occurs at small value of N_x and for $\theta = 60°$ laminate slope change occurs at high value of N_x.For $\theta = 45°$ laminate and for cross ply laminate there is no change in the slopes of their stability envelops.

- For $\theta = 30°$ and $\theta = 60°$ laminates the portion where the slopes of the two envelops are the same, the values of $(N_x + N_y)$ are also same.

- From the stability envelops shown in Fig. 4.34 no such unique point, as mentioned earlier (Fig. 4.29) can be observed.Instead here it can be observed that for $\theta = 30°$ and $\theta = 60°$ laminates there are two points (approximately at $\frac{N_x}{N_y} = 0.175$ and $\frac{N_y}{N_x} = 0.175$) between which both the laminates have the same interaction curve For the combinations of loads where N_x is less than the critical value ($\frac{N_x}{N_y} = 0.175$) $\theta = 60°$ laminate buckles at a greater value of N_y for the same amount of N_x and for the combinations of loads where N_y is less than the critical value ($\frac{N_y}{N_x} = 0.175$) $\theta = 30°$ laminate buckles at a greater value of N_x for the same amount of N_y.Stability envelops of both the cross ply laminate and $\theta = 45°$ laminate donot intersect any any other curves.

For $a/b = 1$ and $a/h = 10$ (Fig. 4.35) the following observations can be made.There is a change in the nature of the stability envelops for thick square laminate from that of the thin laminate though the basic shapes of the stability envelops remains the same (linear or piecewise linear curves).

- Except for cross ply laminate (linear stability envelop) the sability envelops for the angle ply laminates are all piecewise linear.

- $\theta = 45°$ laminate gives the highest value of $(N_x + N_y)$ for almost all combinations of biaxial load except for very high and very low values of N_x and for cross ply laminate $(N_x + N_y)$ is the minimum for any combination of biaxial loading.For very high values of N_x, $\theta = 30°$ laminate gives the maximum value of $(N_x + N_y)$ and for very low values of N_x, $\theta = 60°$ laminate gives the maximum value of $(N_x + N_y)$.

- Change in slope for both $\theta = 30°$ and $\theta = 60°$ laminates occur when both N_x and N_y are moderate.For $\theta = 45°$ laminate change in slope occurs both at very high and very low values of N_x.In all the cases a change in slope is aasociated with a corresponding change in mode shape which is evident from Figs. 4.38 - 4.45.

- The portion for which $(N_x + N_y)$ is same for both $\theta = 30°$ and $\theta = 60°$ laminates is less as compared to thin laminate.

- Here again, observations, similar to that for thin laminates regarding intersection points of the stability curves of different laminates, can be made for $\theta = 30°$ and $\theta = 60°$ laminates.Unlike for thin laminate here $\theta = 45°$ laminate cuts the $\theta = 60°$ laminate at very high value of N_y and the $\theta = 30°$ laminate at very high value of N_x.

The stability boundaries for rectangular laminated plates $(a/b = 2)$ are quite different from that of square laminates.

For $a/b = 2$ and $a/h = 100$ (Fig. 4.36) the following observations can be made.

- Except for $\theta = 30°$ laminate (linear stability envelop) the sability envelops of other angle ply laminates and cross ply laminate are all piecewise linear.

- For different combinations of N_x and N_y, either $\theta = 45°$ laminate or $\theta = 60°$ laminate gives the maximum value of $(N_x + N_y)$.

- For cross ply laminate, the slope of the stability envelop changes at a high value of N_y, for $\theta = 45°$ laminate change in slope occurs at a high value of N_x whereas for $\theta = 60°$ laminate change in slope occurs twice.One is when both N_x and N_y are high and another is when only N_x is high and N_y is moderate.

- Here four points can be observed at which different laminates (two laminates at each points) gives the same value of $(N_x + N_y)$.That is at these points the biaxial load carrying capacities of two different laminates are the same.

For $a/b = 2$ and $a/h = 10$ (Fig. 4.37) the following observations can be made.

- Here the stability envelops are piecewise linear but for certain portions of the envelops, slope changes very frequently.

- The curves are almost perpendicular to the Y axis (denoting $N_y b^2/E_T h^3$) for one portion of them and are almost perpendicular (except for $\theta = 45°$ laminate) to the X axis (denoting $N_x b^2/E_T h^3$) for another portion.This manifests to the fact that at these portions of the curves, for a small decrease in the value of N_x, the capacity of the laminates to carry N_y increases rapidly and vice-versa.

- Change in slopes of all the envelops occur at high values of N_x.Similar to a square laminate here also a change in slope is is aasociated with a corresponding change in mode shape which can be observed from Figs. 4.46 - 4.57.

- As that for thin rectangular laminates, similar kind of intersection points can also be observed for thick rectangular laminates.Here the number of such unique points are six.

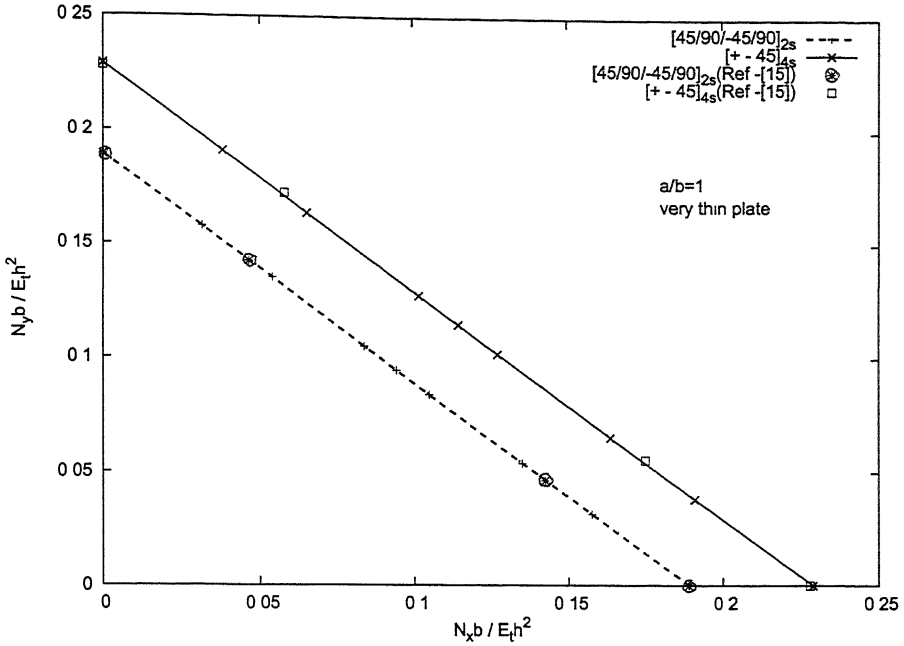

Figure 4.28: **Comparative study of Stability envelop for biaxial in-plane compressive loads N_x and N_y, (Material- M4), ($b = 254mm, h = 2.112mm$), from [15].**

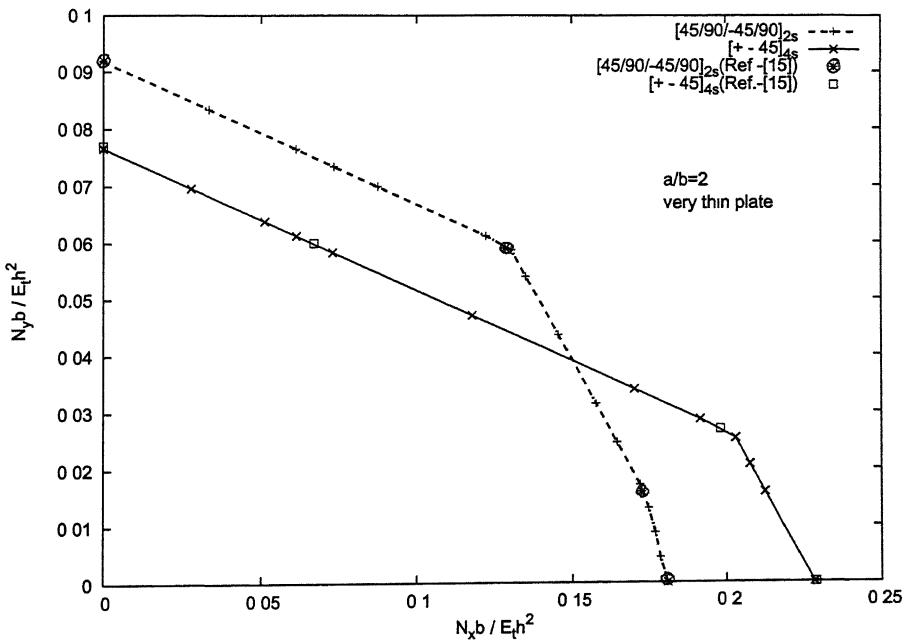

Figure 4.29: **Comparative study of Stability envelop for biaxial in-plane compressive loads N_x and N_y, (Material- M4), ($b = 254, h = 2.112mm$), from [15].**

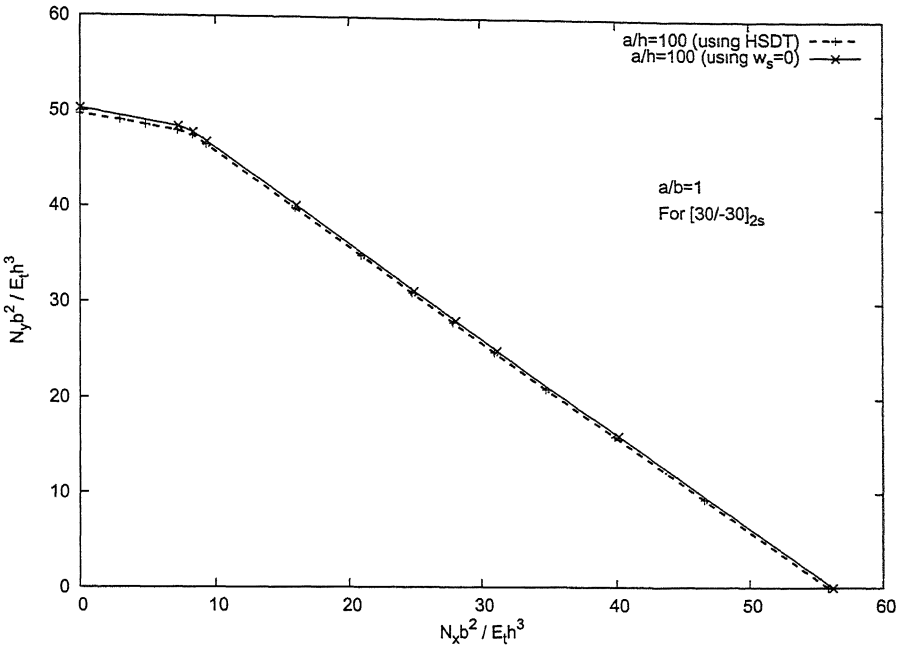

Figure 4.30: **Effect of transverse shear on stability envelop for biaxial in-plane compressive loads N_x and N_y, (Material- M2).**

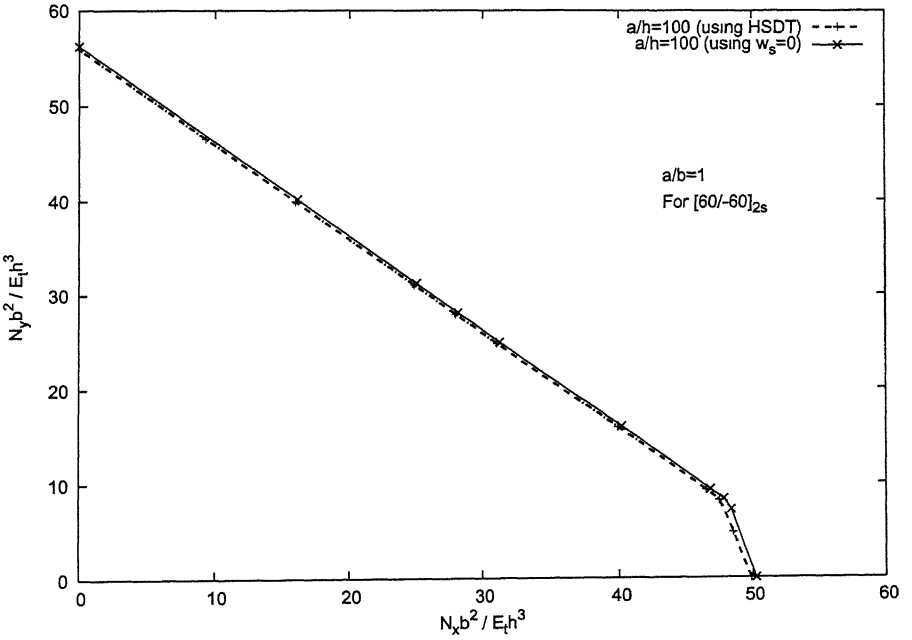

Figure 4.31: **Effect of transverse shear on stability envelop for biaxial in-plane compressive loads N_x and N_y, (Material- M2).**

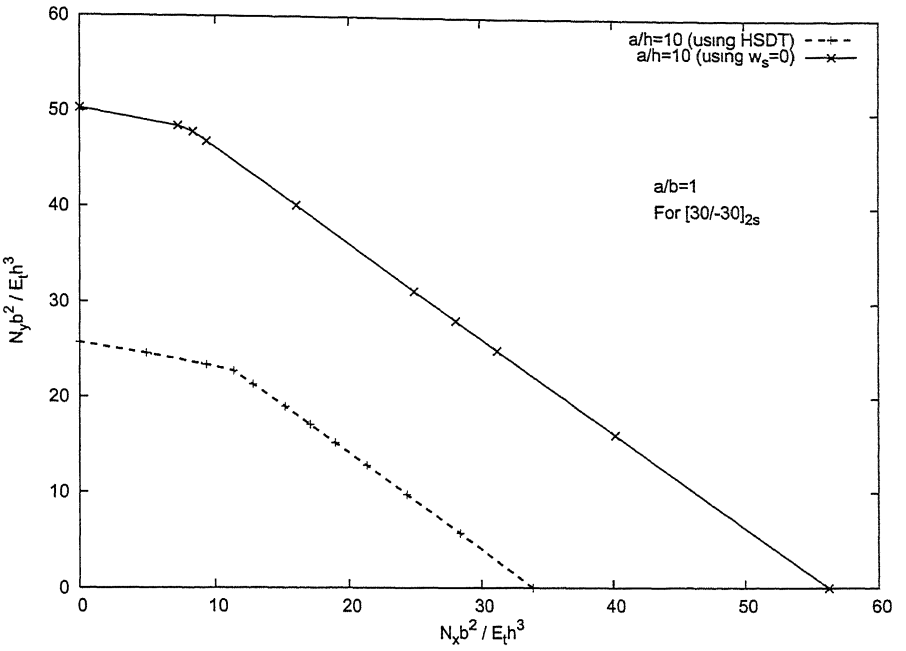

Figure 4.32: **Effect of transverse shear on stability envelop for biaxial in-plane compressive loads N_x and N_y, (Material- M2).**

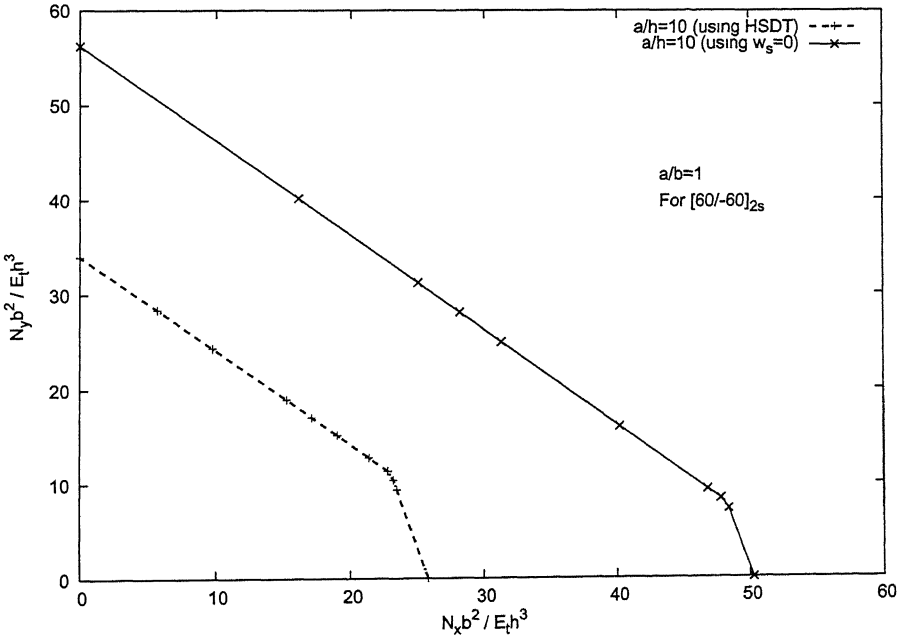

Figure 4.33: **Effect of transverse shear on stability envelop for biaxial in-plane compressive loads N_x and N_y, (Material- M2).**

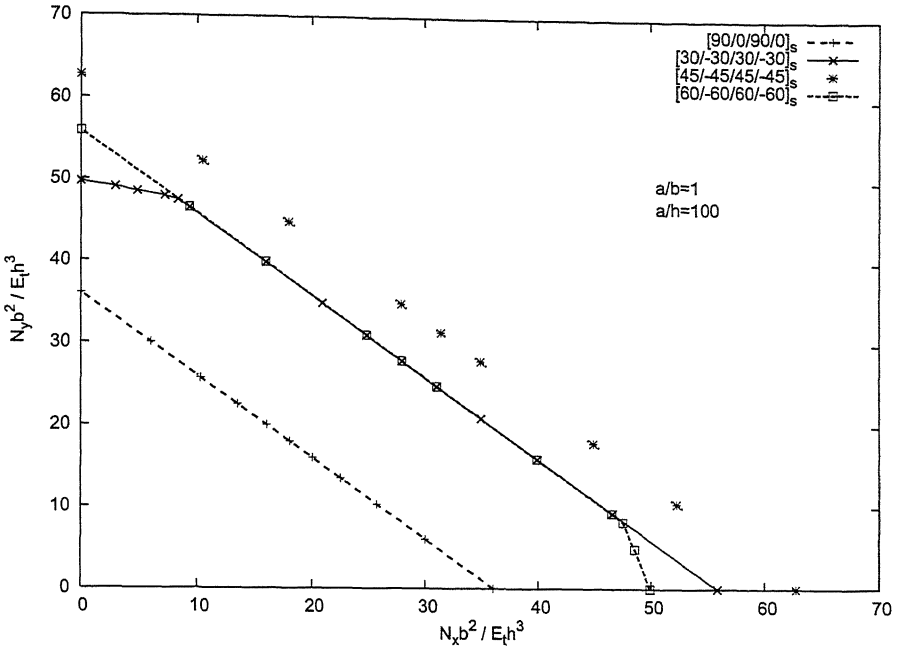

Figure 4.34: **Stability envelop for biaxial in-plane compressive loads N_x and N_y, (Material- M2).**

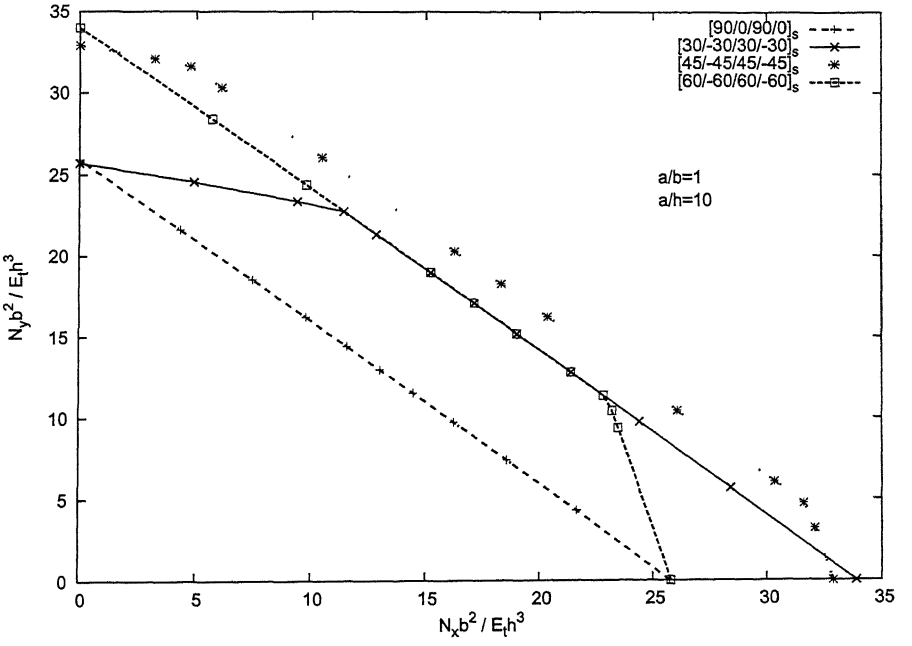

Figure 4.35: **Stability envelop for biaxial in-plane compressive loads N_x and N_y, (Material- M2).**

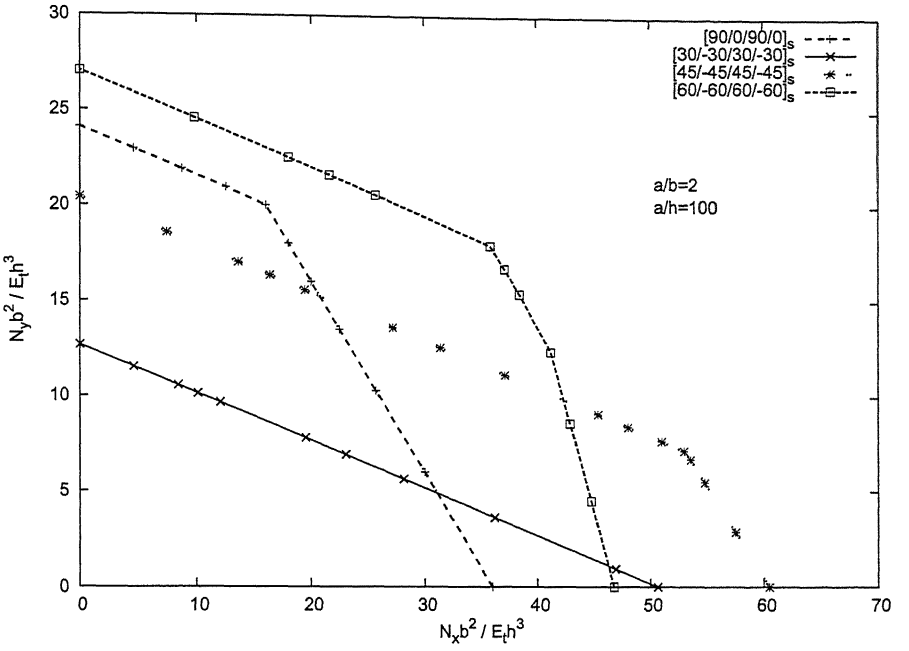

Figure 4.36: **Stability envelop for biaxial in-plane compressive loads N_x and N_y, (Material- M2).**

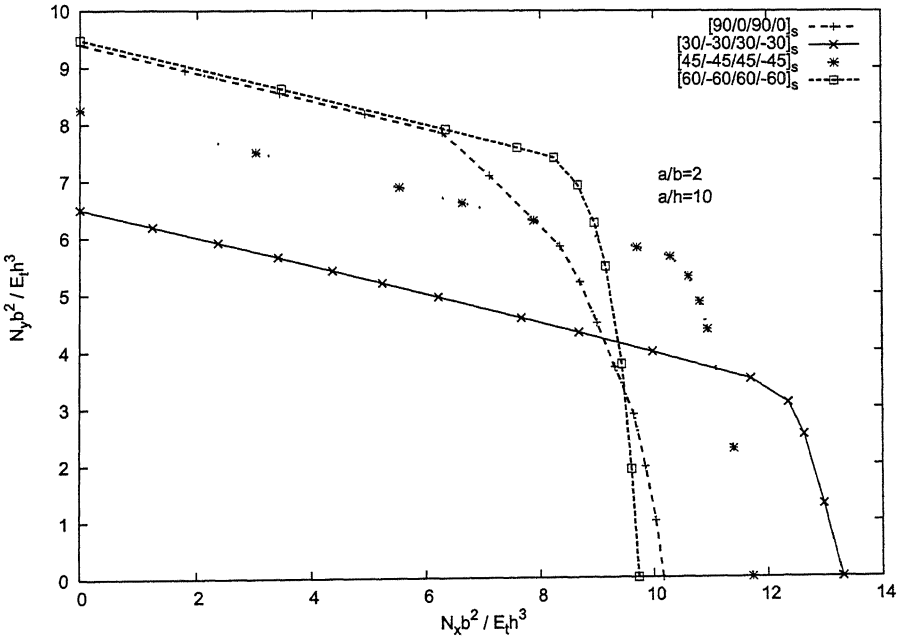

Figure 4.37: **Stability envelop for biaxial in-plane compressive loads N_x and N_y, (Material- M2).**

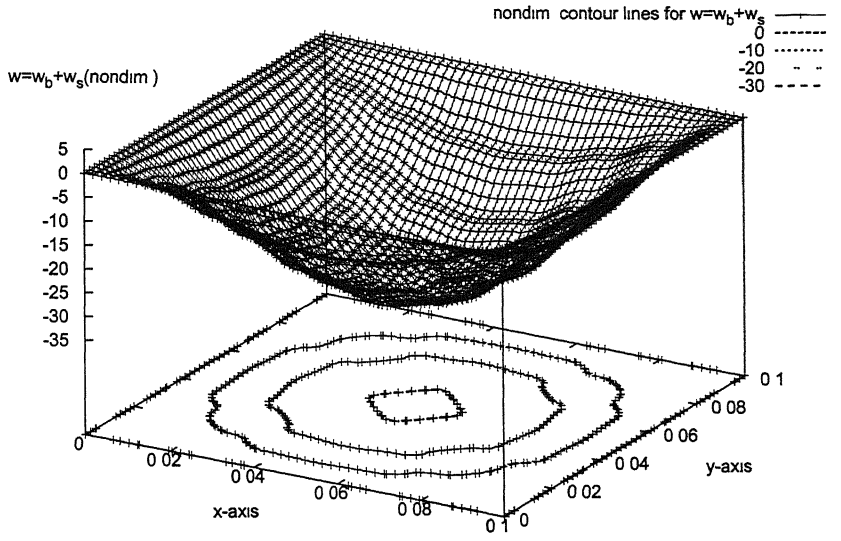

Figure 4.38: **Mode shape of symmetric cross ply laminate** $[90/0]_{2s}$ **for** $a/b = 1, a/h = 10$ **at** $\frac{N_y}{N_x} = 0.6$.

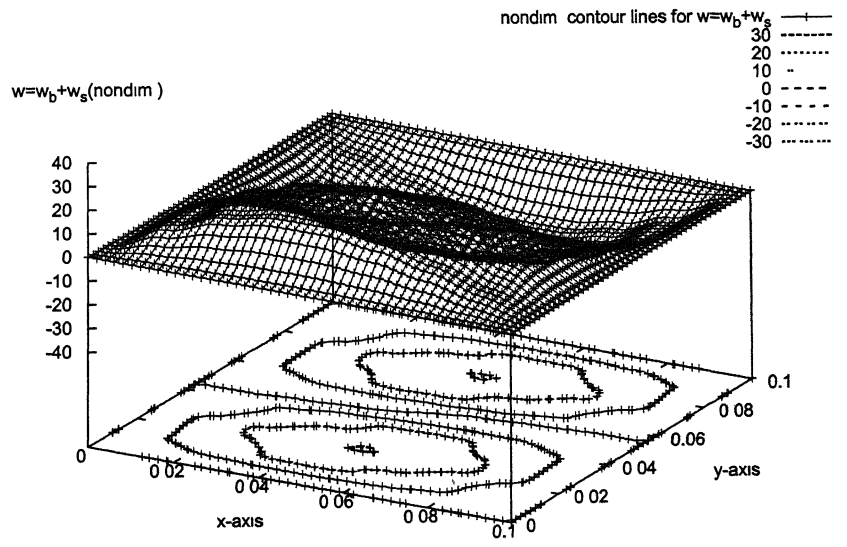

Figure 4.39: **Mode shape of symmetric angle ply laminate** $[\pm 30]_{2s}$ **for** $a/b = 1, a/h = 10$ **at** $\frac{N_x}{N_y} = 0.2$.

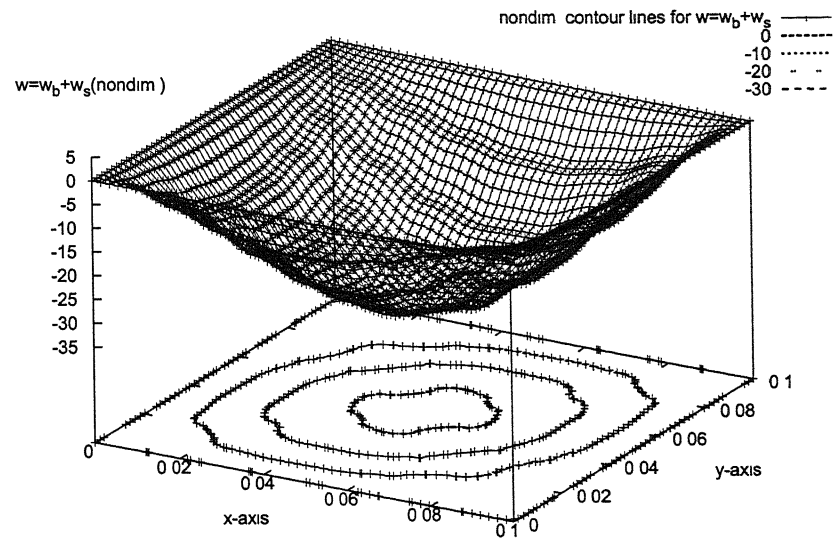

Figure 4.40: **Mode shape of symmetric angle ply laminate** $[\pm 30]_{2s}$ **for** $a/b = 1, a/h = 10$ **at** $\frac{N_y}{N_x} = 0.4$**.**

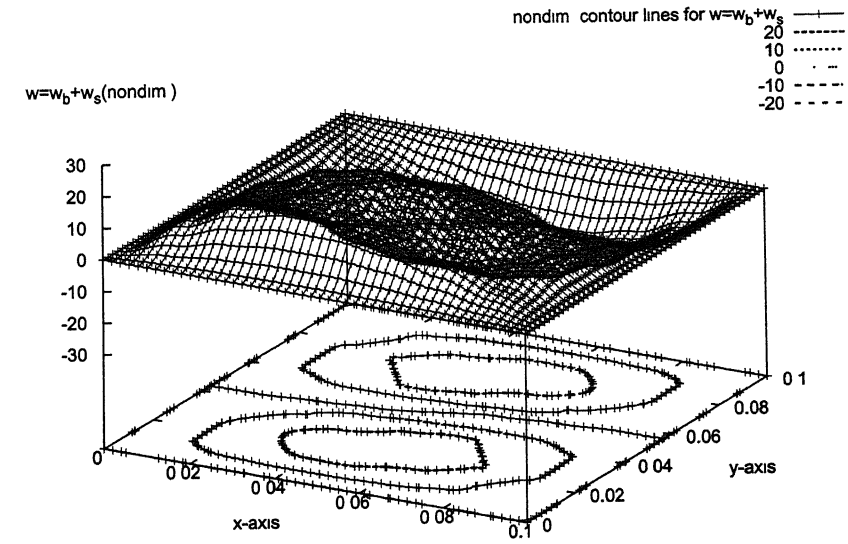

Figure 4.41: **Mode shape of symmetric angle ply laminate** $[\pm 45]_{2s}$ **for** $a/b = 1, a/h = 10$ **at** $\frac{N_x}{N_y} = 0.1$**.**

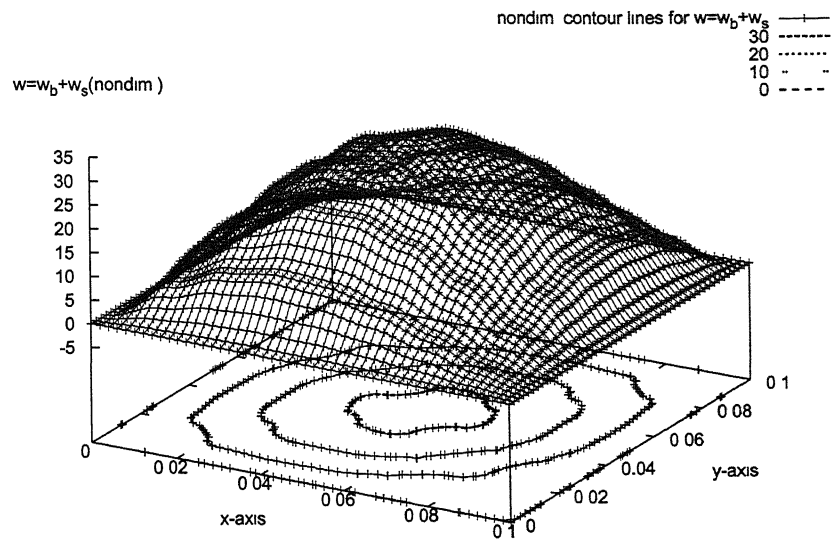

Figure 4.42: **Mode shape of symmetric angle ply laminate** $[\pm 45]_{2s}$ **for** $a/b = 1, a/h = 10$ **at** $\frac{N_x}{N_y} = 0.8$.

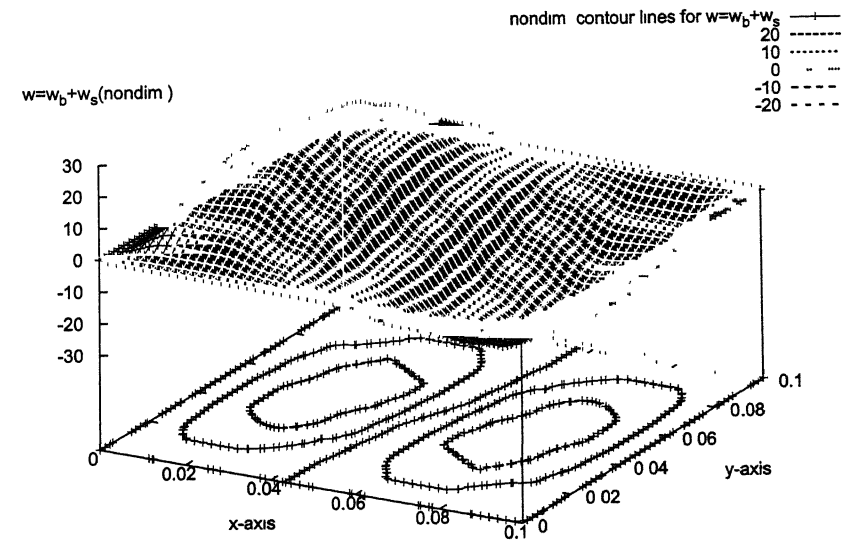

Figure 4.43: **Mode shape of symmetric angle ply laminate** $[\pm 45]_{2s}$ **for** $a/b = 1, a/h = 10$ **at** $\frac{N_y}{N_x} = 0.1$.

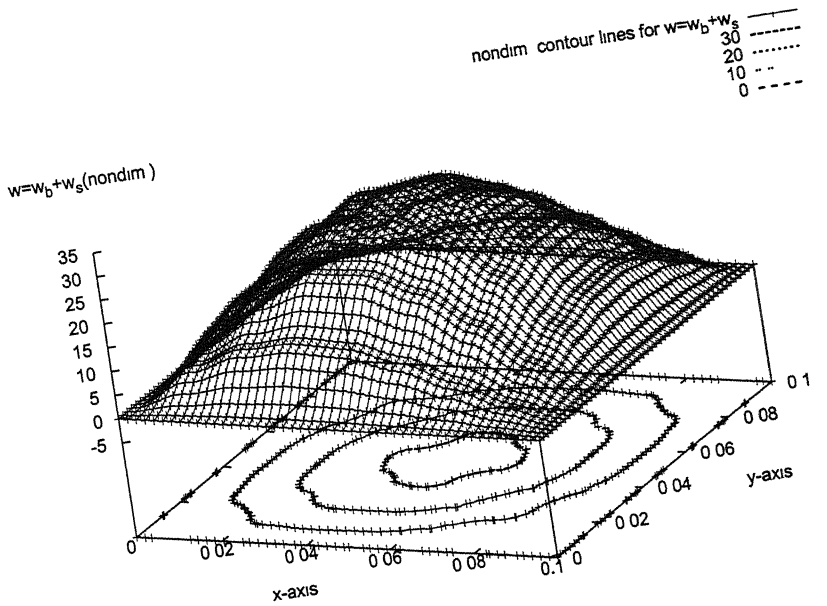

Figure 4.44: **Mode shape of symmetric angle ply laminate $[\pm 60]_{2s}$ for $a/b = 1, a/h = 10$ at $\frac{N_x}{N_y} = 0.4$.**

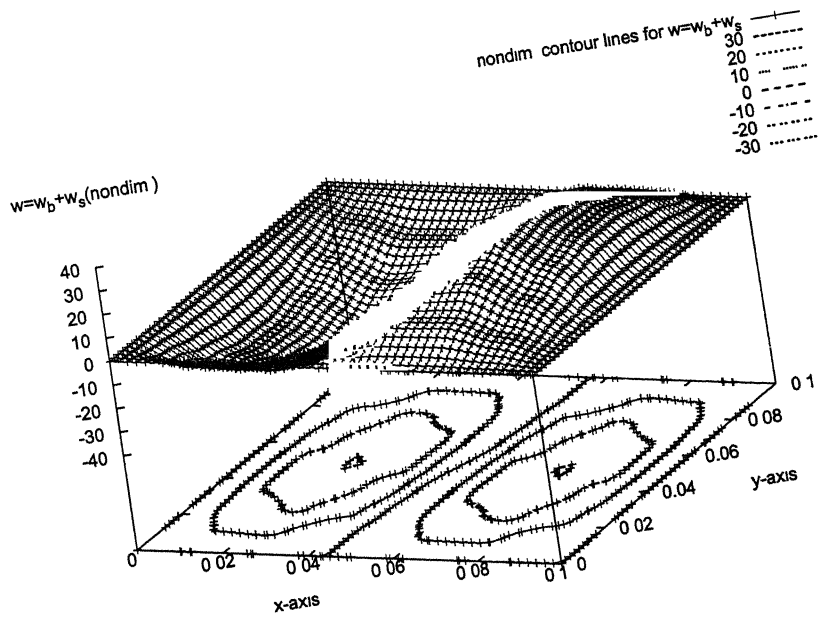

Figure 4.45: **Mode shape of symmetric angle ply laminate $[\pm 60]_{2s}$ for $a/b = 1, a/h = 10$ at $\frac{N_y}{N_x} = 0.2$.**

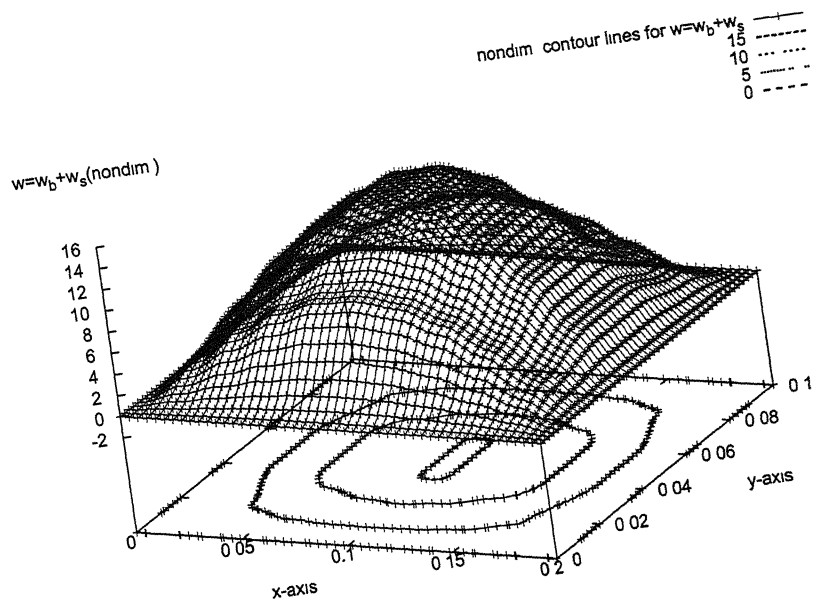

Figure 4.46: **Mode shape of symmetric cross ply laminate $[90/0]_{2s}$ for $a/b = 2, a/h = 10$ at $\frac{N_x}{N_y} = 0.6$.**

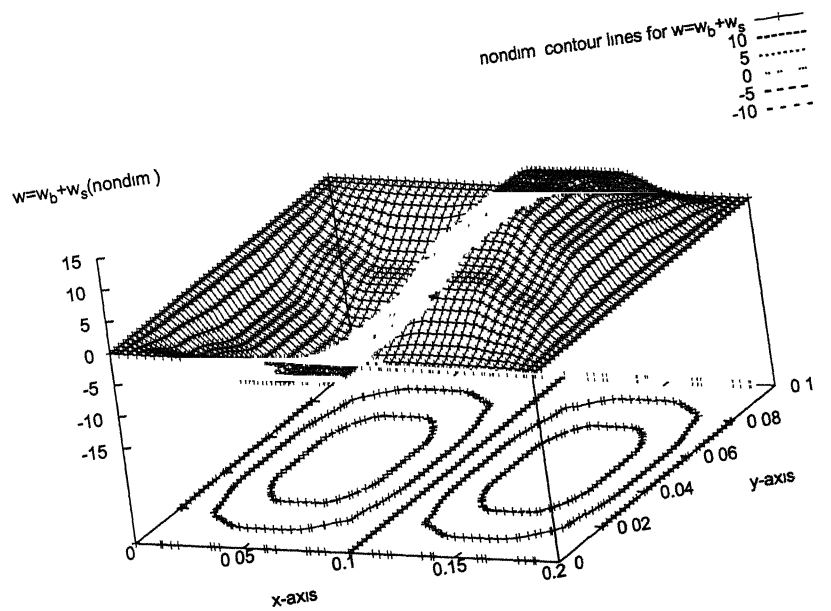

Figure 4.47: **Mode shape of symmetric cross ply laminate $[90/0]_{2s}$ for $a/b = 2, a/h = 10$ at $\frac{N_y}{N_x} = 1.0$.**

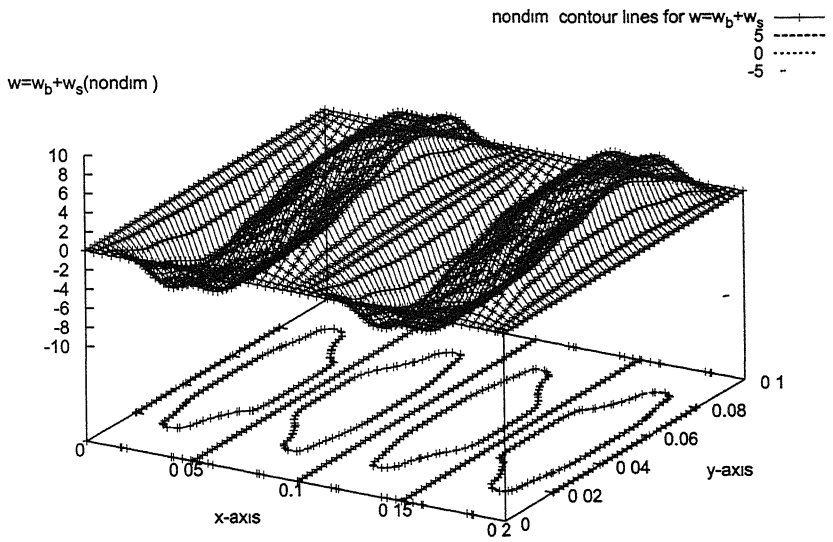

Figure 4.48: **Mode shape of symmetric cross ply laminate** $[90/0]_{2s}$ **for** $a/b = 2, a/h = 10$ **at** $\frac{N_y}{N_x} = 0.2$.

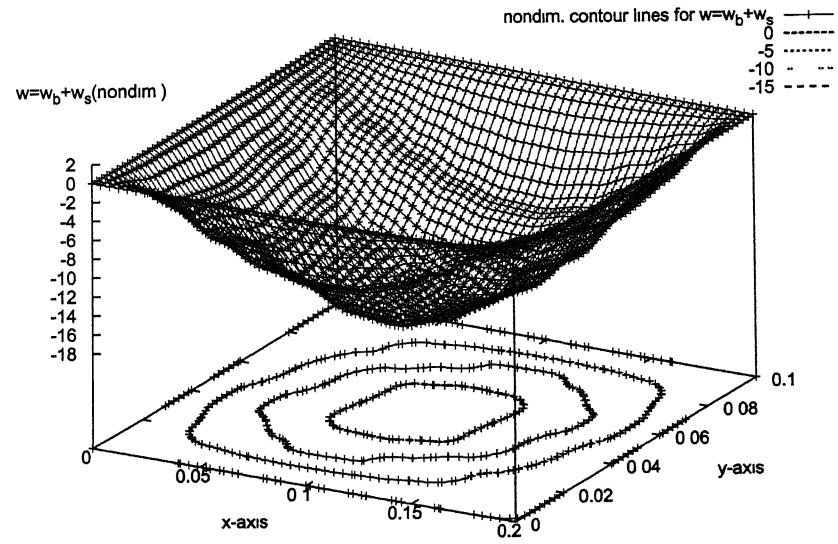

Figure 4.49: **Mode shape of symmetric angle ply laminate** $[\pm 30]_{2s}$ **for** $a/b = 2, a/h = 10$ **at** $\frac{N_y}{N_x} = 0.8$.

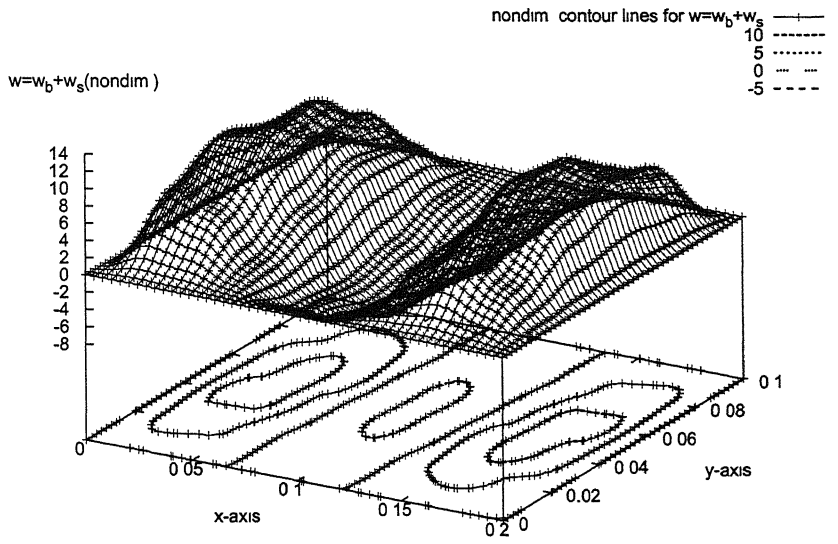

Figure 4.50: **Mode shape of symmetric angle ply laminate** $[\pm 30]_{2s}$ **for** $a/b = 2, a/h = 10$ **at** $\frac{N_y}{N_x} = 0.2$**.**

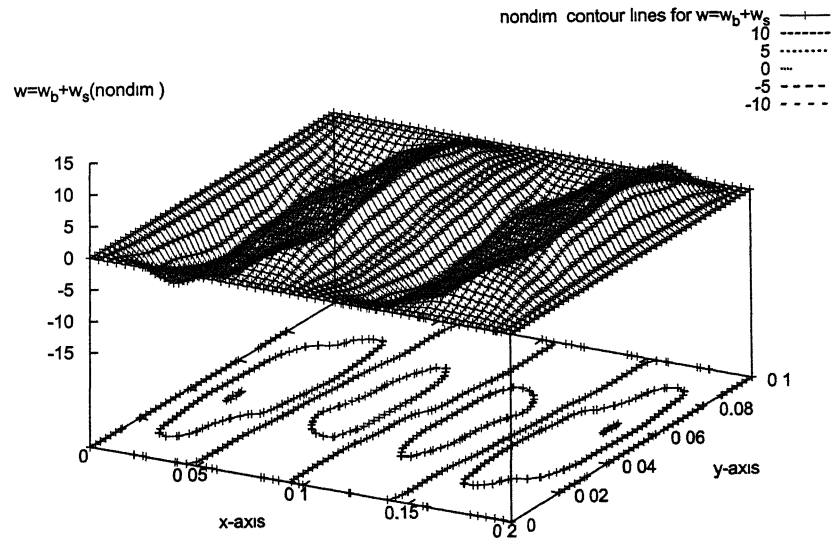

Figure 4.51: **Mode shape of symmetric angle ply laminate** $[\pm 30]_{2s}$ **for** $a/b = 2, a/h = 10$ **at** $\frac{N_y}{N_x} = 0.1$**.**

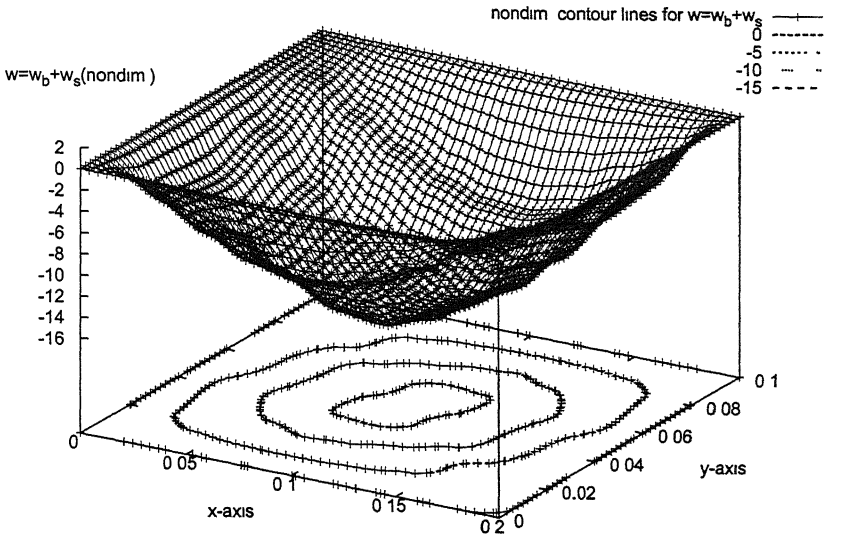

Figure 4.52: **Mode shape of symmetric angle ply laminate** $[\pm 45]_{2s}$ **for** $a/b = 2, a/h = 10$ **at** $\frac{N_y}{N_x} = 0.6$.

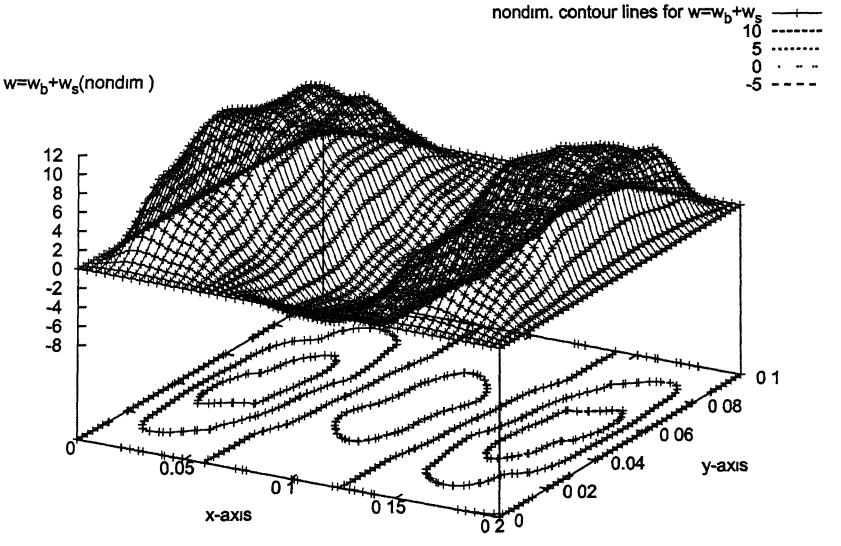

Figure 4.53: **Mode shape of symmetric angle ply laminate** $[\pm 45]_{2s}$ **for** $a/b = 2, a/h = 10$ **at** $\frac{N_y}{N_x} = 0.5$.

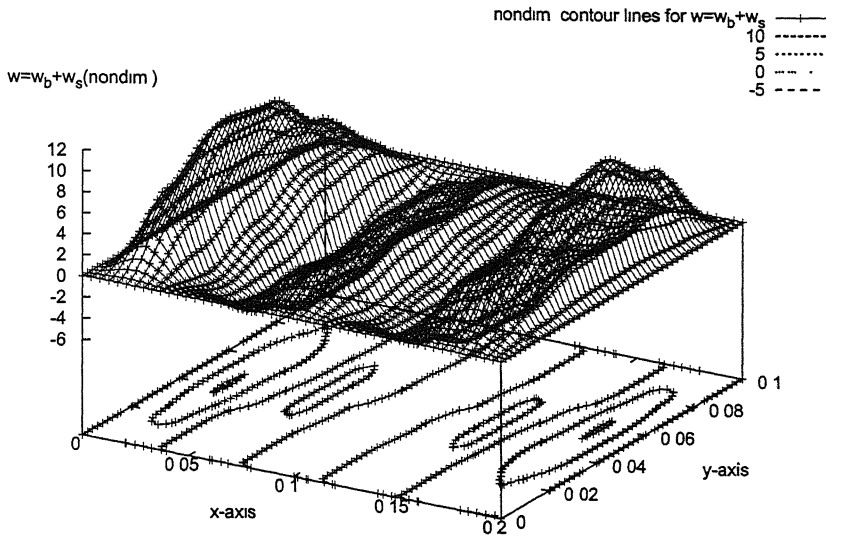

Figure 4.54: **Mode shape of symmetric angle ply laminate** $[\pm 45]_{2s}$ **for** $a/b = 2, a/h = 10$ **at** $\frac{N_y}{N_x} = 0.2$**.**

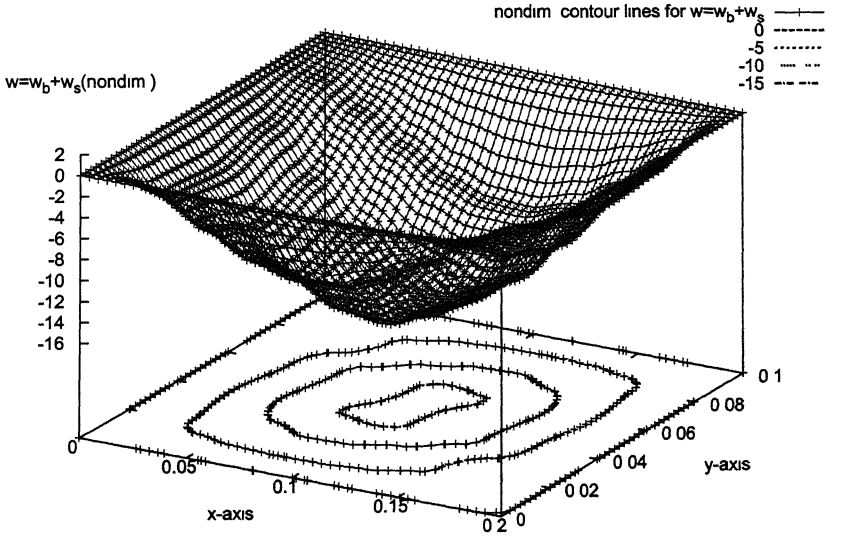

Figure 4.55: **Mode shape of symmetric angle ply laminate** $[\pm 60]_{2s}$ **for** $a/b = 2, a/h = 10$ **at** $\frac{N_x}{N_y} = 1.0$**.**

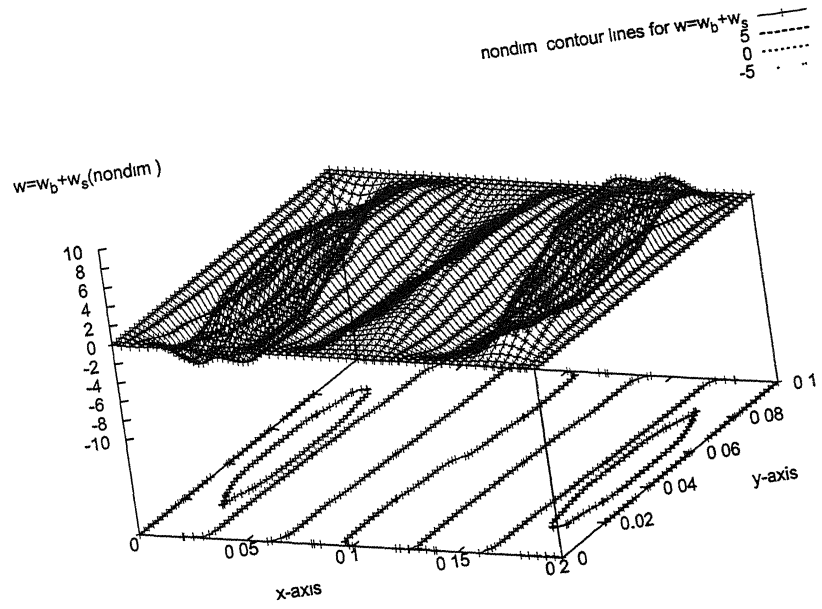

Figure 4.56: **Mode shape of symmetric angle ply laminate $[\pm 60]_{2s}$ for $a/b = 2, a/h = 10$ at $\frac{N_y}{N_x} = 0.2$.**

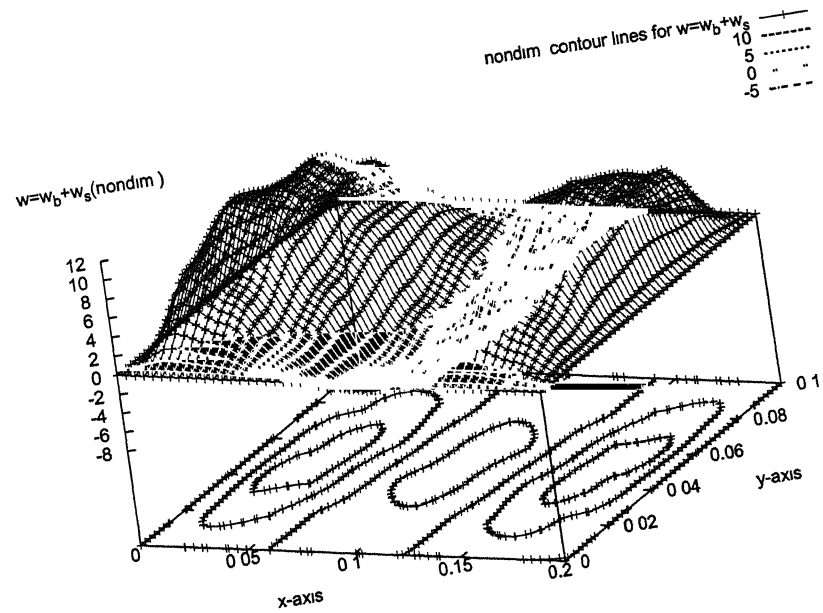

Figure 4.57: **Mode shape of symmetric angle ply laminate $[\pm 60]_{2s}$ for $a/b = 2, a/h = 10$ at $\frac{N_y}{N_x} = 0.8$.**

4.7.2 BIAXIAL IN-PLANE LOADINGS N_x AND $\pm N_{xy}$

First the results from the present study are compared with standard results available in the literature [15].It is found that the results of the present study are in good agreement with the results in the reference.These are shown in Fig 4.58 (for $a/b = 1$) and Fig 4.59 (for $a/b = 2$).It can be observed, that, for rectangular laminates (in Fig. 4.59) there is a unique point (at about $\frac{N_x}{-N_{xy}} = 0.148$) at which both the laminates ($[45/90/-45/90]_{2s}$ and $[\pm 45]_{4s}$) carry the same amount of axial compressive and shear loads, N_x and N_{xy}.Also when only positive shear load is applied both the laminates carry the same amount of loads whereas the same is not true for negative shear load. For square laminate no such obseravations can be made.

In the following section stability envelops are shown for both cross ply and angle ply symmetric laminates $[\pm\theta]_{2s}$ with plate aspect ratios 1 and 2 and length/thickness ratios 100 and 10 for both square and rectangular laminates.The analysis is done using simple HSDT for all the cases.

For $a/b = 1$ and $a/h = 100$ (Fig. 4.60) the following observations can be made.

- Stability envelops are not symmetric about $N_{xy} = 0$ line except for the cross ply laminate.It is observed that the value of $(N_x + |N_{xy}|)$ for initial buckling load is more for negative shear as compared to positive shear.
- For all combinations of biaxial loading cross ply laminate gives the lowest value of $(N_x + |N_{xy}|)$ and $\theta = 45°$ laminate gives the highest value of $(N_x + |N_{xy}|)$.
- Stability envelops of $\theta = 30°$ and $\theta = 60°$ laminates are comparable though $\theta = 30°$ laminate gives slightly higher value of $(N_x + |N_{xy}|)$.
- There is no such unique point for biaxial loading at which two or more laminates carry the same amount of axial compressive and shear loads.When only shear load is applied $\theta = 30°$ and $\theta = 60°$ laminates carry the same amount of load.

For $a/b = 1$ and $a/h = 10$ (Fig. 4.61) the following observations can be made.

- Stability envelops are not symmetric about $N_{xy} = 0$ line except for the cross ply laminate.It is observed that the value of $(N_x + |N_{xy}|)$ for initial buckling load is more for negative shear as compared to positive shear.

- For positive shear loading the stability envelops of $\theta = 30°$ and $\theta = 45°$ laminates are comparable with each other while $\theta = 60°$ and cross ply laminates are comparable with each other.

- For negative shear loading the stability envelops of $\theta = 30°$ and $\theta = 45°$ laminates are comparable with each other but $(N_x + |N_{xy}|)$ is more for $\theta = 60°$ laminate than for cross ply laminate.

- Here the stability envelops of different laminates intersect each others at some unique points.At these points different laminates carry the same amount of biaxial loads, N_x and N_{xy}.In other words it can be said that there are some unique combinations of in-plane compressive and shear loadings that can be carried by different laminates.

For $a/b = 2$ and $a/h = 100$ (Fig. 4.62) the following observations can be made.

- Stability envelops are not symmetric about $N_{xy} = 0$ line except for the cross ply laminate.It is observed that the value of $(N_x + |N_{xy}|)$ for initial buckling load is more for negative shear as compared to positive shear.

- For all combinations of biaxial loading except for very high values of N_{xy} (both positive and negative), $\theta = 45°$ laminate gives the highest value of $(N_x + |N_{xy}|)$.

- The range of shear loading (defined as: positive shear - negative shear) which a laminate can withstand is minimum for $\theta = 45°$ laminate.

- Similar kind of obseravtions that were made for square thin laminates can also be made for rectangular thin laminates regarding intersection poins of stability envelops.

For $a/b = 2$ and $a/h = 10$ (Fig. 4.62) the following observations can be made.

- Stability envelops are not symmetric about $N_{xy} = 0$ line except for the cross ply laminate.It is observed that the value of $(N_x + |N_{xy}|)$ for initial buckling load is more for negative shear as compared to positive shear.

- For low values of shear load (both positive and negative), the difference in $(N_x + |N_{xy}|)$ is substantial for different laminates whereas for high values of positive shear load this difference is very nominal.For very high values of negative shear load the above mentioned difference is medium.

- For negative shear load cross ply laminate gives the minimum value of $(N_x + |N_{xy}|)$ except for very low values of negative shear load.

- For high values of N_x, $\theta = 30°$ laminate gives maximum value of $(N_x + |N_{xy}|)$.

- Here also one can observe some unique points at which different laminates carry the same amount of biaxial loads, N_x and N_{xy}.

* In the above discussion $|N_{xy}|$ denotes the absolute value of nondimensionalized in-plane shear buckling load.

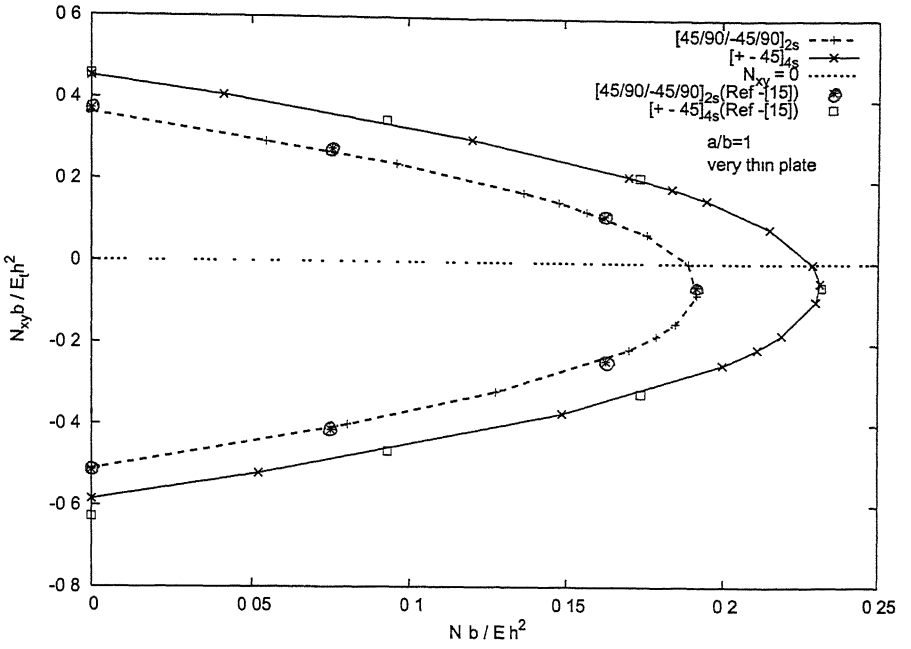

Figure 4.58: **Comparative study of Stability envelop for biaxial in-plane compressive and shear loads N_x and N_{xy}, (Material- M4), ($b = 254mm, h = 2.112mm$), from [15].**

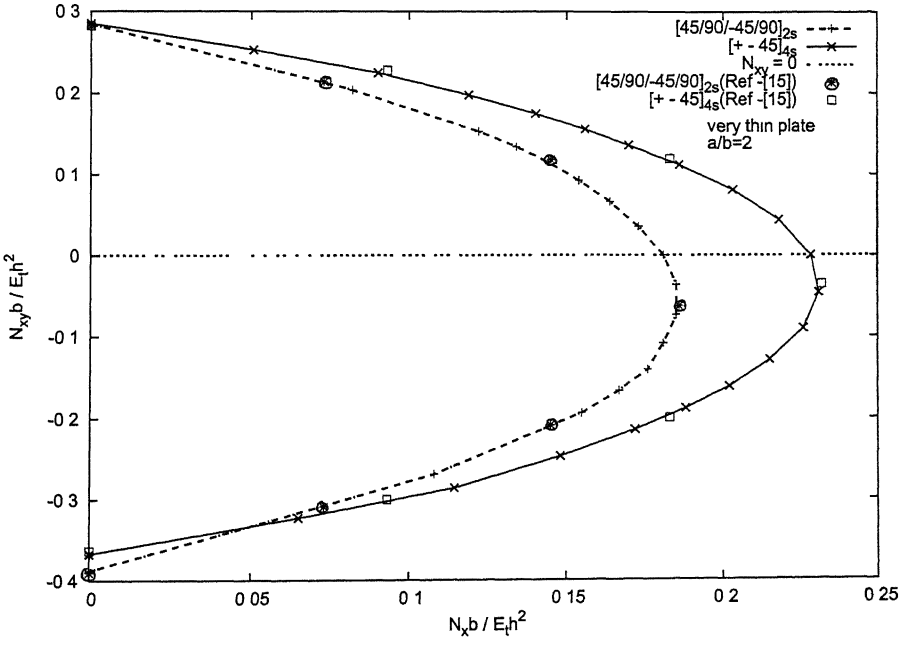

Figure 4.59: **Comparative study of Stability envelop for biaxial in-plane compressive and shear loads N_x and N_{xy}, (Material- M4), ($b = 254mm, h = 2.112mm$), from [15].**

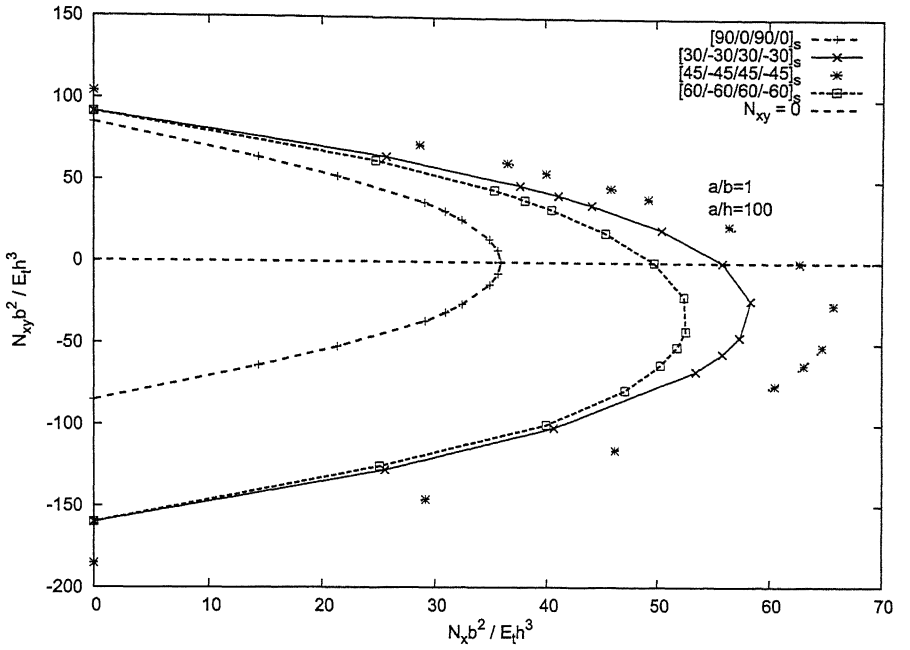

Figure 4.60: **Stability envelop for biaxial in-plane compressive and shear loads N_x and N_{xy}, (Material- M2).**

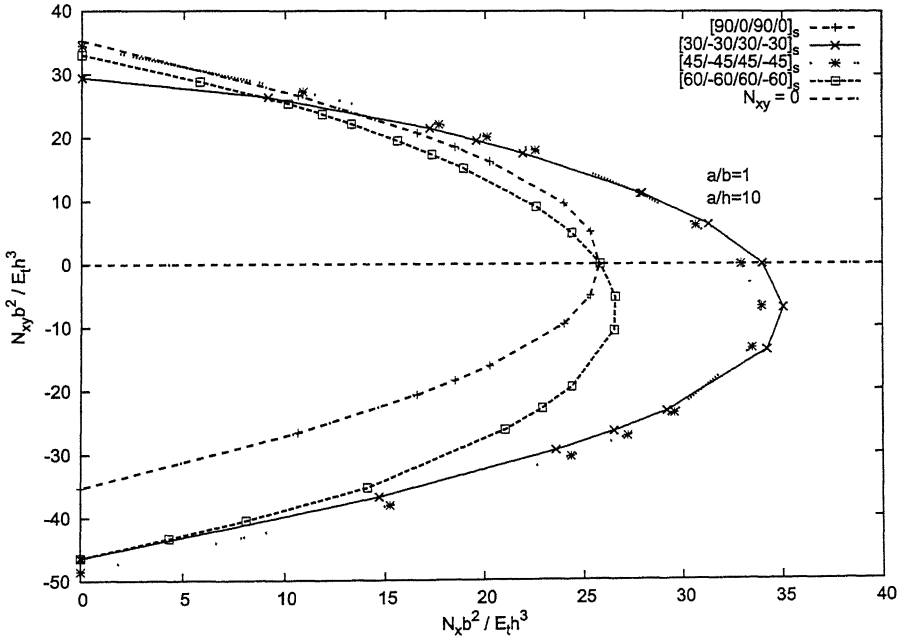

Figure 4.61: **Stability envelop for biaxial in-plane compressive and shear loads N_x and N_{xy}, (Material- M2).**

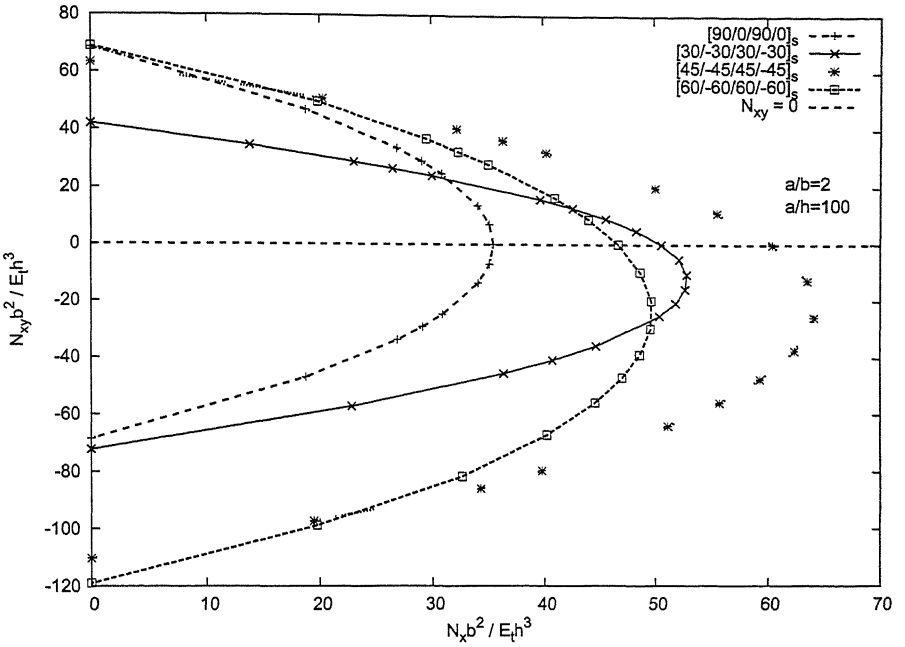

Figure 4.62: **Stability envelop for biaxial in-plane compressive and shear loads N_x and N_{xy}, (Material- M2).**

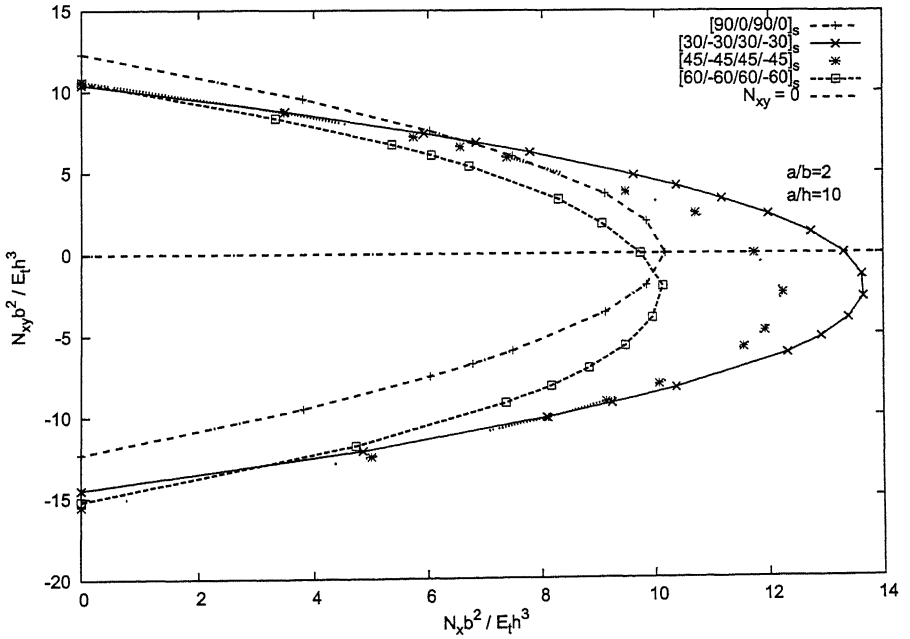

Figure 4.63: **Stability envelop for biaxial in-plane compressive and shear loads N_x and N_{xy}, (Material- M2).**

Chapter 5

CONCLUSIONS AND FUTURE SCOPE

5.1 CONCLUSIONS

In the present work initial buckling behaviour of composite laminated plates was carried out with both uniaxial and biaxial loads (both compressive and shear) including transverse shear effect.The response has been obtained for different plate aspect ratios, fibre orientation angles and length/thickness ratios.The analysis is performed using finite element method and the eigenvalues (which gives the initial buckling load) and the corresponding eigenvectors (which gives the mode shape for the corresponding buckling load) are obtained from the finite element solution using standard NAG routines.The following main conclusions can be drawn from the present investigation.

1. For thin laminates the effect of transverse shear is negligible and CLT is sufficient for predicting buckling loads.However as the length/thickness ratio increases transverse shear plays a dominant role and it has to be duly accounted for accurate prediction of critical loads..For moderately thick laminates there is substantial change in the values obtained by CLT and HSDT.For accurate analysis HSDT must be used for thick/moderately thick laminate.

2. The effect of lamina orientation angle of antisymmetric laminate on the initial

buckling load decreases with the increase in length/thickness ratio.

3. For thick laminates, the effect of lamina orientation angle of antisymmetric laminate on the initial buckling load decreases as the aspect ratio increases.

4. The critical fibre orentation angle reduces as the length/thickness ratio of the laminate increases.

5. For thick laminate the critical fibre orentation angle becomes smaller as the aspect ratio of the laminate increases.

6. For shear buckling load, as the aspect ratio increases the effect of fibre orientation angle on the value of initial buckling load decreases substantially.

7. The critical value of the fibre orientation angle remains almost same for shear buckling load with change in aspect ratio.

8. Interaction curves for N_x and N_y are either linear or piecewise linear.

9. There are some combinations of N_x and N_y for which different laminates give same value of critical load.

10. For combined shear and compressive load (N_{xy} and N_x) the stability envelops are not symmetric about the the line $N_{xy} = 0$ except for cross ply laminate.For same N_x lamiante can withstand more negative shear loading than positive one.

11. For some combinations of combined compressive and shear loadings, the stability envelops for different laminates are culsered and for some other portions they are widely seperated.

5.2 SCOPE FOR FUTURE WORK

Some of the areas which need to be investigated further are mentioned below.

1. The analysis for laminates with cut-outs of different geometries (practical laminates).

2. Response of laminates with plydrops need to be investigated.

3. Stability characteristics of thick laminates under the application of partial edge loading and concentrated loading can also be looked into.

4. Post-buckling analysis of laminates using non-linear strain-displacement relations.

5. Stability envelops of thick laminates with different combinations of thermal/hygroscopic and static in-plane loading.

APPENDIX A

$$\begin{Bmatrix} N_x \\ N_y \\ N_{xy} \\ M_x \\ M_y \\ M_{xy} \\ P_x \\ P_y \\ P_{xy} \\ Q_x \\ Q_y \end{Bmatrix} = \sum_{K=1}^{NL} \begin{bmatrix} [A]_{3\times3} & [B]_{3\times3} & [E]_{3\times3} & [0]_{3\times2} \\ [B]_{3\times3} & [D]_{3\times3} & [F]_{3\times3} & [0]_{3\times2} \\ [E]_{3\times3} & [F]_{3\times3} & [H]_{3\times3} & [0]_{3\times2} \\ [0]_{2\times3} & [0]_{2\times3} & [0]_{2\times3} & [G]_{2\times2} \end{bmatrix}_k \begin{Bmatrix} \epsilon_{0x} \\ \epsilon_{0y} \\ \epsilon_{0xy} \\ k_{0x} \\ k_{0y} \\ k_{0xy} \\ k_{lx} \\ k_{ly} \\ k_{lxy} \\ \gamma_x \\ \gamma_y \end{Bmatrix} \tag{1}$$

where,

$$[A]_k = \begin{bmatrix} \bar{Q}_{11}H_1 & \bar{Q}_{12}H_1 & \bar{Q}_{16}H_1 \\ \bar{Q}_{12}H_1 & \bar{Q}_{22}H_1 & \bar{Q}_{26}H_1 \\ \bar{Q}_{16}H_1 & \bar{Q}_{26}H_1 & \bar{Q}_{66}H_1 \end{bmatrix}_k$$

$$[B]_k = \begin{bmatrix} \bar{Q}_{11}H_2 & \bar{Q}_{12}H_2 & \bar{Q}_{16}H_2 \\ \bar{Q}_{12}H_2 & \bar{Q}_{22}H_2 & \bar{Q}_{26}H_2 \\ \bar{Q}_{16}H_2 & \bar{Q}_{26}H_2 & \bar{Q}_{66}H_2 \end{bmatrix}_k$$

$$[D]_k = \begin{bmatrix} \bar{Q}_{11}H_3 & \bar{Q}_{12}H_3 & \bar{Q}_{16}H_3 \\ \bar{Q}_{12}H_3 & \bar{Q}_{22}H_3 & \bar{Q}_{26}H_3 \\ \bar{Q}_{16}H_3 & \bar{Q}_{26}H_3 & \bar{Q}_{66}H_3 \end{bmatrix}_k$$

$$[E]_k = \begin{bmatrix} \bar{Q}_{11}H_4 & \bar{Q}_{12}H_4 & \bar{Q}_{16}H_4 \\ \bar{Q}_{12}H_4 & \bar{Q}_{22}H_4 & \bar{Q}_{26}H_4 \\ \bar{Q}_{16}H_4 & \bar{Q}_{26}H_4 & \bar{Q}_{66}H_4 \end{bmatrix}_k$$

$$[F]_k = \begin{bmatrix} \bar{Q}_{11}H_5 & \bar{Q}_{12}H_5 & \bar{Q}_{16}H_5 \\ \bar{Q}_{12}H_5 & \bar{Q}_{22}H_5 & \bar{Q}_{26}H_5 \\ \bar{Q}_{16}H_5 & \bar{Q}_{26}H_5 & \bar{Q}_{66}H_5 \end{bmatrix}_k$$

$$[H]_k = \begin{bmatrix} \bar{Q}_{11}H_7 & \bar{Q}_{12}H_7 & \bar{Q}_{16}H_7 \\ \bar{Q}_{12}H_7 & \bar{Q}_{22}H_7 & \bar{Q}_{26}H_7 \\ \bar{Q}_{16}H_7 & \bar{Q}_{26}H_7 & \bar{Q}_{66}H_7 \end{bmatrix}_k$$

$$[G]_k = \begin{bmatrix} \bar{Q}_{44}H_8 & \bar{Q}_{45}H_8 \\ \bar{Q}_{45}H_8 & \bar{Q}_{55}H_8 \end{bmatrix}_k$$

in which,

$H_i = \frac{1}{i}\left({z^i}_k - {z^i}_{k-1} \right)$, $i = 1, 2, 3, 4, 5, 7$

and $H_8 = [\{z_k - z_{k-1}\} - \frac{8}{3h^2}\{{z^3}_k - {z^3}_{k-1}\} + \frac{16}{5h^2}\{{z^5}_k - {z^5}_{k-1}\}]$.

also

$$[D_r] = \begin{bmatrix} [A] & [B] & [E] & [0] \\ [B] & [D] & [F] & [0] \\ [E] & [F] & [H] & [0] \\ [0] & [0] & [0] & [G] \end{bmatrix} \tag{2}$$

APPENDIX B

The element shape functions of a four noded rectangular C^1 continuous finite element in local co-ordinates are:

$$
\begin{aligned}
N_1' &= (2\frac{\bar{X}^3}{\bar{a}^3} - 3\frac{\bar{X}^2}{\bar{a}^2} + 1)(2\frac{\bar{Y}^3}{\bar{b}^3} - 3\frac{\bar{Y}^2}{\bar{b}^2} + 1)\\
N_2' &= -(2\frac{\bar{X}^3}{\bar{a}^3} - 3\frac{\bar{X}^2}{\bar{a}^2})(2\frac{\bar{Y}^3}{\bar{b}^3} - 3\frac{\bar{Y}^2}{\bar{b}^2} + 1)\\
N_3' &= (2\frac{\bar{X}^3}{\bar{a}^3} - 3\frac{\bar{X}^2}{\bar{a}^2})(2\frac{\bar{Y}^3}{\bar{b}^3} - 3\frac{\bar{Y}^2}{\bar{b}^2})\\
N_4' &= -(2\frac{\bar{X}^3}{\bar{a}^3} - 3\frac{\bar{X}^2}{\bar{a}^2} + 1)(2\frac{\bar{Y}^3}{\bar{b}^3} - 3\frac{\bar{Y}^2}{\bar{b}^2})\\
N_5' &= (\frac{\bar{X}^3}{\bar{a}^2} - 2\frac{\bar{X}^2}{\bar{a}} + \bar{X})(2\frac{\bar{Y}^3}{\bar{b}^3} - 3\frac{\bar{Y}^2}{\bar{b}^2} + 1)\\
N_6' &= (\frac{\bar{X}^3}{\bar{a}^2} - \frac{\bar{X}^2}{\bar{a}})(2\frac{\bar{Y}^3}{\bar{b}^3} - 3\frac{\bar{Y}^2}{\bar{b}^2} + 1)\\
N_7' &= -(\frac{\bar{X}^3}{\bar{a}^2} - \frac{\bar{X}^2}{\bar{a}})(2\frac{\bar{Y}^3}{\bar{b}^3} - 3\frac{\bar{Y}^2}{\bar{b}^2})\\
N_8' &= -(\frac{\bar{X}^3}{\bar{a}^2} - 2\frac{\bar{X}^2}{\bar{a}} + \bar{X})(2\frac{\bar{Y}^3}{\bar{b}^3} - 3\frac{\bar{Y}^2}{\bar{b}^2})\\
N_9' &= (2\frac{\bar{X}^3}{\bar{a}^3} - 3\frac{\bar{X}^2}{\bar{a}^2} + 1)(\frac{\bar{Y}^3}{\bar{b}^2} - 2\frac{\bar{Y}^2}{\bar{b}} + \bar{Y})\\
N_{10}' &= -(2\frac{\bar{X}^3}{\bar{a}^3} - 3\frac{\bar{X}^2}{\bar{a}^2})(\frac{\bar{Y}^3}{\bar{b}^2} - 2\frac{\bar{Y}^2}{\bar{b}} + \bar{Y})\\
N_{11}' &= -(2\frac{\bar{X}^3}{\bar{a}^3} - 3\frac{\bar{X}^2}{\bar{a}^2})(\frac{\bar{Y}^3}{\bar{b}^2} - 2\frac{\bar{Y}^2}{\bar{b}})\\
N_{12}' &= (2\frac{\bar{X}^3}{\bar{a}^3} - 3\frac{\bar{X}^2}{\bar{a}^2} + 1)(\frac{\bar{Y}^3}{\bar{b}^2} - 2\frac{\bar{Y}^2}{\bar{b}})\\
N_{13}' &= (\frac{\bar{X}^3}{\bar{a}^2} - 2\frac{\bar{X}^2}{\bar{a}} + \bar{X})(\frac{\bar{Y}^3}{\bar{b}^2} - 2\frac{\bar{Y}^2}{\bar{b}} + \bar{Y})\\
N_{14}' &= (\frac{\bar{X}^3}{\bar{a}^2} - \frac{\bar{X}^2}{\bar{a}})(\frac{\bar{Y}^3}{\bar{b}^2} - 2\frac{\bar{Y}^2}{\bar{b}} + \bar{Y})\\
N_{15}' &= (\frac{\bar{X}^3}{\bar{a}^2} - \frac{\bar{X}^2}{\bar{a}})(\frac{\bar{Y}^3}{\bar{b}^2} - \frac{\bar{Y}^2}{\bar{b}})\\
N_{16}' &= (\frac{\bar{X}^3}{\bar{a}^2} - 2\frac{\bar{X}^2}{\bar{a}} + \bar{X})(\frac{\bar{Y}^3}{\bar{b}^2} - \frac{\bar{Y}^2}{\bar{b}})
\end{aligned}
$$

The aforementioned shape functions can be expressed in natural co-ordinates as:

$$\hat{N}'_1 = \frac{1}{16}(\xi - 1)^2(-\xi - 2)(\eta - 1)^2(-\eta - 2)$$

$$\hat{N}'_2 = \frac{1}{16}(\xi + 1)^2(\xi - 2)(\eta - 1)^2(-\eta - 2)$$

$$\hat{N}'_3 = \frac{1}{16}(\xi + 1)^2(\xi - 2)(\eta + 1)^2(\eta - 2)$$

$$\hat{N}'_4 = \frac{1}{16}(\xi - 1)^2(-\xi - 2)(\eta + 1)^2(\eta - 2)$$

$$\hat{N}'_5 = \frac{1}{16}(\xi - 1)^2(-\xi - 1)(\eta - 1)^2(-\eta - 2)$$

$$\hat{N}'_6 = -\frac{1}{16}(\xi + 1)^2(\xi - 1)(\eta - 1)^2(-\eta - 2)$$

$$\hat{N}'_7 = -\frac{1}{16}(\xi + 1)^2(\xi - 1)(\eta + 1)^2(\eta - 2)$$

$$\hat{N}'_8 = \frac{1}{16}(\xi - 1)^2(-\xi - 1)(\eta + 1)^2(\eta - 2)$$

$$\hat{N}'_9 = \frac{1}{16}(\xi - 1)^2(-\xi - 2)(\eta - 1)^2(-\eta - 1)$$

$$\hat{N}'_{10} = \frac{1}{16}(\xi + 1)^2(\xi - 2)(\eta - 1)^2(-\eta - 1)$$

$$\hat{N}'_{11} = -\frac{1}{16}(\xi + 1)^2(\xi - 2)(\eta + 1)^2(\eta - 1)$$

$$\hat{N}'_{12} = -\frac{1}{16}(\xi - 1)^2(-\xi - 2)(\eta + 1)^2(\eta - 1)$$

$$\hat{N}'_{13} = \frac{1}{16}(\xi - 1)^2(-\xi - 1)(\eta - 1)^2(-\eta - 1)$$

$$\hat{N}'_{14} = -\frac{1}{16}(\xi + 1)^2(\xi - 1)(\eta - 1)^2(-\eta - 1)$$

$$\hat{N}'_{15} = \frac{1}{16}(\xi + 1)^2(\xi - 1)(\eta + 1)^2(\eta - 1)$$

$$\hat{N}'_{16} = -\frac{1}{16}(\xi - 1)^2(-\xi - 1)(\eta + 1)^2(\eta - 1)$$

APPENDIX C

The details of $[B_0]$ and $[B_g]$ matrices are as shown:

$$[B_0] = \begin{bmatrix} N_{i,x} & 0 & 0 & 0 \\ 0 & N_{i,y} & 0 & 0 \\ N_{i,y} & N_{i,x} & 0 & 0 \\ 0 & 0 & -N_{i,xx} & 0 \\ 0 & 0 & -N_{i,yy} & 0 \\ 0 & 0 & -2N_{i,xy} & 0 \\ 0 & 0 & 0 & -\frac{4}{3h^2} N_{i,xx} \\ 0 & 0 & 0 & -\frac{4}{3h^2} N_{i,yy} \\ 0 & 0 & 0 & -\frac{8}{3h^2} N_{i,xy} \\ 0 & 0 & 0 & N_{i,x} \\ 0 & 0 & 0 & N_{i,y} \end{bmatrix}_{11\times 56} \tag{1}$$

and.

$$[B_g] = \begin{bmatrix} 0 & 0 & N_{i,x} & N_{i,x} \\ 0 & 0 & N_{i,y} & N_{i,y} \end{bmatrix}_{2\times 56} \tag{2}$$

In the above matrices, for columns 1 and 2, $i = 1-12$ (shape functions corresponding to u_0 and v_0) and for columns 3 and 4, $i = 1-16$ (shape functions corresponding to w_b and w_s).

Bibliography

[1] J. N. Reddy. An Introduction to Finite Element Method. McGraw-Hill International Editions, Engineering Mechanics Series, 1993.

[2] S. P. Lim, K. H. Lee, S. T. Chow and N. R. Senthilnathan, "Linear and Nonlinear Bending of Shear Deformable Plates," *Computers and structures, Vol. 30, 1988, pp. 945-952.*

[3] J. M. Whitney, "The effect of transverse shear deformation on the bending of laminated plates," *J. Comp. Mat., Vol. 3, 1969, pp. 534-547.*

[4] J. M. Whitney and N. J. Pagano, "Shear deformation in heterogeneous anisotropic plates," *J. Appl. Mech., Vol. 37, 1970, pp. 1031-1036.*

[5] E. Reissner, "The effect of transverse shear deformation on the bending of ela stic plates," *J. Appl. Mech., Vol. 12, 1945, pp. A69-A77.*

[6] R. D. Mindlin, "Influence of rotary inertia and shear on flexural motions of isotropic, elastic plates," J. Appl. Mech., Vol. 18, 1951, pp. A31-A38.

[7] J. N. Reddy, "A Simple Higher Order Theory for Laminated Composite Plates," *Journal of Applied Mechanics, Vol. 51, 1984, pp. 745-752.*

[8] J. N. Reddy and N. D. Phan, "Stability and vibration of isotropic, orthotropic and laminated plates according to a higher-order shear deformation theory," *J. Sound and Vibration, Vol. 98(2), 1985, pp. 157-170.*

[9] J. N. Reddy and A. A. Khdeir, "Buckling and vibration of laminated composite plates using various plate theories," *AIAA Journal, Vol. 27(12), 1989, pp. 1808-1817.*

[10] Gajbir singh, "Nonlinear Bending,Vibration and Buckling of Composite Beams and Plates," *Ph. D. dissertation at Indian Institute of technology, Kanpur. March 1993.*

[11] B. D. Agarwal and L. J. Broutman. Analysis and Performance of Fiber Composites. John Willy and Sons, New Delhi, 2^nd Ed., 1990.

[12] Robert M. Jones. Mechanics of Composite Materials. Scripta Book Company, McGraw-Hill Kogakusha, Ltd. New Delhi, 1975.

[13] Bogner, F. K., Fox, R. L. and Schmit, L. A., "The generation of interelement compatible stiffness and mass matrices by the use of interpolation formulas," *Proc. Conf. Matrix Methods in Structural Mech., AFFDL-TR-66-80, Wright-Patterson A.F.B., Ohio, October 1966, pp. 397-444.*

[14] M. Sharma, "Response and strength of axially compressive square laminates with a cutout," *M. Tech. dissertation at Indian Institute of technology, Kanpur. March 1999.*

[15] G. J. Turvey and I. H. Marshal. Buckling and Postbuckling Analysis of Composite Plates. Chapman and Hall, 1995.

[16] C. J. Brown, Alan L. Yettram and Mark Burnett, "Stability of plates with rectangular holes," *Journal of Structural Engineering, Vol. 113(5), 1987, pp. 1111-1116.*

[17] N. G. R. Iyengar. Structural Stability of Columns and Plates. Affiliated East-West Press Pvt. Ltd., Nwe Delhi, 1986.

[18] R. D. Cook. Concepts and Application of Finite Element Analysis.2nd edition, John Willy and Sons, 1981.

[19] T. J. R. Huges. Finite Element Method.Prentice-Hall, Inc, 1987.

[20] O. Ochoa and J. N. Reddy. Finite Element Analysis of Composite Laminates. Kluwert Academic Publishers, 1992.

[21] O. C. Zienkiewicz. The Finite Element Method. Tata McGraw-Hill Publishing Co. Ltd., New Delhi, 1979.